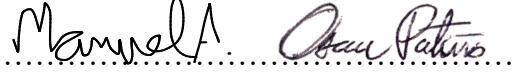




University of
Stavanger

Faculty of Science and Technology

MASTER'S THESIS

Study program/Specialization: Petroleum Engineering / Natural Gas Engineering	Spring semester, 2020 Open
Author: Manuel Alejandro Alfonso Alarcón Oscar Giovanni Patiño Hernández	 (Author's signature)
Faculty supervisor: A. H. Rabenjafimanantsoa Kjell Kåre Fjelde	
Thesis title: Experimental Investigation and Transient Flow Modelling of the Bullheading Process	
Credits (ECTS): 30	
Key words: Well control Bullheading Hydrostatic pressure Drift flux model Slug Flow AUSMV	Pages: 104 + enclosure: 36 Stavanger, 15.07.2020 Date/year

Contents

Abstract	i
Acknowledgment	ii
Nomenclature	iii
1 Introduction	1
2 Theoretical Background	3
2.1 Multiphase Flow in pipes	3
2.1.1 Multiphase Vertical Flow	3
2.1.2 Multiphase Horizontal Flow	5
2.2 Well Control	6
2.2.1 Circulating Well Control Techniques	6
2.2.2 Bullheading Applications	11
3 Experimental Investigation of the Bullheading Process	17
3.1 Experimental set-up for the bullheading Investigation	17
3.1.1 Equipment Installation	17
3.1.2 Practical tests	19
3.2 Flow loop of the experimental process	23
3.2.1 Experimental procedure	23
3.2.2 Software and Physical properties monitoring	26
4 The Transient Drift Flux Model	27
4.1 Conservation Laws	27
4.1.1 Conservation of Mass	27
4.1.2 Conservation of momentum	28
4.2 Closure laws	29
4.2.1 Gas slip model	29
4.2.2 Density models	31
4.2.3 Friction gradient model	32
4.2.4 Reynolds number	32
4.3 AUSMV scheme for the small-scale experimental setup	33
4.3.1 Discretization Process and Numerical Scheme	34
4.3.2 CFL Condition	35
4.3.3 Numerical diffusion and application of slope limiters	36
4.3.4 Boundary Conditions	37
5 Results and Discussion	39
5.1 Flow Visualization	40
5.2 Monitoring of physical properties	41

5.2.1 Absolute Pressure	43
5.2.2 Average Gas Velocity	57
6 Conclusions and Recommendations	65
A Flow calibration	69
B Numerical model	71
C 3D set-up pieces	103

List of Figures

2.1 Vertical fluid flow pattern for multiphase flow systems	4
2.2 Flow pattern map modeled for a vertical 5 cm diameter pipe upflow	4
2.3 Horizontal fluid flow pattern for multiphase flow systems	5
2.4 Flow regimes map in horizontal two phase flow	6
2.5 Kick circulation to surface using killing fluid	7
2.6 Pressure gradient mud profile	7
2.7 Gas kick appearance by swab effect	8
2.8 Driller's method pressure profile during circulation	9
2.9 W&W method pressure profile during circulation	10
2.10 Bullheading a well through the annular	12
2.11 Bullheading a well through tubing string	13
2.12 Bullheading process for a production well	14
2.13 Differences between MCD and PMCD	16
3.1 Initial laboratory Set-up	18
3.2 PASCO Capstone interface	19
3.3 Flow rate pump test with power supply variation	20
3.4 Sketch of the final set-up in 3D	22
4.1 Mass conservation in a production well	28
4.2 Reynolds Flow Classification Pattern	33
4.3 Example of a well discretization scheme	34
4.4 Gas volume fraction for different discretizations	36
4.5 Gas injection at bottom in the simulation	37
5.1 Bubble shape change	40
5.2 Absolute Pressure with flow rate of 0.61 l/s	47
5.3 Differential Pressure with flow rate of 0.61 l/s	48
5.4 Absolute Pressure with flow rate of 0.74 l/s	50
5.5 Differential Pressure with flow rate of 0.74 l/s	51
5.6 Absolute Pressure with flow rate of 0.90 l/s	52
5.7 Differential Pressure with flow rate of 0.90 l/s	53

5.8	<i>Absolute Pressure with flow rate of 1.08 l/s</i>	55
5.9	<i>Differential Pressure with flow rate of 1.08 l/s</i>	56
5.10	<i>Gas volume fraction - Test 0.61 l/s</i>	58
5.11	<i>Gas volume fraction at different flow rates</i>	59
5.12	<i>Taylor bubble gas volume for the four Bullheading rates</i>	60
5.13	<i>Gas Phase velocity response for a bullheading rate of 0.61 l/s</i>	60
5.14	<i>Gas Phase velocity response for a bullheading rate of 0.74 l/s</i>	61
5.15	<i>Gas Phase velocity response for a bullheading rate of 0.90 l/s</i>	62
5.16	<i>Gas Phase velocity response for a bullheading rate of 1.08 l/s</i>	62
5.17	<i>Gas Phase velocity compilation for each circulation rate</i>	63

List of Tables

3.1	Absolute pressure for each sensor	23
4.1	Flow parameters for different flow patterns	30
5.1	Liquid rate scenarios	43
5.2	Average experimental results	57
5.3	Gas velocities from the models	63

Abstract

The main objective of this thesis was to design and study a physical laboratory scale model, to simulate a kick and push it through the bullheading method. The air bubble was injected in a cylindrical loop system filled with water acting as a multiphase flow system. In drilling operations this is imperative to handle or prevent the migration effect of kicks through the Surface.

This study was focused on the implementation of the bullheading method applied in laboratory, with gas bubble injected into a Newtonian fluid filled system. The main goal was the circulation of the gas using liquid at a downward direction to push it to its injection position using four different flow rate tests. The difference in each test lies in the progressive increase in the liquid rate, which gradually shortens the time it takes for the gas to return to the site where it was injected. The amount of gas induced was monitored in all the four tests by using a reference height in the pipe, to decrease calculation variations for the gas rate results.

The hydrostatic pressure of the system was monitored with the use of PASCO Capstone equipment for the measurement of the absolute pressure. The gas rate was calculated with the pressure drop in a time interval when the sensor perceives the pass of the bubble and then when it only perceives liquid as an indicator of constant pressure in the sensor reading.

The average speed of the bubble was determined with the distance and the time it took to pass between the Top and Mid pressure sensors when bullheading. The increase in liquid rates produced an increase in the average velocity of the gas, decreasing the time it takes for the bubble to pass through the two sensors in each of the flow liquid rates.

The gas and liquid rates were determined in the laboratory. The same was the geometries of the experimental scale model and other initial conditions these were used as inputs for the numerical model and thus obtaining the average gas velocity. On this study, gas velocity was the parameter to be compared with experimental results and simulation due to the initial conditions of the flow model. It creates a different scenario than the real one making futile any further comparison for the moment. The numerical model conditions differed from the experimental model, due to the size of the bubble obtained from the numerical simulation which was different from the bubble injected experimentally. Because the physical parameters are dependents of the bubble area e.g. pressure, volume, etc.

The bullheading experiment allowed the visualization of the Slug flow and Dispersed flow pattern characteristic for the vertical multiphase flow patterns at a range of superficial gas and liquid velocities.

Acknowledgment

This project is especially dedicated to my aunt, Yaneth Alarcón Galindo, despite the fact that she is no longer in this world, she gave me the motivation to continue and complete this stage, being my guide and example to follow, regardless the difficulties.

To our supervisor Andrianifaliana Herimonja Rabenjafimanantsoa, for giving us their wisdom, dedication, knowledge to the development and completion of this project.

Our other supervisor Kjell Kåre Fjelde, for their generosity in granting his acquired experiences and instructing us with his knowledge, and patience to correct our stumbling blocks.

My thesis partner Oscar Giovanni Patiño Hernandez for correcting my mistakes with a “slap on the wrist”, and for teaching me about his experiences and knowledge acquired in the oil sector. I wish you “Fair winds and Following seas” in your future projects.

Manuel Alfonso.

This thesis is dedicated to my family who always support me, without them I wouldn't be where I am. To my friends who despite the distance always are there for me when needed.

To my supervisors Benja and Kjell, for their patience and guidance during this masters road. And to my thesis partner Mañe for making so much fun this ride. Thank you buddy.

Oscar Patiño

Nomenclature

P&A	=	Plug and Abandonment
AUSMV	=	Advection Upstream Splitting Method
U_{Gs}	=	Superficial Gas velocity
U_{Ls}	=	Superficial Liquid Velocity
BOP	=	Blow Out Preventer
KWM	=	Kill Weight Mud
W&W	=	Wait and Weight
BHP	=	Bottom Hole Pressure
HP	=	Hydrostatic Pressure
MPD	=	Managed Pressure Drilling
MCD	=	Mud Cap Drilling
PMCD	=	Pressurized Mud Cap Drilling
NPT	=	Non-Productive Time
IADC	=	International Association of Drilling Contractors
RCD	=	Rotating Control Device
LAM	=	Light Annular Mud
ECD	=	Equivalent Circulation Density

1 Introduction

The presence of gas bubble inside flow stream during well operations has been a challenge for the petroleum industry since the early 1900's. The need to discover new technologies for well control, arose from the occurrence of incidents known as blowouts. Those consequences are associated with the non-control of inflows during flowing wells.

The bullheading method is an alternative technique for well control pressure operations assuring the correct circulation of gas into the formation, compared with conventional well control techniques. Initially the gas bubbles are confined within the geological formations and migrate to a position with lower restrictions, then the motion occurs moving towards the wellbore space by density difference to the uppermost part of the well. Sometimes the safety equipment is not able to handle the fluid pressures and a different technique must be used. This method is functional when the bubble pressure is expected to be higher than the surface control equipment. The applications vary between well operations like Special Drilling operations, Completion and Plug and abandonment (P&A) among others, however this project was developed to make an approach as the Well Control Method.

The bullheading technique consists of forcing formation fluids back into formation by pumping mud downhole through the string or annulus (*depending on well condition*) monitoring flow rate and pressures to do not exceed safe operative conditions. The main downside of this technique, is if the open hole section is too large. In that scenario there is no real control of where the gas is going to be bullheaded due to the possibility of fracturing another formation which are weaker than the one the kick came from.

The purpose of this study was to build a small scale experimental facility where gas can be injected through an inlet allowing it to migrate a distance during a fixed period of time before being bullheaded down by a certain liquid flowrate. The flowrate needed for this is the critical flow variable that we were to investigate.

Pressure sensors were used to deduct what the negative gas velocity will be, for a given bullheading scenario. The experimental results will be compared with the simulated results obtained by using a transient flow model. This flow model is based on the application of the gas slippage that is taken from literature.

The transient flow modelling uses a mathematical model and a numerical scheme (AUSMV) for fluid dynamics of the bullheading process. The model is based on the

drift flux model using a gas slip relation. The slip parameters were taken from literature and adapted to the geometry. The objective was to find out, which rates were needed to force gas bubbles *downward* and compare this with theoretical results using a transient flow model.

A motivation for this study is the application of the bullheading method through the design and construction of the first laboratory small scale model. This model is applied in the multiphase flow laboratory facilities at the University of Stavanger in Norway. This investigation is divided into experimental and numerical model, being prominent in the experimental model using the results for the application of the numerical model using the calculation of gas velocity, and mass of air through pressure drops.

In chapter 2, the theoretical background is presented describing the multiphase flow in vertical and horizontal pipes, circulating well control techniques and bullheading operations are also described. A detailed description of the experimental process in chapter 3. In chapter 4, the transient drift flux model is presented using a mathematical model and the application of the conservation laws. Results and discussions from the experimental and numerical models are presented in chapter 5. This study ends with conclusions of the successful design of bullhead experiments, and recommendations for improvements in chapter 6.

2 Theoretical Background

Two-phase flow or Multiphase flow system is nearly everywhere, from waterfalls that change part of its current into mist to particles that move through the plasma in our blood, it can be confused as a single-phase flow. In the O&G (*Oil and Gas*) industry multiphase flow can occur while a well is in production, also while drilling a well (a kick scenario can develop).

The single-phase flow is discriminated between laminar and/or turbulent flow; in the same way the multiphase flow is characterized by flow regimes, which depends on time and space distribution for the gas/liquid flow (transient flow conditions). These flow patterns have been studied over the years to understand how they occur, develop and behave with variations in superficial velocities. Nevertheless the final goal is always to assure flow from the reservoir to the surface using well control systems correctly and safely.

2.1 Multiphase Flow in pipes

During the flow of fluids, multiphase flow can occur during production but can also happen when having a kick while drilling a well. There is a variety of flow patterns occurring during the process. During drilling operations unfortunately, it is not possible to identify the flow pattern by direct contact, but along the years with the help of different experimental studies it is known that for both vertical and horizontal wells different flow patterns can be present all depending on the superficial velocities of the fluids involved.

2.1.1 Multiphase Vertical Flow

Figure 2.1 shows a classification distinguished by Taitel and Dukler [Taitel et al., 1980]¹, for a vertical up flow, where the type of flow pattern will depend on the magnitude of the superficial velocities.

From the left to right the composition of the fluid flow varies along with the increase in superficial velocity for each of the phases. The flow pattern can be categorized by the superficial velocities for each of the phases (U_{GS} and U_{LS}) given any pipe size and a set of fluid properties. The classification was made for an air-water system considering the ratios between the fluids of interest.

Taitel and Dukler described a theoretical transition between the flow regimes classifying the velocity ratio of the phases. Figure 2.2 depicts various vertical flow regimes, as a function of the superficial velocities for the liquid and gas phase. The pipe diameter used for this classification was 5 cm with 1 bar pressure and a temperature of 25°C.

¹[Taitel et al., 1978]

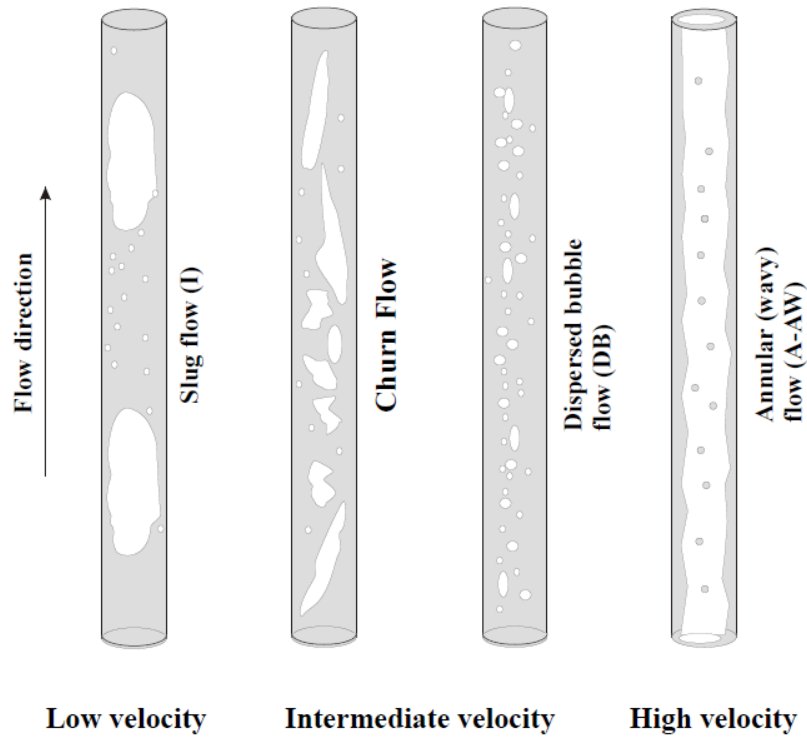


Figure 2.1: Vertical fluid flow pattern for multiphase flow systems [Time, 2017]

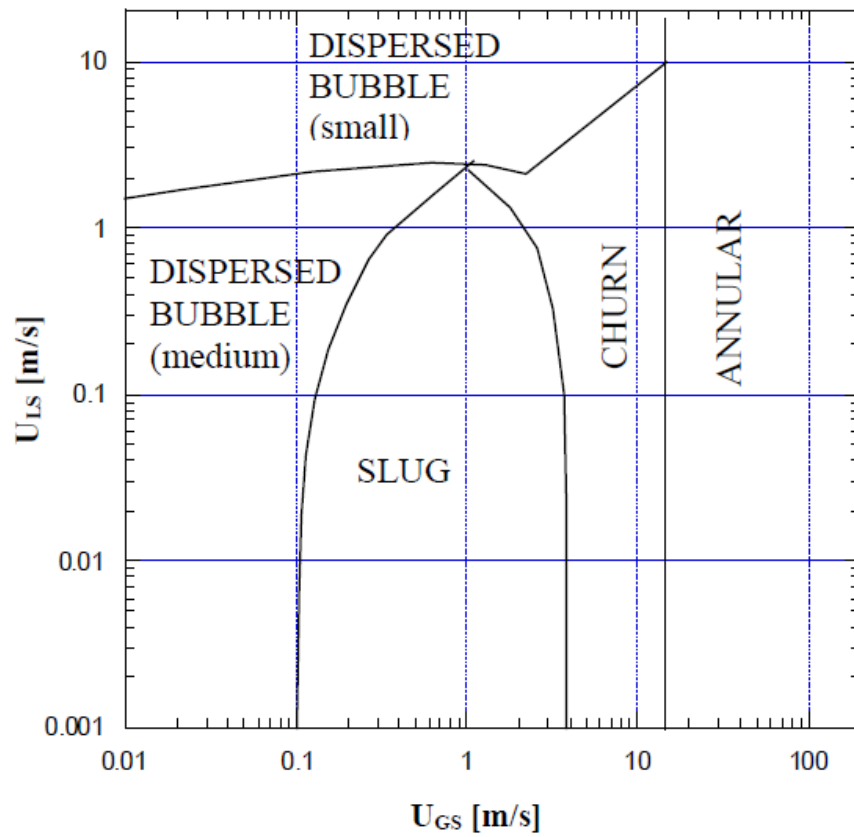


Figure 2.2: Flow pattern map modeled for a vertical 5 cm diameter pipe upflow [Time, 2017]

2.1.2 Multiphase Horizontal Flow

For horizontal flow, gas-liquid flow behaves differently with respect to flow patterns. There are six flow patterns as shown in Figure 2.3. The flow pattern is the result from the liquid-gas distribution in the tube, shifting from steady state conditions to transient flow conditions.

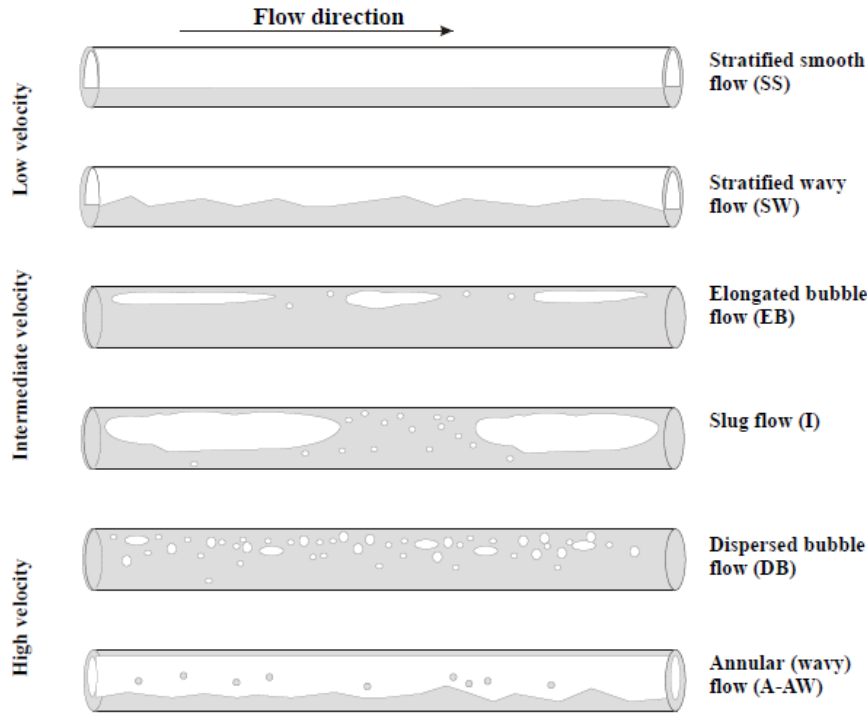


Figure 2.3: *Horizontal fluid flow pattern for multiphase flow systems*
[Time, 2017]

The horizontal flow patterns also can be classified as the vertical flow using the superficial velocities for the liquid and gas phase. Figure 2.4 shows the classification using the Mandhane plot, with higher initial velocities compared with vertical flow superficial velocities for each of the phases (horizontal superficial velocities are ten times higher than vertical superficial velocities). It was observed experimentally for a pipe with internal diameter 2.5 cm according to these authors.

The fluid is characterized by possessing different physical properties, for instance: volume of liquid or gas occupied on a predefined space, temperature of the system, viscosity, velocity of the phases, density of each phase, superficial tension, etc. It is possible to predict the fluid behavior monitoring their physical properties using flow models in situations where it is not feasible to be in direct contact with the fluid.

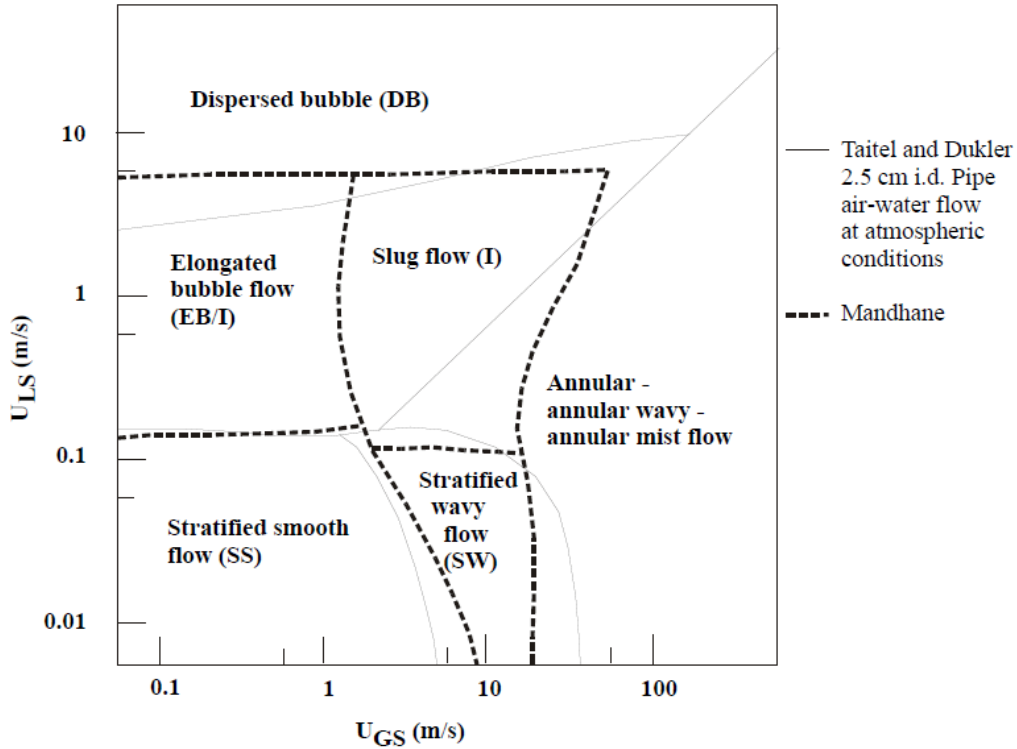


Figure 2.4: Flow regimes map in horizontal two phase flow [Time, 2017]

2.2 Well Control

Well control methods are operational techniques to prevent or minimize the potential release of uncontrolled pressurized fluids (known as kicks) coming from the wellbore to the surface. If those fluids are not controlled and reach surface can produce a blowout. A blowout is defined as an uncontrolled flow of fluids from the wellbore to surface and can happen at different stages of the life of a well with catastrophic consequences including human lives.

Well control applies for different operations: Drilling, Well Completion, Workover and P&A (*Plug and Abandonment*); in other words, the main objective is the pressure control during the lifetime of the well specially during Drilling operations. The next subsections describe the circulating techniques and the Bullheading applications for different operations.

2.2.1 Circulating Well Control Techniques

These methods are commonly practiced for kicks circulation, monitoring the bottom hole pressure to establish a steady circulation rate to displace the kick up to the surface through the kill line. The kill fluid is pumped from surface through the drillpipe displacing the kicks within the flow direction as shown in Figure 2.5. The arrows indicate flow direction.

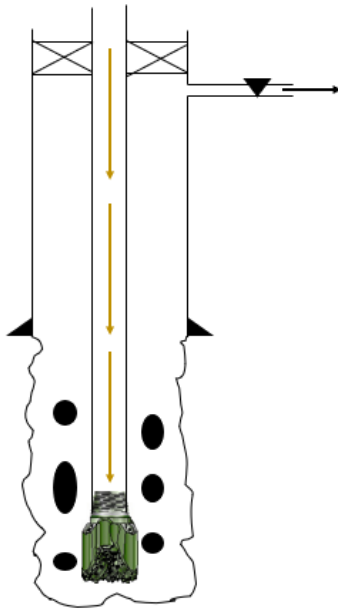


Figure 2.5: *Kick circulation to surface using killing fluid*
 [Koederitz, 1995]

Figure 2.6 is an example of a typical pressure gradient mud profile, for different mud weight design. The hydrostatic pressure and the dynamic pressure must be lower than the fracture pressure and higher than the pore pressure to be ideally within the drilling window to avoid kicks and well collapses.

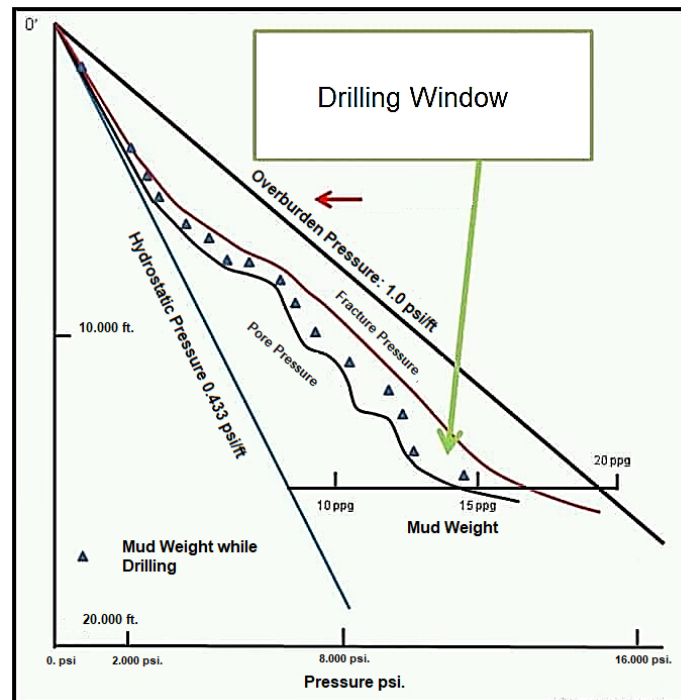


Figure 2.6: *Pressure gradient mud profile*
 [Ortiz, 2019]

The x-axis represents pressure of the system in pounds per square inch ($\frac{lb}{in^2}$) and the y-axis represents the well depth in feet (ft) for a casing setting design. The mud weight is gradually increased as the well is being drilled. Also in Figure 2.7 an example of one of the causes of a kick can be seen. This is known as swabbing and can be produced by pulling out of the hole the string too fast, creating a suction that allows the formation pressure to be higher than hydrostatic thus allowing formation fluids into the wellbore (*kick*).

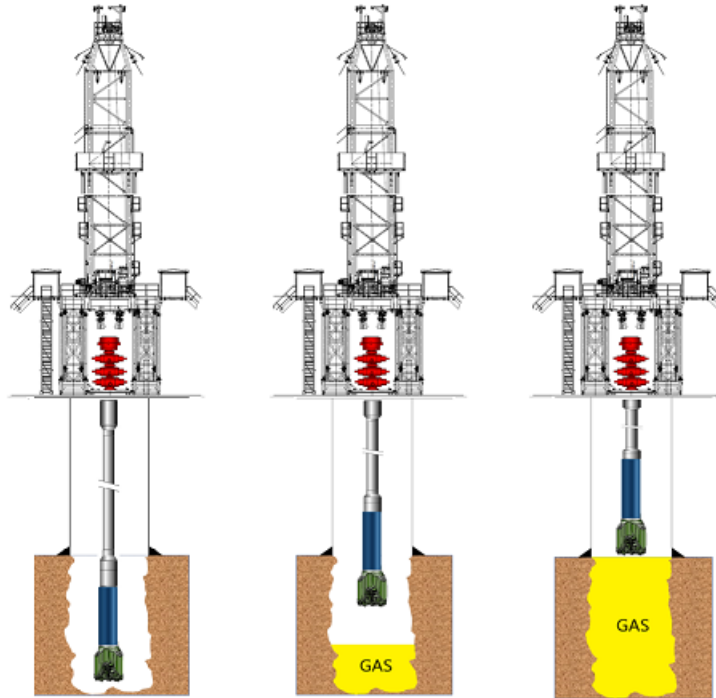


Figure 2.7: *Gas kick appearance by swab effect*
[Lyons et al., 2015]

- **Drillers Method^{II}**

This is one of the most used methods for well kicks handling, due to its simplicity and reduction in time to start the process. The kicks can occur due to multiple reasons. For instance, when tripping out a swabbing effect can occur where the pressure in the well is reduced such that a kick is taken.

This method consists as follows: once the kick is detected the BOP (*Blow Out Preventer*) is closed and let pressure build-up. Pipe and choke pressures are recorded. Kill sheet is updated and recalculated for the required parameters. Using this method, the kick is circulated out of the well keeping bottomhole pressure fixed. The choke pressure is used to control this.

^{II}[API,]

Two circulations are required for this procedure. The 1st circulation is performed with the same drilling fluid to take out the kick to surface, always taking care to not exceed the critical pressures when the kick pass the casing shoe and reach surface. Once the kick is out of the well, the 2nd circulation start with the kill weight mud (KWM). As the KWM is pumped, the Drillpipe pressure goes down due to hydrostatic relief, when reaching the bit, it start to be constant as the KWM goes up through the annulus, the choke pressure goes down. If at the end of the circulation schedule the choke pressure is not zero, it means that probably there is a new kick or miscalculations on the circulation schedule were made. Utmost care have to be taken while planning those control stages. Figure 2.8 shows the pressure behavior during this procedure.

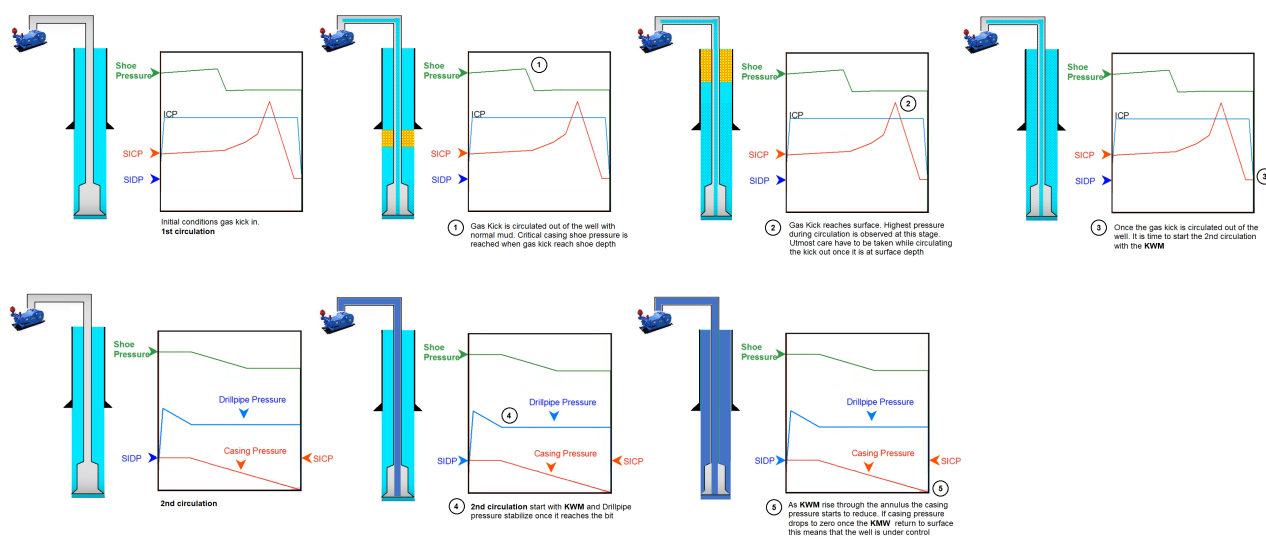


Figure 2.8: *Driller's method pressure profile during circulation*
[Brasil, 2020]

- **Wait and Weight Method (W&W)**

This is also known as the Engineer Method. The well is shut in when the kick occurs. Shut in pressures are recorded. The kill mud density is calculated and the mud weight is increased before kill circulation starts.^{III}.

With the W&W method, the kick is circulated out of the well and the well is controlled in one circulation instead of two as the *Driller's method*. Once the circulation of the KWM start, utmost care have to be taken when the kick is passing through the casing shoe to avoid fractures. Once again when the KWM return to surface through the annulus, the casing pressure should go down to zero meaning that the well is under control. Most companies prefer to use Driller's

^{III}[API,] pp. 11

method instead of W&W, to avoid risks for collapse or stuck pipe incidents for keeping the string static while the mud system weight is increased. Figure 2.9 illustrates a well being killed by the Wait and Weight method where the kill mud is first displacing the drillpipe and then the annulus.

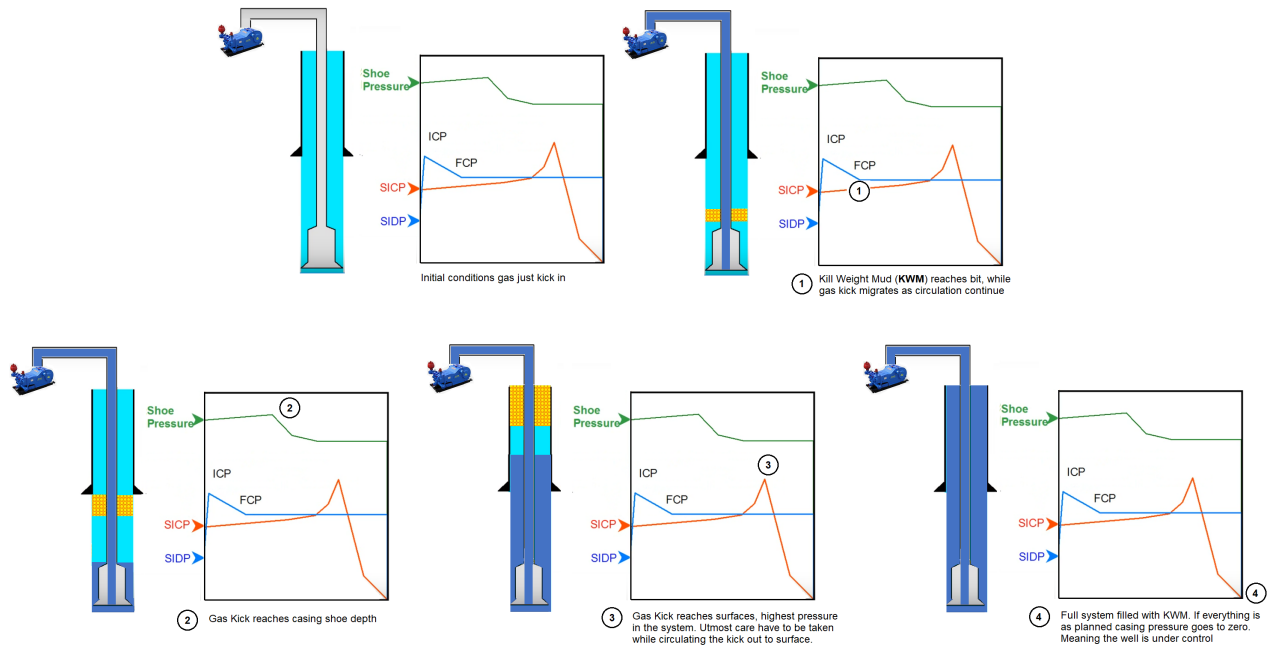


Figure 2.9: *W&W method pressure profile during circulation* [Brasil, 2020]

• Concurrent Method

Also known as Slow Weight-up Method, it is designed to circulate the gas kick out with a mud weight that is gradually increased. The well is closed in when the kick is detected, the circulation is resumed as soon the pressure stabilizes. The drilling fluid increases the weight by the addition of weight material as soon the circulation has started, the rate at which the fluid density increases depends on the rate which the weight material is being added. The fluid circulation is established with predefined parameters because of gas expansion in the annulus space, the drillpipe pressure must be controlled to keep the bottom hole pressure balanced; when the drillpipe volume is displaced by kill mud, the pumping pressure is maintained constant until kill mud reaches surface.

• Volumetric Method

It is a gas expansion controlling technique that allow gas to migrate, while replacing the increase recorded in choke pressure for an equivalent volume of mud in the annular to control the bottom hole pressure (*BHP*), keeping it constant.

In this method the increase in hydrostatic pressure does not occur by growth in fluid weight, but by fluid replacement. Some of the situations this method can be used: Stuck pipe, Snubbing operations, Shut-in periods where the surface or downhole equipment needs to be repaired.

2.2.2 Bullheading Applications

The Bullheading technique is based on trying to force the kick fluids downwards in the well back into the formation. It is applied until the influx is displaced into the exposed open hole formation and the well is filled with kill fluid to control the reservoir pressure (*Details on this technique will be discussed later*) the fluid circulation rate must be enough to overcome the gas migration.^{IV}

The Bullheading can be applied for well control, production/intervention and for special drilling operations: Managed Pressure Drilling (MPD) and its variants known as Mud Cap Drilling (MCD), and Pressurized Mud Cap Drilling (PMCD).

• Bullheading during drilling operations

Bullheading operations are applicable for the drilling process when well control incidents occur. As discussed on previous chapters, the Bullheading technique is an alternative when the conventional well control techniques like the Driller's Method and the Wait and Weight method, cannot be applied *e.g. when the pressures becomes too large for the well to handle.*^V

One of the main factors for which the Bullheading technique is selected, is the capacity to handle large influx volumes into the well, and it avoids the high pressures that can occur in the well with conventional well kill methods. Nevertheless, with the application of bullheading some factors should be considered: one of them is the pressure management at the casing shoe, because it is a critical weak spot where one should avoid to fracture the formation.^{VI} Some of other factors influencing the technique selection are:

- Circulation unavailability due to stuck pipe (by Pack-off).
- Bit tripped out.
- Gas kicks with sulfides are risky.
- Excessive pressures downhole or at the surface.
- Unavailability to handle high gas volumes at surface.

^{IV}[Ghauri et al., 2016] pp.1

^V[Ghauri et al., 2016] pp.2

^{VI}[Sun et al., 2014] pp.10

In general, the bullheading technique for drilling operations require a high internal pressure casing strength to avoid casing burst. A rule of thumb suggests that the maximum well head pressure should not exceed eighty percent of the casing strength according to well control.^{VII} Figure 2.10 is an illustration when a kick is forced downwards into the annulus and back into e.g. a fractured formation.

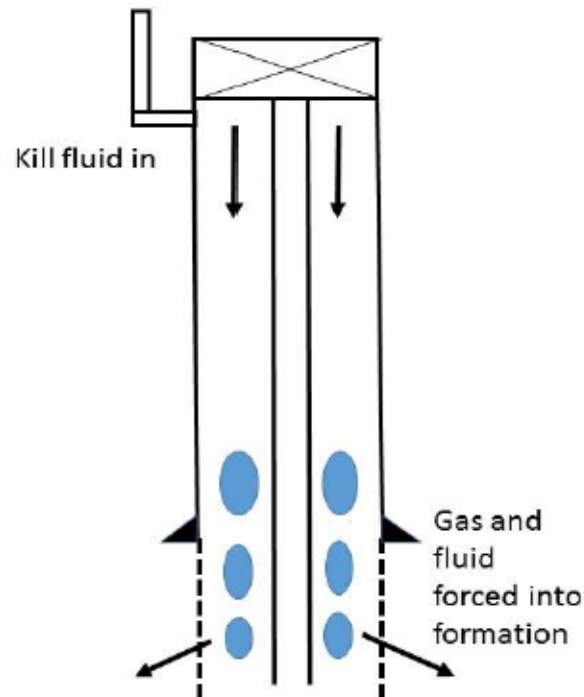


Figure 2.10: *Bullheading a well through the annular*
[Ghauri et al., 2016]

- **Bullheading during Well production / Well intervention**^{VIII}

As discussed before, bullheading operations can also be applied for production wells prior to workover operations. A live well in some cases has to be killed before workover. One of the techniques that can be used for this is bullheading. Being a production well operation, the bullhead technique consist of pumping fluids through the production tubing downhole. Since production well is full of hydrocarbons, the first step is to circulate seawater to force the hydrocarbons back to the reservoir. Then the kill pill replaces the sea water for the first circulation step to block the formation pores, followed by a denser brine or a heavy kill fluid.

The main function of the kill pill is to plug the pores such that the fluids do not migrate into the formation. The kill pill and the dense brine must create

^{VII}[Sun et al., 2014] pp.11
^{VIII}[Ghauri et al., 2016] pp.2

enough hydrostatic pressure to keep the wanted hydrocarbons inside the formation. Figure 2.11 illustrates the situation where a production well is killed through a conventional string.

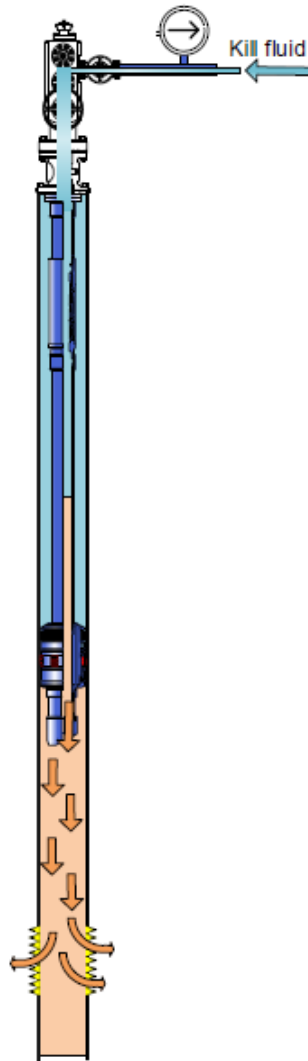


Figure 2.11: *Bullheading a well through tubing string*
[Crumpton, 2018]

Figure 2.12 depicts different zones for the bullheading operation, the kill fluid is pumped inside the tubing and traveling through three different zones (from bottom to surface):

1. The gas zone contains mainly gas during the kill process; the length should decrease gradually as the kill operation progress.
2. The transition zone contains gas and liquid which grow as more liquid arrives to the formation zone. The gas bubbles tend to move upwards against the flow by density differential.
3. The liquid zone contains only kill fluid moving downward. Here the gas is swept away and the kill is completed. The gas zone and the liquid zone are

characterized as single-phase fluid zones.

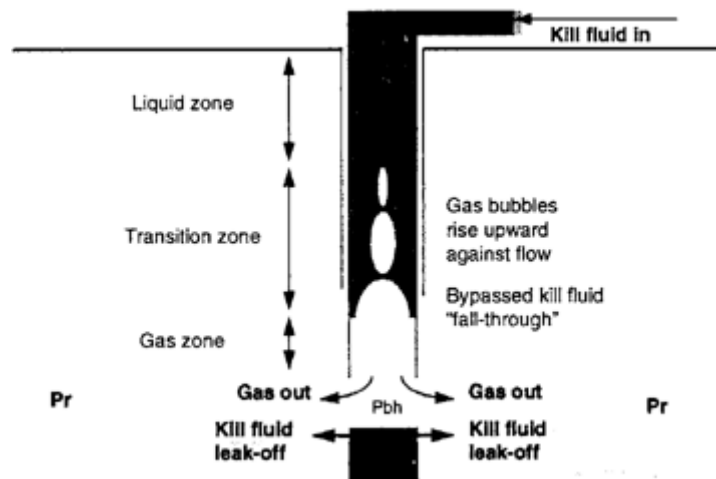


Figure 2.12: *Bullheading process for a production well*
 [Pieter et al., 1994]

- **Bullheading for special drilling operations**

The special drilling techniques described are a result of different drilling challenges that occur when there is a large potential for huge drilling fluid losses. These can typically occur when drilling in fractured carbonated formations where one also can encounter karst structures. In the next section, a description of some special drilling systems developed for handling difficult well prospects are discussed, with special focus on Pressurized Mud Cap Drilling (PMCD) where the application of Bullheading is part of the standard procedure used when carrying out this kind of operation.

- **Managed Pressure Drilling (MPD)**

Managed Pressure Drilling is a technology to address well drilling challenges. The application of the MPD lies on make it possible to drill wells with narrow drilling window (Figure 2.6) by making use of different techniques ranging from controlling circulation friction to adjusting mud density.

The Underbalanced Operations and Managed Pressure Drilling Committee of the International Association of Drilling contractors has defined the MPD “an adaptive drilling process used to precisely control the annular pressure profile throughout the wellbore. The objectives are to ascertain the downhole pressure environment limits and to manage the annular hydraulic pressure profile accordingly. MPD is intended to avoid continuous influx of formation

fluids to the surface. Any influx incidental to the operation will be safely contained using an appropriate process”^{IX}.

The main objective is for well prospect with very narrow margins between formation pore pressure and the formation fracture pressure for those wells, which are not drillable in a conventional method. The MPD technique objectives are the mitigation of risks associated with drilling operations (Lost circulation, stuck pipe, Wellbore instability and Well-control incidents). These problems are associated with the increase of NPT where the MPD application can increase the operational efficiency diminishing the NPT^X.

– **Mud Cap Drilling (MCD)**

The Mud Cap Drilling is a variant of the MPD for lost circulation matters. The principle here is the circulation of two drilling fluids (one as a sacrificial fluid and the other as a mud cap). The fluid pumped through the annular can be heavy mud or sea water, circulated until reaching a specific height (normally below the previous casing shoe) acting as an annular barrier, and the lightweight sacrificial fluid through the drillpipe. the sacrificial fluid carries all the cuttings into the formation where nothing returns to surface. The heavy mud remains in the annulus as a “mud cap” above the affected zone for the sacrificial fluid. The main goal is to keep the heavy mud in the annular side without provoking a backpressure or circulation returns.^{XI}

– **Pressurized Mud Cap Drilling (PMCD)**

When drilling through highly fractured carbonate formations, huge fluid losses can occur. These losses generate nonproductive time (*NPT*) and therefore extra costs. A technology to avoid this, is named Pressurized Mud Cap Drilling (*PMCD*). The IADC defined the PMCD as “*a variation of MPD that involves drilling with no returns to surface and where an annulus fluid column, assisted by surface pressure [made possible with the use of a rotating control device (RCD)], is maintained above a formation that is capable of accepting fluid and cuttings. A sacrificial fluid with cuttings is accepted by the [lost] circulation zone. This technique is applicable for cases of severe [lost] circulation that preclude the use of conventional wellbore construction techniques.*”^{XII}

^{IX}[Gedge et al., 2013]

^X[Malloy, 2007]

^{XI}[Malloy, 2007] pp.3.

^{XII}[Gedge et al., 2013] pp.3.

The PMCD technique also uses a sacrificial fluid called Light Annular Mud (LAM). The sacrificial fluid is also lost within the formation along with the cuttings. The PMCD is a MPD variation but an improvement of the MCD to operate with thick fractured formations. The annular fluid above the formation fractures is controlled using a Rotary Control Device (*RCD*) which keeps the well-sealed on top to create a backpressure from open to a closed system (pressurized annulus). The RCD can identify kick migrations events since the pressure at the RCD will start to increase if a kick starts migrating in the annulus. However it is important to avoid the kick migration to the surface since the RCD cannot handle large kick pressures after a certain increase, the annulus will be Bullheaded using (LAM) that fills the whole well fluid column, and the kick will be forced back into the fractures.

Some of the differences between the MCD and the PMCD lies on the well pressure balance. With the MCD the well is open to the atmosphere thus a latent risk of overbalance is present that may cause a higher fluid loss as the drilling continues. Figure 2.13 is a comparison visualization between the MCD and the PMCD techniques. The PMCD reduces the risk of fluid loss, monitoring the pressure on top using a surface device and achieving a pressurized annulus resulting in a reduction of drilling costs in extreme-loss situations.

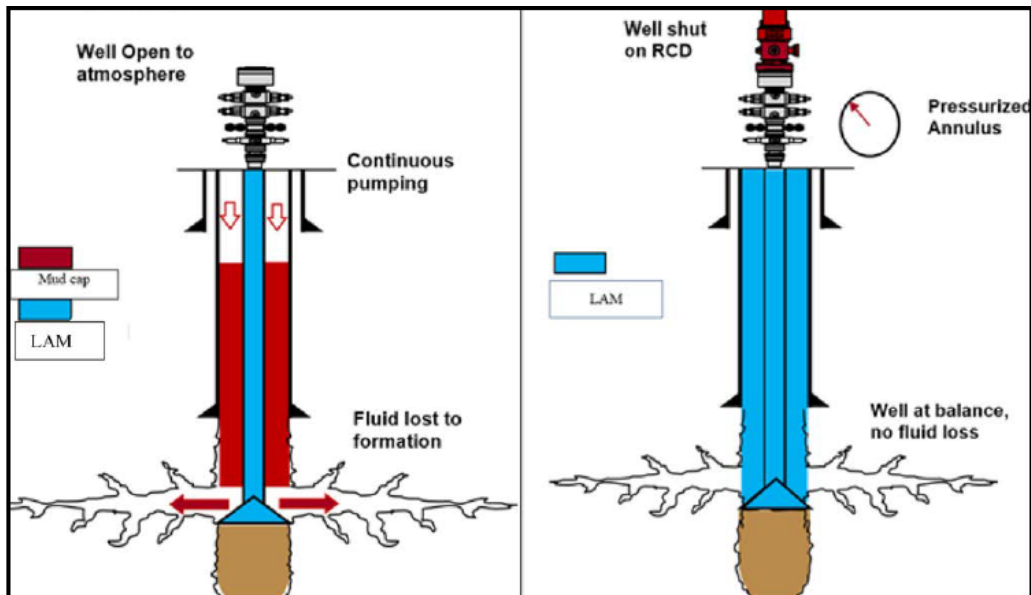


Figure 2.13: *Differences between MCD and PMCD*
 [Al-Otaibi et al., 2020]

3 Experimental Investigation of the Bullheading Process

In this work, main focus has been on developing a small scale experimental setup to investigate gas migration and the bullheading process. From the experimental setup and conditions the following can be observed:

- Temperature of the system is fixed, i.e. room temperature.
- Only Newtonian fluids will be considered (water and air).
- Two types of flow patterns can be seen from the experiments (slug flow and dispersed bubble).
- The geometry will be a uniform vertical pipe.

In the following section the experimental model describes the laboratory set-up process, the equipment installation for the experiment, equipment calibration and procedure, the measurement of the physical properties using the PASCO software and direct visualization. The experiment includes the visual observation of the multiphase flow pattern, the gas bubble migration effect and the physical interaction between gas-liquid flow.

3.1 Experimental set-up for the bullheading Investigation

An initial set up was installed using the tools available in the laboratory. During the laboratory work new attachments were included to give a practical and a correct function of the system.

Figure 3.1 illustrates the initial laboratory set-up including the changes throughout the practice after different hydrostatic tests. The set-up was improved to obtain a close loop system avoiding leakages and decreasing the probability of pressure losses.

The gas bubbles were injected to simulate gas migration from the gas inlet by using a two way valve attached to the system and causing a Slug flow which was identified with direct visualization; the bubbles were found of different sizes and after different observations the bullheading process was not able to be effective using the original set up. Therefore, a second design was sketched by adapting new equipment to the set-up for bullhead the experiments.

3.1.1 Equipment Installation

As seen in Figure 3.3 the system consist of:

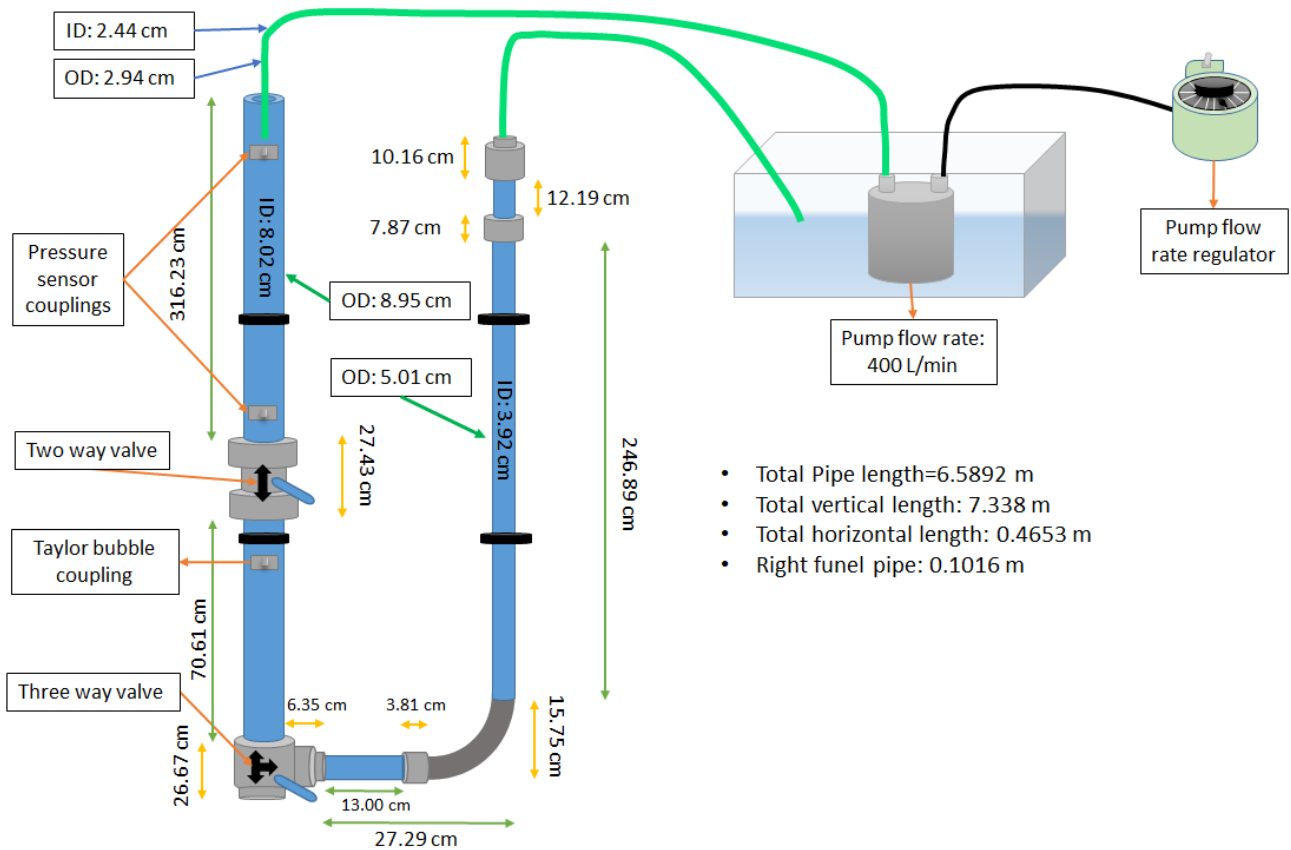


Figure 3.1: *Initial laboratory Set-up*

- Two acrylic glass tubes of 3 m height with different diameters ($ID_1 = 8.02 \text{ cm}$ - $ID_2 = 3.92 \text{ cm}$).
- A Honeycomb filter placed in top of the small pipe.
- A 90 degrees elbow to change the flow direction of the system.
- Three way ball valve from the bottom.
- Two funnels connected to the inlet and outlet of the system.
- Four threaded sensor couplings attached to the pipe.
- Four flexible silicone hoses to send the real time pressure data.
- One centrifugal pump with operative specifications (95 l/m, 12 V, 9 A).
- DC High current power supply (SPS-9602) - (Output Voltage/Current - 1-30 V / 30 A).
- A tank filled with Newtonian fluid.
- Two silicone hoses to connect the inlet/outlet of the system.
- Pressure transducers (PASCO Dual Pressure Sensor - PS-2181).
- PASCO Capstone software for monitoring the pressures.

Note: *PASCO* is a software tool used as datalogging solution using sensors, interfaces, data collection and software analysis. Figure 3.2 illustrates the PASCO

solution tools for data acquisition, allowing users to display the required data according to the sensor used.



Figure 3.2: *PASCO Capstone interface*

3.1.2 Practical tests

Experimental tests are important to obtain reliable results. This must be ensured before comparing experimental results.

The first tests were carried out to check the efficiency of the pumping system. These tests consisted of equipment calibrations for flow rate and absolute pressure monitoring. The equipment calibrations consisted of the direct use of the pump; thus, the pump efficiency was measured with a fluid filling process using different methods. The ideal pump flow rate capacity is 1.5 l/s at the maximum power supply of 12.5 V or 9 A. The tests were made using two methods:

1. The first method consisted of two vessels one filled with water and the other empty, the main goal was to pump water from one vessel to the other to reach a reference in volume of 20 liters. The procedure involved a variation in the voltage adjusting the flow rate of the pump monitoring the current of a power supply. The flow rate test had been performed with an initial power value of 4 volts to the maximum voltage the pump can support without any damage (12.5 V), increasing the voltage in steps of 1 volt monitoring the time it takes to reach the reference volume of 20 liters. The data are in the Appendix.
2. The second method was practiced pumping water between two vessels but this time using an electronic weight scale to measure the difference in weight (before and after the operation) gauging the time it took to reach a specific level. This time, the mass rate difference is measured and compared from a reference weight of 16 Kg (*initial weight*), subsequently the flow rate is calculated dividing the mass rate difference with the water density which is constant. Equation 3.1 is

the representation of the flow rate calculation changing the voltage from a minimum supply of 4V up to 12V with steps of 0.5V approximately. The data are in the Appendix.

Figure 3.3 is the representation of fluid pumping in the two different methods, to observe the operation of the equipment in different practices.

$$Q = \frac{\Delta \mathcal{M}}{\rho} \left[\frac{\frac{Kg}{s}}{\frac{Kg}{m^3}} \right] \quad (3.1)$$

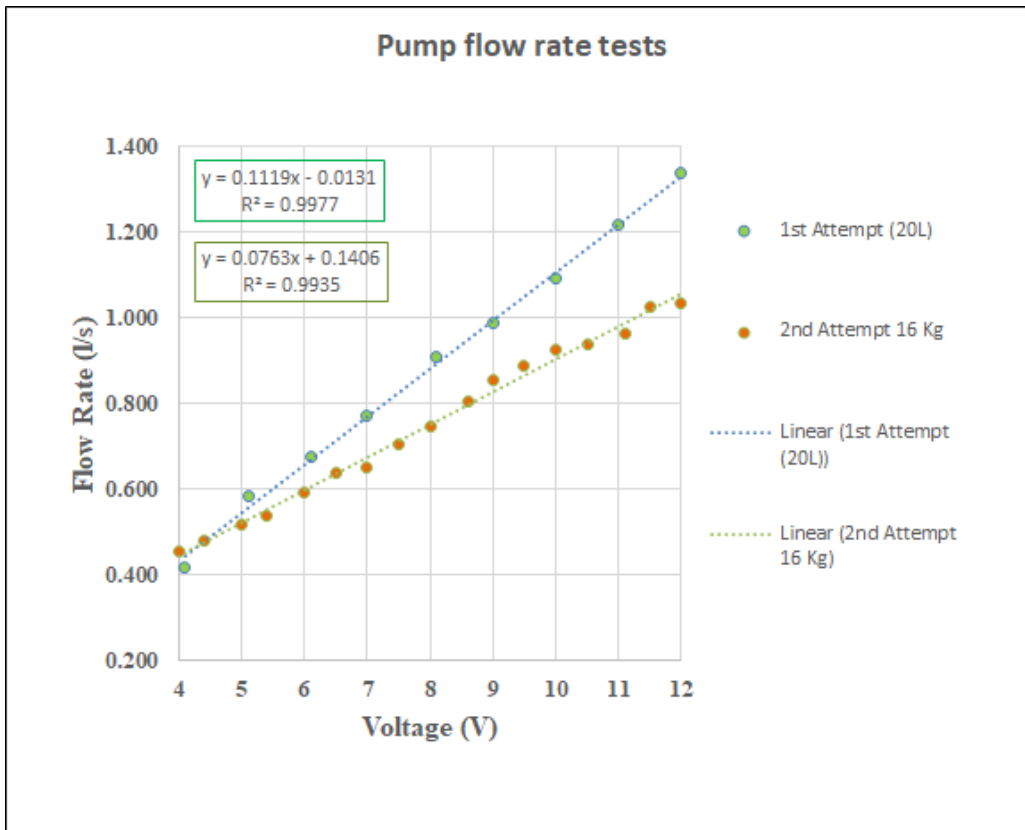


Figure 3.3: Flow rate pump test with power supply variation

Comparing the two methods that were performed it showed a linear tendency of the system from an initial value of 4V up to 12V. However, it can be seen a power difference comparing the maximum voltage obtaining an approximate difference of 0.3 l/s. The real flow rate efficiency is calculated comparing the ideal pump flow rate with the apparent flow rates for each of the tests. Accordingly the first method showed the best linearity with a maximum flow rate of 1.33 l/s, even though the second method was measured using a calibrated weight scale with a constant initial weight of 16 Kg and lastly obtaining a flow rate 1.03 l/s. The calculated efficiencies were 88.7% and 68.8% respectively, this shows that the pump is working with an efficiency of nearly 70%.

The efficiency was calculated with a rule of three using brand new pump specification (1.5 l/s) and comparing with the pump output calculated with each method.

Method #2 was decided as the way to go due to some discrepancies while performing method #1 e.g. when the pump was shut down the pump keep sucking for gravity and was difficult to have a proper reading of what was the real volume pumped and what was sucked after shut down. While option #2, the reading was immediately recorded after a fixed period of time pumping thus reducing the uncertainty of the pump sucking after being shut down. The difference between the two attempts, lies on the direct measurement of the test using a constant reference value monitored directly from an electronic device and the amount of data obtained to produce a more accurate response.

The monitoring of the absolute pressure is essential to obtain a real value with the intention of being compared with the theory, therefore the pressure obtained from the sensors must be calibrated. The pressure data obtained from the sensors, are the result of the sum of different effects affecting the results. The change in pressure data are small, but highlighting the set-up size, it is important to monitor these small variations. The calibration of the pressure sensors involved the theoretical calculation of the hydrostatic pressure combined with the atmospheric pressure (absolute pressure) for each of the sensors for a better data resolution. The atmospheric pressure was taken from the laboratory pressure gauge to calibrate the absolute pressure sensors.

Figure 3.4 shows the laboratory set-up sketch with the height and diameters to calculate different properties of the system as: volume of the gas, hydrostatic pressure. these data must be used in the flow model so one can compare the experimental results with the theoretical model for gas slip.

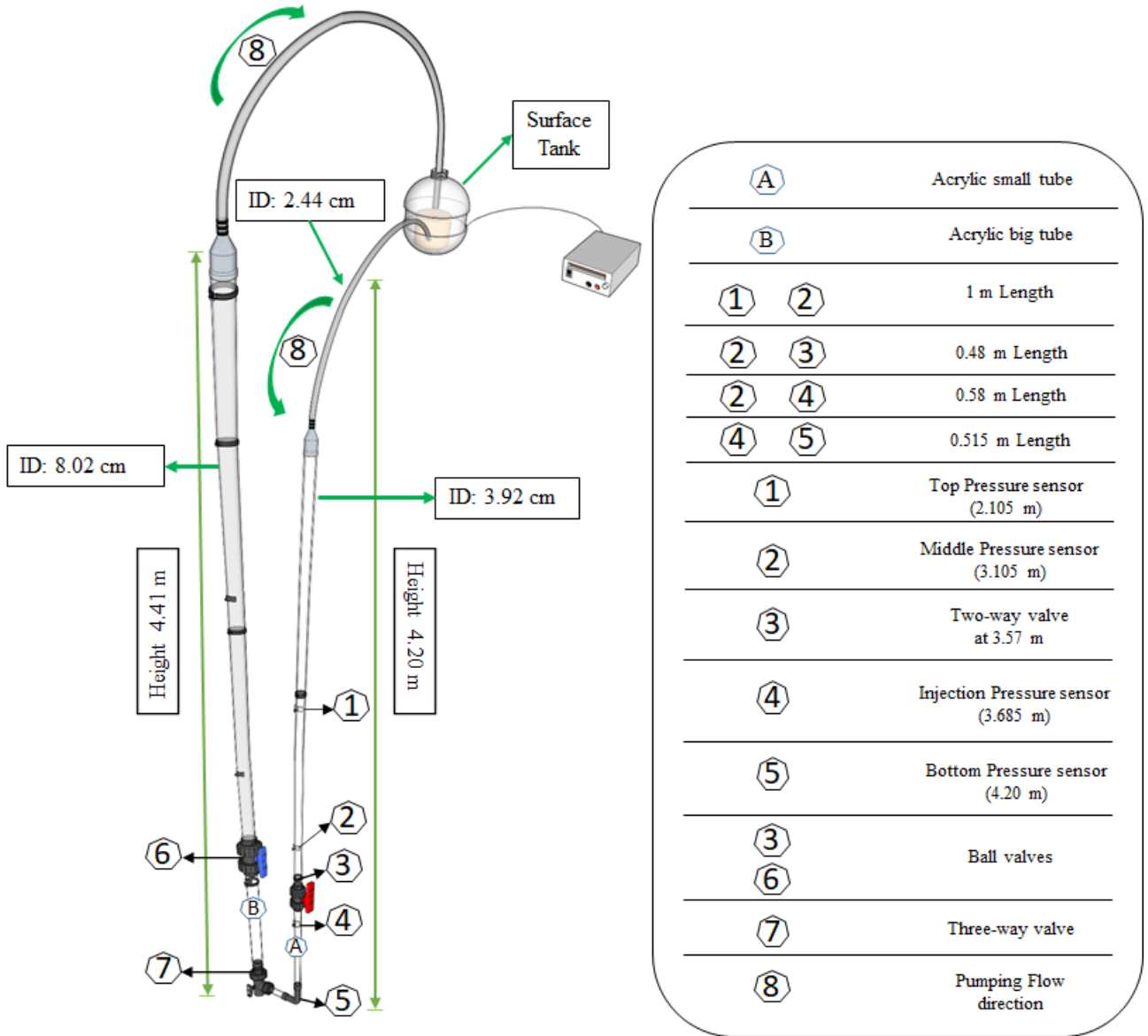


Figure 3.4: Sketch of the final set-up in 3D

Equation 3.2 shows how the hydrostatic pressure from the sensors is calculated, using the density of the fluid in the system, the gravity and the height where the sensors are located. The sensors used in the setup are absolute pressure sensors thus the value of hydrostatic pressure is calculated, the atmospheric pressure must be added to have the correct values.

$$HP \left(\frac{N}{m^2} \right) = \rho \left(\frac{Kg}{m^3} \right) * g \left(\frac{m}{s^2} \right) * h(m) \quad (3.2)$$

Table 3.1 is the pressure summary for all the pressure sensor locations, considering that the hydrostatic pressure changes when the column height varies.

In every test all the sensors are calibrated with the calculated static conditions for

Table 3.1: Absolute pressure for each sensor

Properties	Sensors					
	Top	Middle	Differential	Inj.	Bottom	Differential
Height (m)	2.105	3.105	1.00	3.685	4.20	0.515
Hyd. Pressure (kPa)	20.65	30.46	9.81	36.15	41.20	5.05
Abs. Pressure (kPa)	123.08	132.89	9.81	138.58	143.63	5.05
Press. (mbar)	1230.79	1328.89	98.1	1385.79	1436.31	50.52

hydrostatic pressure according to the values in Table 3.1. The actual atmospheric pressure was taken at the moment in the laboratory.

3.2 Flow loop of the experimental process

It is important to design an experimental procedure considering the different challenges of direct measurement of the physical properties. These challenges are linked to different inaccuracy; for instance: calibrations, monitoring of physical properties, gross errors and systematic errors that affects the obtention of valid results.

3.2.1 Experimental procedure

In this section the experimental bullheading process is explained using the set-up described on Figure 3.4. The procedure consists of the following steps:

1. PASCO Capstone is configured. Pressure recording begins.

2. Both ball valves (3) and (6); must be open to allow fluid to pass through the system, as well the Three-way valve (7) must be in this position \perp to avoid drainage of the system.

3. The surface tank must be filled with water preferably 10 cm above the intake of the pump to avoid suction of bubbles directly coming from the return hose. Circulate liquid through the acrylic tube (A), and receives the fluid coming out from the tube (B), to purge any trapped air bubbles and ensure that the system is filled with water. Then stop circulation.

4. Calibrate pressure sensors with the atmospheric pressure under laboratory conditions and the calculated hydrostatic pressure using the data from **Table 3.1**.

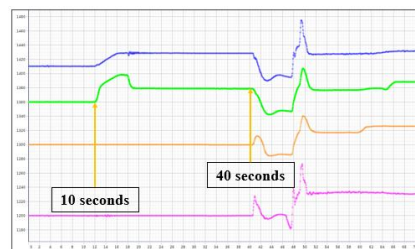
5. The next step is to close the red valve (3).



6. Open the air inlet valve around the 10 sec. and let the air displace the liquid column bellow (4) until the *Injection Mark*. The amount of displaced liquid is supported with a pressure difference visualized in the software pressure recording.



7. Wait until second 40 to open the valve and allow the pressure to stabilize.



8. Open red valve (3). The air bubble migration effect can be seen through the translucent acrylic tube. Taylor bubble migration begins.



9. The bubble is allowed to migrate to a second mark previously measured which gives the migration reference for 6 seconds.



10. The pump is turned on at the voltage determined for the test being evaluated. It pumps liquid downward through the tube (A). If the flow rate is low, the gas will still migrate upwards creating a countercurrent flow situation. If the flow rate is sufficiently large the Taylor bubble will start moving downwards.

11. Bullheading is performed until the bubble completely passes the injection sensor. The experimental attempts should be repeated several times varying voltage supply to study the results with different flow rates.



12. Stop pump and sensor recording.

3.2.2 Software and Physical properties monitoring

As discussed previously, “PASCO Capstone” is used to facilitate the monitoring of the physical properties; “*it is an advanced program for data collection, display and software analysis*”^{XIII}. It can be complemented with a wide variety of sensors ranging from Thermodynamics to Atomic & nuclear sensors all very sensitive to small changes in the properties measured.

For this experimental work, PASPORT Dual Pressure Sensors were used (“*Dual pressure sensors are a device capable of reading two absolute pressures, one gauge pressure, or one differential pressure. Dynamic variable over-sampling automatically reduces the measurement noise at low sampling rates. Sample rates up to 1000 Hz make studies of both transient and steady-state pressure possible*”)^{XIV}. These were attached to measure the hydrostatic pressure combined with the atmospheric pressure of the system. the sensor requires the Capstone software for data collection and analysis to display the data information.

The pressure sensor devices are connected to the transparent tube (A) using capillaries for a direct visualization. These tubing allows the measurement of the absolute and differential pressure for the flow inside the system. In total two dual pressure sensors were installed for four pressure tubing inlets as seen in Figure 3.4 (1, 2, 4 and 5). The theoretical hydrostatic pressure of the system differs from the measured pressure due to the presence of different effects that alters the real pressure of the system, probably these effects are linked to pressure loss due to capillary action and friction, which makes difficult the intrusive measurement of the fluid properties.

^{XIII}[PASCO, 2020]

^{XIV}[PASCO, 2020] Product Summary

4 The Transient Drift Flux Model

In order to be able to model two-phase flow, a mathematical model is needed. It can either use a 1D two fluid model or a simpler 1D drift flux model. One can also choose between studying steady state situations where there are no time variations or transient flow where time variation occurs. The Bullheading process is transient in nature hence a transient flow model is needed.

The mathematical model obtained will typically be a system of nonlinear partial differential equations that has to be solved by an appropriate numerical method. In this thesis, the Advection Upstream Splitting Method (AUSMV) scheme will be used for solving the transient 1D drift flux model.

4.1 Conservation Laws

The drift flux model has based on conservation laws for mass, momentum and energy. If the system is been assumed with a fixed temperature and isothermal conditions, one can neglect the conservation law for energy. The model consists of mass conservation law for each phase and a mixture momentum equation. It must be supplied by sub models for the physical properties for each phase, i.e a model for phase density, gas slippage and friction.

The Drift Flux Model must be supplied by a gas slip relation which describes the gas motion relative to the liquid. The gas slip relation is very dependent on which flow pattern that is present in a certain location. Hence, there is a need both to be able to predict what kind of flow pattern is present at a certain depth of the well and a suitable model for how gas moves relative to the liquid for the specific flow pattern. This model will be important if we shall simulate the bullheading process and compare this with the experimental results.

The drift flux model to be presented here consists of two mass conservation laws (one for each phase) and a mixture momentum equation.

4.1.1 Conservation of Mass

The conservation of mass is described by the application of partial differential equations for each phase formulated across a segment.

Figure 4.1 shows a production well with flow in one direction (x) along the production tubing. The tubing can be discretized in different cells and the mass conservation principles can be applied for each phase and for each of the cells. These are formulated as partial differential equations and they are shown in Equation 4.1 and Equation 4.2.

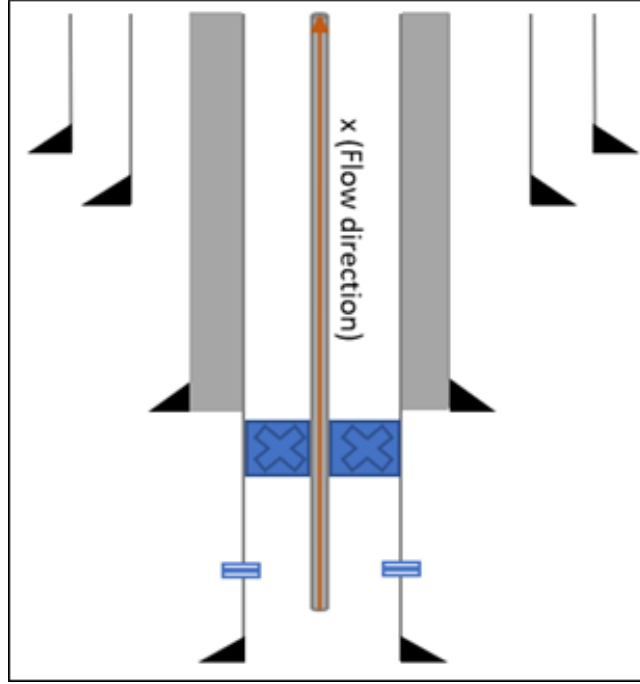


Figure 4.1: Mass conservation in a production well

$$\frac{\partial}{\partial t}(A\rho_l\alpha_l) + \frac{\partial}{\partial x}(A\rho_l\alpha_l\nu_l) = s1 \quad (4.1)$$

$$\frac{\partial}{\partial t}(A\rho_g\alpha_g) + \frac{\partial}{\partial x}(A\rho_g\alpha_g\nu_g) = s2 \quad (4.2)$$

$$\alpha_l + \alpha_g = 1 \quad (4.3)$$

In the equations above assuming there is no mass exchange between the gas and the liquid $s1 = s2 = 0$. It is important to highlight that the energy equations are neglected assuming that the temperature is a fixed variable (constant).

The mass conservation involves: (A) - area in (m^2), (ρ) - density in ($\frac{Kg}{m^3}$), (α) - phase volume fraction, and (ν) - velocity ($\frac{m}{s}$) for each phase.

Equation 4.3 is the sum of the phase volume fractions, where for a multiphase system (liquid-gas) this must be equal to 1, indicating that the whole system is filled with pure liquid/gas or the fraction of one phase relative to the other.

4.1.2 Conservation of momentum

The conservation of momentum can be express in terms of mass times acceleration equal to the sum of forces shown in Equation 4.4.

The first terms in the momentum on Equation 4.4 are related to acceleration and it is only when these are nonzero value that there are sonic waves. Sonic waves are generated when there is acceleration. e.g when starting up and shutting down the pump, there will be acceleration and therefore the production of sonic waves. These waves propagate in the pipe for a while until it is dampened completely by friction acting as a fluctuation. The right-hand side of the Equation 4.4 represent gravitational and frictional losses.

$$\frac{\partial}{\partial t}(A(\rho_l \alpha_l \nu_l) + (\rho_g \alpha_g \nu_g)) + \frac{\partial}{\partial x}(A(\rho_l \alpha_l \nu_l^2) + (\rho_g \alpha_g \nu_g^2)) + A \frac{\partial}{\partial x} P = -A(\rho_{mix} g + \frac{\Delta P_{fric}}{\Delta z}) \quad (4.4)$$

4.2 Closure laws

Only three conservation laws are present within the numerical model, but there are several unknowns associated with the physical properties like pressure, phase velocities, phase densities, friction. Hence there is a need to supply with additional closure laws to be able to find all the unknown variables.

4.2.1 Gas slip model

Since there is a mixture momentum equation, it is required to supply a gas slip relation that includes the effect that gas moves faster than the liquid. This will depend on the flow pattern which is present during the fluid flow. For instance, the model for dispersed bubble flow in vertical pipes is different than the model for slug flow.

The general model for the gas slip is represented in Equation 4.5, here the “ S ” expresses the gas rise velocity. In a static closed well the gas velocity will be determined from “ S ”. The “ $K\nu_{mix}$ ” term plays a role if the system is circulating or if the gas is moving upwards and expands causing an additional mixture flow in one direction. The “ K ” value reflects the gas distribution across the flow area.

$$\nu_g = K\nu_{mix} + S \quad (4.5)$$

Hasan^{XV} describes how the values of the flow parameter “ K ” and the gas rise velocities are dependent on the type of flow and flow pattern. The “ K ” parameter is denoted as “ Co ”. Table 4.1 is the result of experimental work to find average approximations for the “ K ” parameter for the different vertical multiphase flow patterns. The variation in the flow parameter “ Co ” depends on the flow configuration (Upward

^{XV}[Hasan et al., 2007]

concurrent, Countercurrent and Downward flow).

The Upward concurrent flow can be depicted when the gas and liquid phase flows in the same upward direction. Countercurrent flow occurs when the gas and liquid phases flow in the opposite direction e.g when the gas is injected inside a pipe with opposite liquid flow direction, and the Downward flow occurs when both phases flow in the same downward direction.

The experimental work of this project will focus on the Slug flow model, using two flow parameter “ K ” of 1.2 and 1.12 respectively to the three types of flow configurations. The “ K ” value will be 1.2 while injecting the kick and when it migrates upwards, but from the point where the pump is turn on producing the Bullheading effect, the “ K ” value will be reduced to 1.12 using interpolation to ensure a smooth transition.

The Taylor bubble rise velocity^{XVI} “ S ” has been investigated by many researchers; it is shown in Equation 4.6 where it was estimated for vertical cylindrical channels.

Table 4.1: Flow parameters for different flow patterns

[Hasan et al., 2007] pp.2.

Properties	Flow Parameter, Co			Rise Velocity ν_∞
	Upward cocurrent	Countercurrent	Downward	
Bubbly / D.Bubbly	1.2	2.0	1.2	ν_{∞_b}
Slug	1.2	1.2	1.12	$\bar{\nu}_\infty$
Churn	1.15	1.15	1.12	$\bar{\nu}_\infty$
Annular	1.0	1.0	1.0	0

$$S = 0.35 \sqrt{\frac{gD(\rho_l - \rho_g)}{\rho_l}} \quad (4.6)$$

It is possible to note that this depends on the diameter of the pipe and the density differences between gas and liquid, an example of calculation will be shown. A vertical pipe with inner diameter of 3.92 cm is considered. It is filled with water ($1000 \frac{Kg}{m^3}$), a gas bubble with a density of $1.2 \frac{Kg}{m^3}$ is injected. What would be the Taylor bubble rise velocity?.

^{XVI}[Hasan et al., 2007] pp.2

Using Equation 4.6 we obtain

$$S = 0.35 \sqrt{9.81 \frac{m}{s^2} * 0.0392 * \left(1 - \frac{1.2 \frac{Kg}{m^3}}{1000 \frac{Kg}{m^3}}\right)} = 0.217 \frac{m}{s}$$

How will be the bubble rise velocity if the diameter of the pipe is ten times larger?.

$$S = 0.35 \sqrt{9.81 \frac{m}{s^2} * 0.392 * 10 * \left(1 - \frac{1.2 \frac{Kg}{m^3}}{1000 \frac{Kg}{m^3}}\right)} = 0.686 \frac{m}{s}$$

How will be the bubble rise velocity if the gas density is increased ten times?.

$$S = 0.35 \sqrt{9.81 \frac{m}{s^2} * 0.0392 * \left(1 - \frac{10.2 \frac{Kg}{m^3}}{1000 \frac{Kg}{m^3}}\right)} = 0.216 \frac{m}{s}$$

Here it is possible to see that most of the gas bubble velocity variation lies on the diameter change. The increase of the gas phase velocity was found almost at 50 $\frac{cm}{s}$ increasing 10 times the inner diameter of the pipe; nevertheless, an increase in gas density almost 10 times the gas rise velocity decreased not so considerably. Thus, it can be said that the gas slip velocity depends almost exclusively on the diameter variation.

4.2.2 Density models

Since the Drift Flux Model and the AUSMV will try to simulate a small-scale experimental setup, some appropriate density models must be chosen for the planned fluids to be used in the experiment. The original code has some very simple relations for the fluid densities which were only depending on pressure. Hence, it was found appropriate to try to find some more accurate density model.

Water will be used as liquid phase and air will be used for gas. The density models will be dependent on both pressure and temperature. For the water density, Equation 4.7 is used:

$$\rho_l = \rho_o + \frac{\rho_o}{\beta}(P - P_o) - \rho_o \alpha (T - T_o) \quad (4.7)$$

Here, the variables with subscript “o” refers to the standard conditions which are defined as the atmospheric conditions, the Bulk modulus of elasticity “ β ”^{XVII} is an approximate value of the compressibility of a fluid, it describes how easy a unit volume of a fluid changes when changing pressure applied on it.

^{XVII}[EngineeringToolBox, 2004]

The volumetric thermal expansion coefficient “ α ”^{XVIII} is a constant value present in any solid, liquid and gas when is in direct contact with temperature changes. Normally, an object will expand if the temperature increases, however the water expands when the temperature is greater and lower than +4°C. the average bulk modulus “ β ” and volumetric thermal expansion “ α ” for water are $2.20 * 10^9$ ($\frac{N}{m^2}$) and $2.07 * 10^{-4} K^{-1}$ respectively.

For the gas density, an ideal gas law will be used and the formula for this is shown in Equation 4.8 and Equation 4.9. For air, the value of R was set to $R = 286.9 \frac{J}{Kg K}$

$$PV = nRT \quad (4.8)$$

$$\rho_g = \frac{P}{RT} \quad (4.9)$$

Note: *In this study T will be considered a fixed parameter at 20 degrees Celsius for the small scale experimental facility*

4.2.3 Friction gradient model

A simple friction pressure loss model will be used in the simulations. The output of this model is the frictional pressure loss per meter. The Equation 4.10 reads:

$$\frac{\Delta f}{\Delta z} \left(\frac{Pa}{m} \right) = \frac{2f\rho_{mix}\nu_{mix}abs(\nu_{mix})}{(D_{out} - D_{in})} \quad (4.10)$$

We can note that the pressure loss is proportional to the mixture density and to the mixture velocity squared. It also depends on the inner and outer diameter of the flow area. In our case, the inner diameter will become zero. The frictional pressure loss model also includes the friction factor f. The expression for this will depend on whether the flow is laminar or turbulent and it depends on the value of the Reynolds number which is explained more in the next section.

4.2.4 Reynolds number

This is a dimensionless number used for determining whether the flow is laminar or turbulent. The expression for the friction factor discussed in the previous section will also include the Reynolds number. The Reynolds number reflects the ratio between inertial forces and viscous forces. The formula is given by the Equation 4.11.

$$Re = \frac{Inertia Forces}{Viscous Forces} = \frac{\rho\nu\Delta D}{\mu} \quad (4.11)$$

^{XVIII}[College, 2020]

If the viscosity dominates, the flow will be laminar and the opposite way if the inertial forces dominate, then the flow is turbulent. For Reynolds number below 2000, the flow is laminar. For Reynolds numbers above 3000 the flow is considered turbulent. In between, there is a transition region.^{XIX}. Figure 4.2, evidence the flow behavior for the Reynolds flow regime classification.

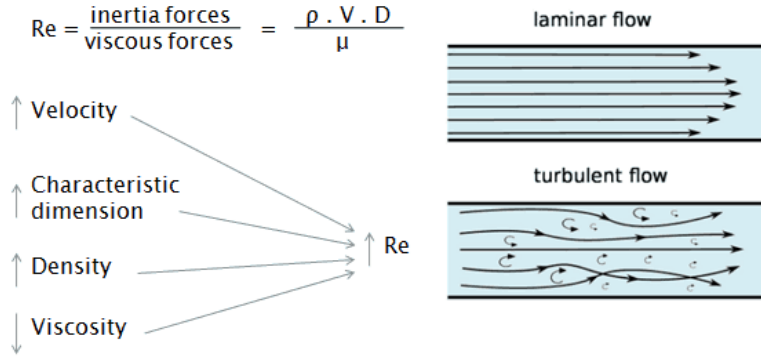


Figure 4.2: *Reynolds Flow Classification Pattern*
[Schlichting and Gersten, 2016]

4.3 AUSMV scheme for the small-scale experimental setup

In this section a brief mathematical analysis of the drift flux model is going to be mentioned.

The drift flux model considered here consisted of two mass conservation laws (Equation 4.1 and Equation 4.2), and a mixture momentum equation (Equation 4.4). This compose a system of nonlinear partial differential equations. It is possible to form a complex mathematical analysis of the system and show that this is a hyperbolic system and that the model described propagation of waves. It is characterized for rapid sonic waves but also a more slowly gas volume fraction wave displacement. The speed of these waves are reflected by the so called eigenvalues of the system. For more details consider the work of Benzoni-Gavage^{XX}. The AUSMV scheme depend on information of the sonic wave propagation and it uses the expression that was obtained in the work of Benzoni-Gavage. The Equation 4.13 for the sound velocity was developed under the assumption shown in Equation 4.12.

$$\alpha_g \rho_g \ll \alpha_L \rho_l \quad (4.12)$$

$$w = \sqrt{\frac{p}{\alpha_g \rho_l (1 - K \alpha_g)}} \quad (4.13)$$

^{XIX}[Schlichting and Gersten, 2016]

^{XX}[Benzoni-Gavage, 1991]

4.3.1 Discretization Process and Numerical Scheme

The first step when developing a transient flow model is to discretize the flow region into a certain number of cells. The conservation laws and the closure laws has then to be solved separately for each of these cells. An example of discretization is shown in Figure 4.3. Here the variable “ U ” refers to the content of masses and momentum inside the cells while the variable “ F ” represents the fluxes of mass and momentum between the cells. It can be noted that the variables reflecting the content of the cell is defined in the midpoint of the cell for the numerical scheme to be considered here. The conservation laws can be written in a condensed vector form as shown in Equation 4.14, Equation 4.15 and Equation 4.16.

$$\frac{\partial}{\partial t}U + \frac{\partial}{\partial x}F(U) = G(U) \quad (4.14)$$

$$U = \begin{pmatrix} \alpha_l \rho_l \\ \alpha_g \rho_g \\ \alpha_l \rho_l \nu_l + \alpha_g \rho_g \nu_g \end{pmatrix} F(U) = F_c + F_p = \begin{pmatrix} \alpha_l \rho_l \\ \alpha_g \rho_g \\ \alpha_l \rho_l \nu_l^2 + \alpha_g \rho_g \nu_g^2 + p \end{pmatrix}, G(U) = \begin{pmatrix} 0 \\ 0 \\ -q \end{pmatrix} \quad (4.15)$$

$$F(U) = F_c + F_p = \begin{pmatrix} \alpha_l \rho_l \\ \alpha_g \rho_g \\ \alpha_l \rho_l \nu_l^2 + \alpha_g \rho_g \nu_g^2 \end{pmatrix} + \begin{pmatrix} 0 \\ 0 \\ p \end{pmatrix} \quad (4.16)$$

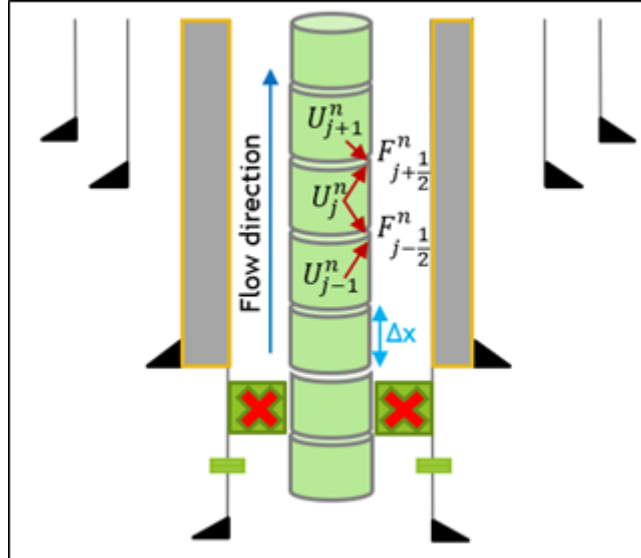


Figure 4.3: Example of a well discretization scheme

A numerical scheme steps forward in time and updates the content for each cell from one-time level to the next stepping forward with a timestep of a certain size. The updating formula can be written as follows in Equation 4.17 and it is just a

discretized version of the conservation laws discussed earlier:

$$U_j^{n+1} = U_j^n - \frac{\Delta t}{\Delta x} \left(F_{j+\frac{1}{2}}^n - F_{j-\frac{1}{2}}^n \right) - \Delta t Q_j^n \quad (4.17)$$

Here “ U ” represents the conservative variables as seen in the vector form of the system above, and “ j ” ranges from 1 to 3 since there are three conservation laws. The time level is reflected by the “ $n + 1$ ” notation which reflects the value at the new time level while “ n ” reflects the value at the old-time level.

The variable “ Q ” is the source term and the only contribution here is for the momentum equation where “ Q ” is defined as the right-hand side of Equation 4.4. “ Δt ” is the chosen time step and “ Δx ” represents the length of the cell. The fluxes between the cells are represented by the vector “ F ”. Here it is possible to observe that these variables are calculated at the old-time level and this indicates that the scheme is explicit. The fluxes between the two cells are calculated based on some average of the values in the two cells. The way this is done can vary from scheme to scheme but in the case of this project, the AUSMV scheme is adopted. For a more detailed description of how the numerical fluxes are calculated in this case refer to Udegbumam^{XXI}.

It is possible to note that the scheme, finds the conservative variables at a new time level. In order to find the physical variables e.g pressure, phase volume fraction, phase densities and phase velocities, one need to use closure laws defined earlier. It is also needed to update the friction pressure gradient and the hydrostatic gradient, since the source term “ Q ” is needed to be updated since it is a part of the numerical scheme.

4.3.2 CFL Condition

Using an explicit scheme like the AUSMV, the timestep will be limited by the CFL condition stated on Equation 4.18.

$$timestep < CFL \frac{\Delta x}{fastest\ wave\ speed} \quad (4.18)$$

The CFL is a numerical value between 0 and 1 and the fastest wave in the system will be the sonic wave. When the scheme is adopted to the experimental arrangement, the number of cells adopted in the experimental setup and the timestep chosen were 25 boxes and $1 * 10^{-5}$ seconds, respectively. The increase in the number of boxes will produce a more accurate solution, nevertheless the timestep of the numerical

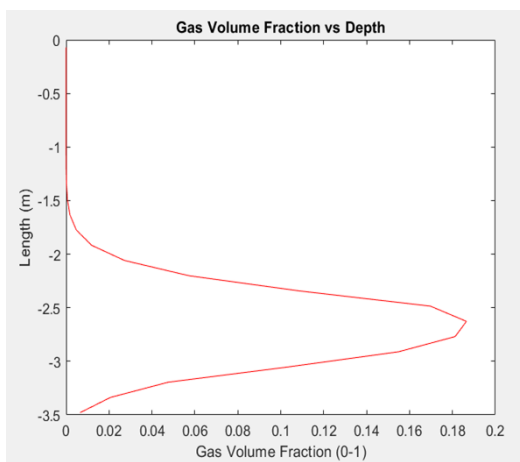
^{XXI}[Udegbumam et al., 2015]

simulation has to be reduced to obtain an accurate response from the simulation tests. A rule of thumb suggests an allowed limit for the CFL number lower than 0.2.

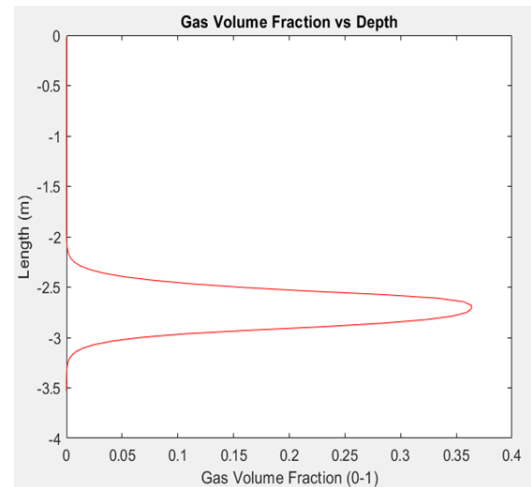
4.3.3 Numerical diffusion and application of slope limiters

The drift flux model will describe sharp interfaces between two phase flow regions and one phase flow regions. The variable that will display these is the gas volume fraction that will change values rapidly. However, the so-called numerical diffusion will tend to smear these sharp transitions out. One alternative to reduce the numerical diffusion is to increase the number of boxes. But in addition, the slope limiter concept can be applied to make the scheme more accurate. For a detailed description of the numerical diffusion reduction, refer to the extension of the second order accuracy.^{XXII}

Figure 4.4a and Figure 4.4b represent simulation result for the small scale setup. The gas volume fraction was the parameter to be evaluated as an example using the same experimental geometries, gas rate and liquid rate for both cases. The idea was to make a comparison identifying the numerical diffusion produced by using the conventional number of boxes (25) and the time step mentioned in the previous section illustrated in the Figure 4.4a, and an increase to 4 times of the number of boxes (100) with a reduction of 10 times the initial timestep represented on the Figure 4.4b.



(a) Gas volume fraction for 25 discretized well boxes and $1 * 10^{-5}$ seconds



(b) Gas volume fraction for 100 discretized well boxes and $1 * 10^{-6}$ seconds

Figure 4.4: Gas volume fraction for different discretizations

The gas volume fraction of the multiphase system was plotted to identify differences when using a rough and fine discretization. It was possible to identify the numerical diffusion when the amount of well boxes was increased by the price of increasing computational time. For the fine grid, the kick is much more concentrated since numerical

^{XXII}[Fjelde et al., 2016]

diffusion has been reduced. In both cases, the slope limiter concept was used where the cell variables are not considered constant when calculating the numerical fluxes. The slope limiter concept calculates the boundary values for each cell which are again used to re calculate the numerical fluxes of the cells.

4.3.4 Boundary Conditions

In the AUSMV scheme, we need to treat the boundary conditions separately. There will be three different situation:

- Injection of gas at bottom.
- Close the well and let the kick migrate.
- Stay injecting liquid at top of the well to bullhead the gas downward.

For the injection of gas, the inlet gas rate in Kg/s has to be specified. This injection will take place in a certain period. The total mass of gas injected in the simulation should be similar to the mass injected in the experiment. (This mass is calculated experimentally once we have the reading from the MID pressure sensor after the bubble pass across it. Pressure difference is calculated between the reading from the sensor before and after the bubble cross it. The difference in pressure is converted as a water level drop inside the system [*Theoretical height of the bubble*]. Then using the volume of the cylinder and the density of the gas. Mass flow rate is calculated).

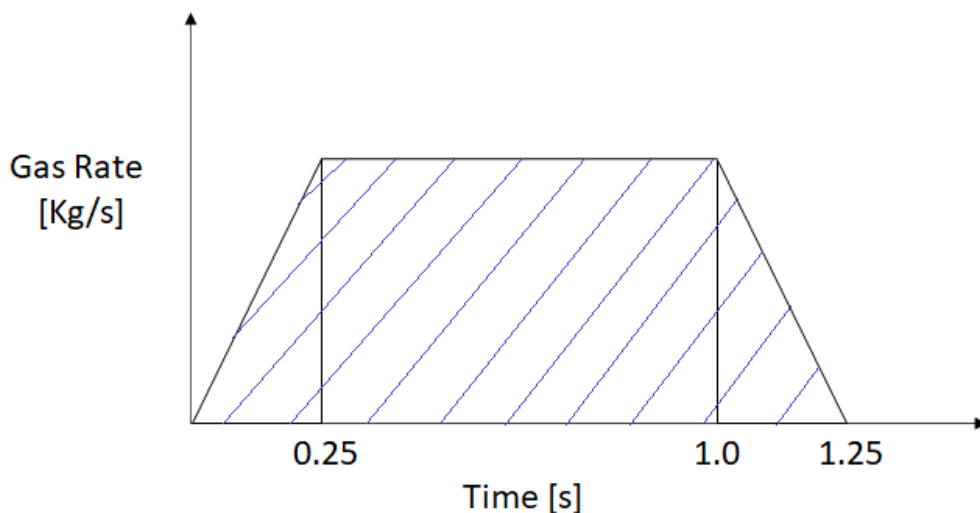


Figure 4.5: Gas injection at bottom in the simulation

The Figure 4.5 above shows how the gas is injected at bottom in the simulation. After the gas was injected, the well was closed until time = 1.25 (s). Then the liquid rate (Kg/s) at the top of the well was ranged up (using a negative value) and the

bullheading process was started.

One can note that all flow rate changes were done gradually to avoid excessive acceleration effects. In the numerical scheme itself, the boundary condition will change depending on the situation discussed above. But we will not go into details on this.

The numerical model formulates the mass change in time for each of the intervals, applying different concepts like the closing of the system and the flow direction when the migration of air and the bullheading technique takes place.

5 Results and Discussion

In this chapter the data obtained from the experimental practice will be discussed. These data will be used as the input for the simulation of the numerical model. To replicate the bullheading method on the laboratory scale circulating at four different liquid rate scenarios with an average variation of 0.153 l/s in flow, to visualize the changes produced increasing it in each of the liquid rate scenarios. With the application of the experimental tests, many challenges were noted in obtaining a Slug flow, since during each circulation the presence of dispersed bubble pattern was evident during the process producing changes in the monitoring of the absolute pressure and the average gas velocity.

As mention earlier, the absolute pressure of the system was monitored using pressure sensors connected to the PASCO Capstone software and in direct contact with the fluid within the flow loop. The visualization and the absolute pressure data for the vertical multiphase flow were essential to obtain the average velocity of the Taylor bubble (Figure ??). The average velocity was then calculated using the distance between the Top-Mid pressure sensors, and the time the bubble spent when it was pushed down. The gas mass rate was calculated using the pressure drop read at the Mid sensor and contrasted with the direct visualization of the Taylor bubble within the system.

The differential pressure showed changes that intensified as circulation rates were increased. This is due to the increase during circulation by the pump. These changes are associated to pressure peaks produced by the Equivalent Circulating Density (ECD) the moment the liquid is circulated against the gas bubble.

In general, independent of the circulated flow rate, the same variations could be observed in all the pressure curves. By classifying the bullhead of the bubble in eight frame, it could be seen that in the curves from Figures 5.2 to 5.9 the only change is the time spent for each flow rate.

The numerical model was updated to simulate the laboratory scale with predetermined inputs like the geometries of the set-up and physical properties for the multiphase fluid e.g. pipe heights, inner and outer diameters, gas, and bullheading rates, among others. For a detailed description of the numerical model and the inputs for the experimental work, refer to the Appendix B.

5.1 Flow Visualization

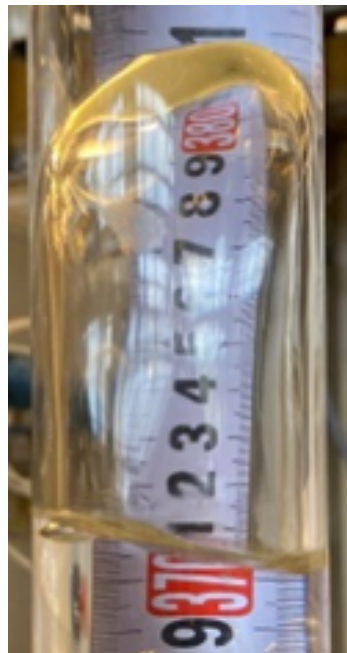
The slug flow and dispersed bubble pattern were seen within the experimental tests. The injected air bubble formed a Slug Flow pattern when the multiphase system starts to flow ^{XXIII}. “describes a symmetric Taylor Bubble about the vertical axis inside a circular pipe”.

The symmetric gas bubble shape shown in Figure 5.1a occurs by the velocity difference between the gas and liquid superficial velocities flowing upwards with the flow assisted by the density difference, however if the Taylor bubble is affected by any force, the bubble may distort when the type of flow is changed e.g Upward concurrent, Countercurrent and Downward flow. This could be seen in Figure 5.1a when normally the Taylor bubbles are characterized by separated liquid slugs.

Figure 5.1a is the visualization of Taylor bubble found within the experiment tests for this project, it is being Bullheaded with the flowing Newtonian liquid (water).



(a) Photograph of a Taylor Bubble moving upwards with no flow in pipe



(b) Photograph of a Taylor Bubble moving downward with flow in pipe

Figure 5.1: Bubble shape change

During the flow tests of the experimental Bullheading method, some dispersed bubbles were found within the flow.

^{XXIII}[Rabenjafimanantsoa et al., 2011]

The system was filled with Methylene blue to improve the visualization of the flow pattern (Figure 5.2 to 5.9), since the migration of the bubble until it is bullheaded back to the Injection zone. The illustration for the Taylor bubble migration and subsequently the bullhead, will be described with the absolute pressure changes for each of the liquid rate scenarios.

Most of the time, when the bubble migrated upwards, a Slug flow pattern was observed. Additionally, the dispersed bubble pattern was identified when the injected gas bubble was pushed by the liquid. Some of the small bubbles flowed from the surface and others were trapped in different parts of the setup.

When the Taylor bubble reaches above the top sensor, the bullheading started. The slug flow pattern is continuing when the pump starts to circulate, and after some seconds later it can be seen some amount of small bubbles passing within the flow direction. This may be due to different reasons:

- The presence of turbulence in the surface tank is due to the amount of liquid derived from the system circulation with small bubbles coming from the injected Taylor bubble. From the Taylor bubble some small bubbles come off traveling within the flow and others get trapped, when the flow decreases or the pump is turned off these bubbles migrate to the surface, being trapped inside the pump. This effect is diminished by purging the pump; however it is not sufficient to completely get rid of the bubbles trapped in the system.
- The pump being used multiple times for the different flow tests carried out in the laboratory, decreased its circulation efficiency. This was determined by trying to circulate at the same rate multiple times, observing that the pump struggled to circulate the liquid from the tank to the system.

5.2 Monitoring of physical properties

The pressure was the parameter measured directly during the experiment within the flow of the multiphase system. Furthermore, the velocity of the system was calculated using the basic displacement of the induced gas between the top and middle sensor over time.

For the measurement of the physical properties, five liquid flow rate tests were carried out for the visualization of the Bullheading process. However only four of the five tests showed the results of the Bullheaded gas. the first test was run using a liquid rate of (0.47 l/s), which was not enough to Bullhead the induced air bubble. The next flow rate of (0.61 l/s) showed good results Bullheading the kick. The liquid rate was increased gradually according to the pump range power supply. To achieve an

approximate equivalence between the liquid flow and the power supply for the pump in voltages, a linear interpolation was calculated using the pump flow rate tests shown in Figure 3.2. For the different liquid flow circulation tests refer to the Appendix A for the equivalence of voltages and flow rates in the power range that the pump can circulate.

During the liquid rate test of (0.61 l/s), it was observed directly and with the pressure data, that the air bubble was Bullheaded slowly. Thus, the minimum liquid flow rate to get a static Taylor bubble ($\nu_g = 0$) is between (0.47 l/s) and (0.61 l/s).

For the experimental set-up was impossible to keep the bubble static for the way the water gets into the pipe while it keeps moving up/down very slowly, probably because the circulation rate is not constant.

The bubble velocity can be calculated when it is stationary within the liquid. Using the gas slip relation, we can derive for which liquid velocity the Taylor bubble will become static employing Equation 4.5. If the gas bubble is in a static position (no gas displacement $\nu_g = 0$) the slip model becomes the Equation 5.1:

$$\begin{aligned}
 \nu_g &= K(\nu_l * \alpha_l + \nu_g * \alpha_g) + S \\
 0 &= K(\nu_l * \alpha_l + 0) + S \\
 -S &= K(\nu_l * \alpha_l) \\
 -S * A &= K(\nu_l * \alpha_l) * A \\
 \frac{-S * A}{K * \alpha_l} &= \nu_l * A = Q_{liq}
 \end{aligned} \tag{5.1}$$

The Equation 5.1 involves the area of tubes (pipe cross section), the rise velocity ratio “S” which depends on the flow pattern, an average phase volume fraction of liquid and the flow parameter “K” for the type of flow direction. here an example will be presented. e.g. for a laboratory scale using a circulation loop system with a cylindrical pipe diameter of 3.92 cm, a Slug flow was found (water and injected air) with a “S” value of 0.2169 m/s, an average liquid volume fraction of 0.4 was determined with the multiphase system. the fluid system was found at a countercurrent direction ($K = 1.2$) to produce a static condition of the kick migration to the surface, how much would be the minimum liquid flow rate needed to obtain a static gas bubble.

$$\begin{aligned}
 \frac{-0.2169(\frac{m}{s}) * \frac{\pi}{4} * 0.0392 m^2}{1.2 * 0.4} &= Q_{liq} \\
 -5.4536 * 10^{-4} \frac{m^3}{s} &\simeq -0.5454 \frac{l}{s} = Q_{liq}
 \end{aligned}$$

With an experimental test with these similar characteristics, is possible to say that if the fluid circulates within an equal or higher flow, the liquid can stop the Taylor bubble and push it down.

Table 5.1 shows the liquid rate scenarios for each of the experimental tests, with a gradual increase of (0.15 l/s) on average for each test.

Table 5.1: Liquid rate scenarios

Exp. Test	Q (l/s)
1 st	0.47
2 nd	0.61
3 rd	0.74
4 th	0.90
5 th	1.08

5.2.1 Absolute Pressure

The absolute pressure measured in this experimental setup is the sum of the atmospheric pressure combined with the hydrostatic and the frictional pressure. These pressures vary with the depth of each sensor. The greater the depth, the greater the pressure exerted by the fluid column.

As mentioned in section 2.2.1, the hydrostatic pressure of a well depends on the fluid density, gravity and TVD, for this project the hydrostatic pressure depends on the water density, gravity, and pipe height.

The pressure sensors are installed at different depths showing an increase in the absolute pressure from low to high value. An example is going to be shown e.g. using Equation 3.2. How large will the hydrostatic pressure and absolute pressure in mbar, measured by the top sensor located at 2.1 m height of the setup, filled with water. Note that the atmospheric pressure is equal to 101325 Pa and 1013 mbar.

$$\begin{aligned}
 HP (Pa) &= \rho \left(\frac{Kg}{m^3} \right) * g \left(\frac{m}{s^2} \right) * h(m) = 1000 \frac{Kg}{m^3} * 9.81 \frac{m}{s^2} * 2.1 m \\
 &= 20601 Pa \\
 20601 Pa + 101325 Pa &= 121926 Pa \simeq 1219.26 mbar
 \end{aligned}$$

The hydrostatic pressure calculated previously combined with the atmospheric pressure (101325 Pa) should be approximate to the absolute pressure value measured by the top sensor of the experiment.

As discussed in previous chapters, the pressure drop was calculated using the reading from the mid sensor when the bubble tip passes through it and after the whole bubble pass across it after the valve is open.

To start with the absolute pressure plot obtained from each of the pressure sensors (Top, Middle and Injection), collected from the PASCO Capstone software and described in the Figure 5.2.

The pressure data was chosen for the first flow rate circulation of (0.61 l/s). The visualization of the Taylor bubble was included in different bubble frames (from 1 to 8) for some absolute pressure variations measured by the sensors:

- The yellow curve showed the absolute pressure data detected by the Mid sensor. From frames 1 to 3, the pressure behavior while the bubble started the migration displacement just until 40.8 seconds approximately. The frame number 2, is where the sensor perceived the tip of the Taylor bubble producing a pressure increase, this occurred when we left a small gap of air between the capillary and the PASCO sensor to avoid it get damaged. The capillary hoses were filled with water to make use of its incompressibility making it easier to transmit pressure changes by the air gap.

Between the bubble frames 2 and 3 is where the “belly” was observed between 41 and 43 seconds, the time it took for the bubble from the tip to the tail to pass through the sensor. The pressure data when the bubble tip is detected by the sensor is approximately 1319.76 mbar, and the pressure when the tail of the Taylor bubble passed and stabilized was approximately 1304.3 mbar. Thus, the gas mass rate is calculated using the pressure drop with this two pressure data points.

To reduce the length of the calculations, an example will be performed using the pressure data from the first test pressure, the results of the other tests will be attached in Table 5.2.

The pressure drop was calculated in the Mid sensor with the column full of water and with the bubble. The absolute pressure was determined at 1304.3 mbar and 1319.76 mbar equal to a pressure drop of 15.46 mbar, with that pressure difference it is possible to calculate the water level drop and therefore the mass of gas inside the multiphase system with the hydrostatic Equation 3.2, where the height variable is isolated from the equation as follows:

$$h[m] = \frac{\Delta P (Pa)}{\rho \left(\frac{Kg}{m^3} \right) * g \left(\frac{m}{s^2} \right)} = \frac{\frac{15.46 \text{ mbar}}{0.01 \text{ Pa}}}{1000 \frac{Kg}{m^3} * 9.81 \frac{m}{s^2}} = 0.1576 \text{ m} \simeq 15.76 \text{ cm}$$

With the obtained height equivalent to the pressure drop for the circulation rate of 0.61 l/s, the volume of gas can be calculated using the cylinder volume formula as Equation 5.2 demonstrates:

$$V (m^3) = \frac{\pi}{4} * D^2 (m^2) * h (m) \quad (5.2)$$

The inputs are the diameter of the pipe equal to 3.92 cm and the pressure differential of the fluid column calculated previously of 0.1576 m \simeq 15.76 cm.

$$V (m^3) = \frac{\pi}{4} * (0.0392 \text{ m})^2 * 0.1576 (m) = 1.9020 * 10^{-4} \text{ m}^3$$

We can calculate the gas density using the Equation 4.9 for the gas density model, the pressure in this case will be when the gas tip hits the middle sensor which is the absolute pressure at that position.

$$\rho_g \left(\frac{Kg}{m^3} \right) = \frac{P (Pa)}{R \left(\frac{J}{Kg K} \right) * T(K)} = \frac{130299 \text{ Pa}}{286.9 \frac{J}{Kg K} * 293.15 \text{ K}} = 1.5492 \frac{Kg}{m^3}$$

With the gas density and its volume, we can proceed to calculate the amount of air mass within the system using the Equation 5.2 for density calculations.

$$\begin{aligned} m (Kg) &= \rho_g \left(\frac{Kg}{m^3} \right) * V (m^3) = 1.5492 \left(\frac{Kg}{m^3} \right) * 1.9020 * 10^{-4} \text{ m}^3 \\ &= 2.9466 * 10^{-4} \text{ Kg} \simeq 2.9466 * 10^{-4} \frac{Kg}{s} \end{aligned}$$

This mass of air will be used in the numerical simulation. This value will be the same in the simulation using the trapezoid principle explained in the section 4.3.4.

The process is being repeated for each of the circulation tests using the pressure data provided by the sensors, where it should be similar in all of the four circulation rate scenarios due to the similar amount of air injected at the beginning of the experiment. At 47.65 seconds the mid sensor perceived an increase in pressure. This is due to the pump start circulation prior to bullhead. From this point not until around 61.25 seconds the Taylor bubble had passed the mid sensor, then the pressure is stabilized by only measuring liquid above it. This

can be verified on frame 7 from Figure 5.2.

- The red curve represents the pressure data recorded by the top sensor shown from frames 4 to 6. The sensors detected a fluid column variation the moment the tip of the bubble goes upward at approximately 46.4 seconds finishing just before at 47.65 seconds just exactly in the moment the surface pump starts the circulation. The turn on of the pump produced an increase in the pressure where some oscillations were found, due to the complexity of power supply deliver for a desired liquid rate e.g. from (0 l/s) to (0.61 l/s) in a single instant. At 49.6 seconds the sensor identified a reduction due to the presence of the lowest part of the Bullheaded Taylor bubble, and around 50.6 seconds the pressure stabilized by sensing only liquid above the sensor. Frame 6 was the proof of it.
- The green curve represents the pressure data from the injection sensor. This curve is plotted for a matter of pressure monitoring since the liquid circulation started at 47.65 seconds until the bubble had reached the injection sensor at 66 seconds, where the Bullheading test finished after 18.35 seconds since the moment the pump starts until the bubble passed completely through the injection sensor. The Upward flow direction is associated to the movement of the bubble, as well the countercurrent direction related to the moment the liquid is circulated and hit the bubble to stop it, and finally the downward flow direction when the bubble is pushed for the circulated liquid. The data for the pressure differential between the sensors can be seen in 5.3.
- The Top-Mid sensor pressure difference corresponded to the data on the blue curve. Here the pressure data is corroborated together with the absolute pressure data, to determine if the ups and downs on the curve correspond to the capillary effect mentioned above. Between 48 and 49 seconds the oscillations produced by turning on the pump were evident. For the average gas velocity, the time was determined to be approximately 50.6 seconds when the top sensor passes, reaching the mid sensor at approximately 61.25 seconds.
- The Inj-Mid sensor pressure difference corresponded to the data on the orange curve. The main purpose was to illustrate the duration of the Bullheading at 66 seconds confirmed with the absolute pressure stabilization after this period. The duration of the test was 26 seconds since the valve was opened.

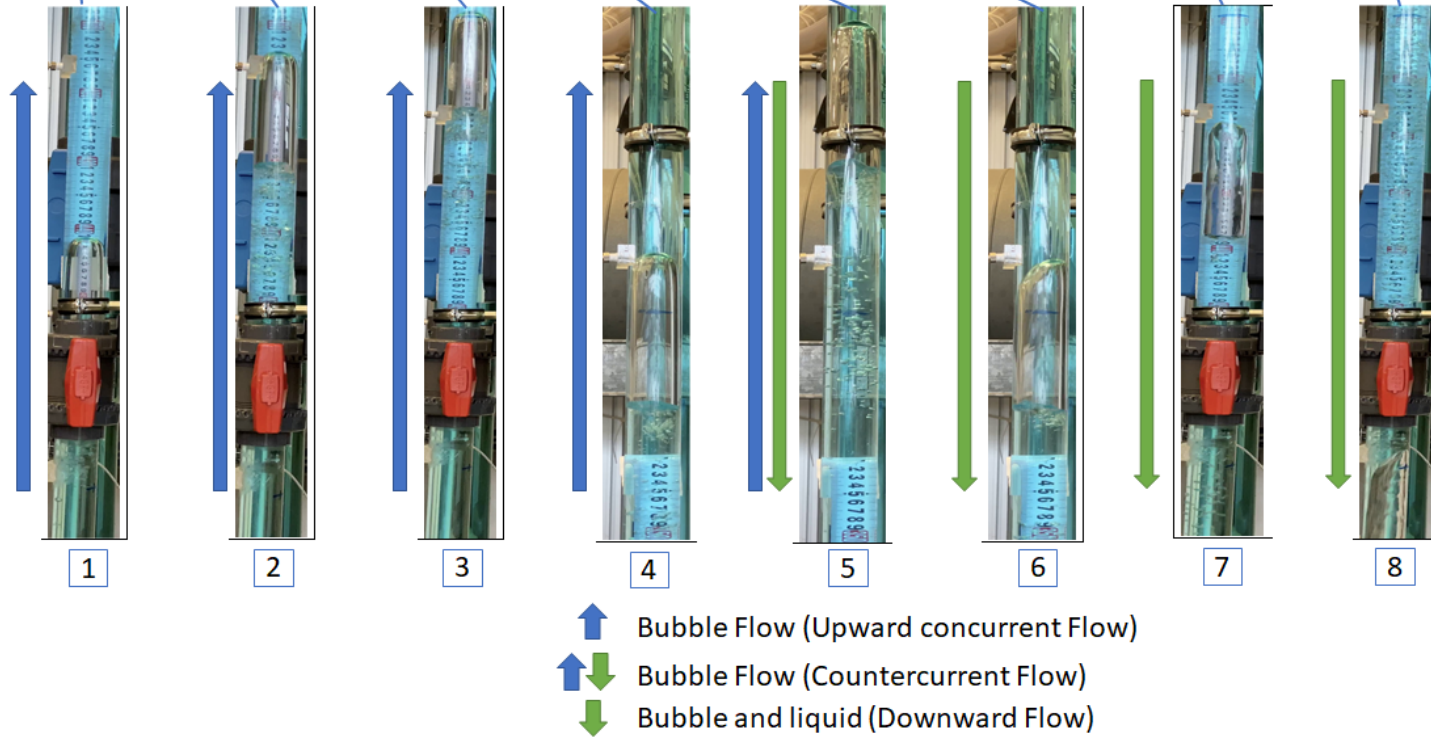
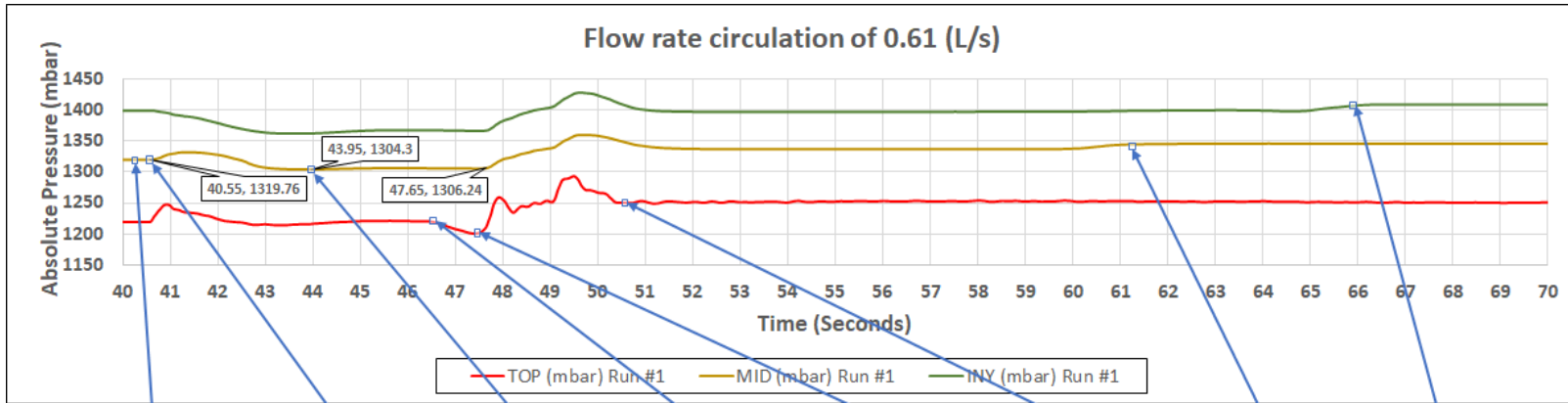


Figure 5.2: Absolute Pressure with flow rate of 0.61 l/s

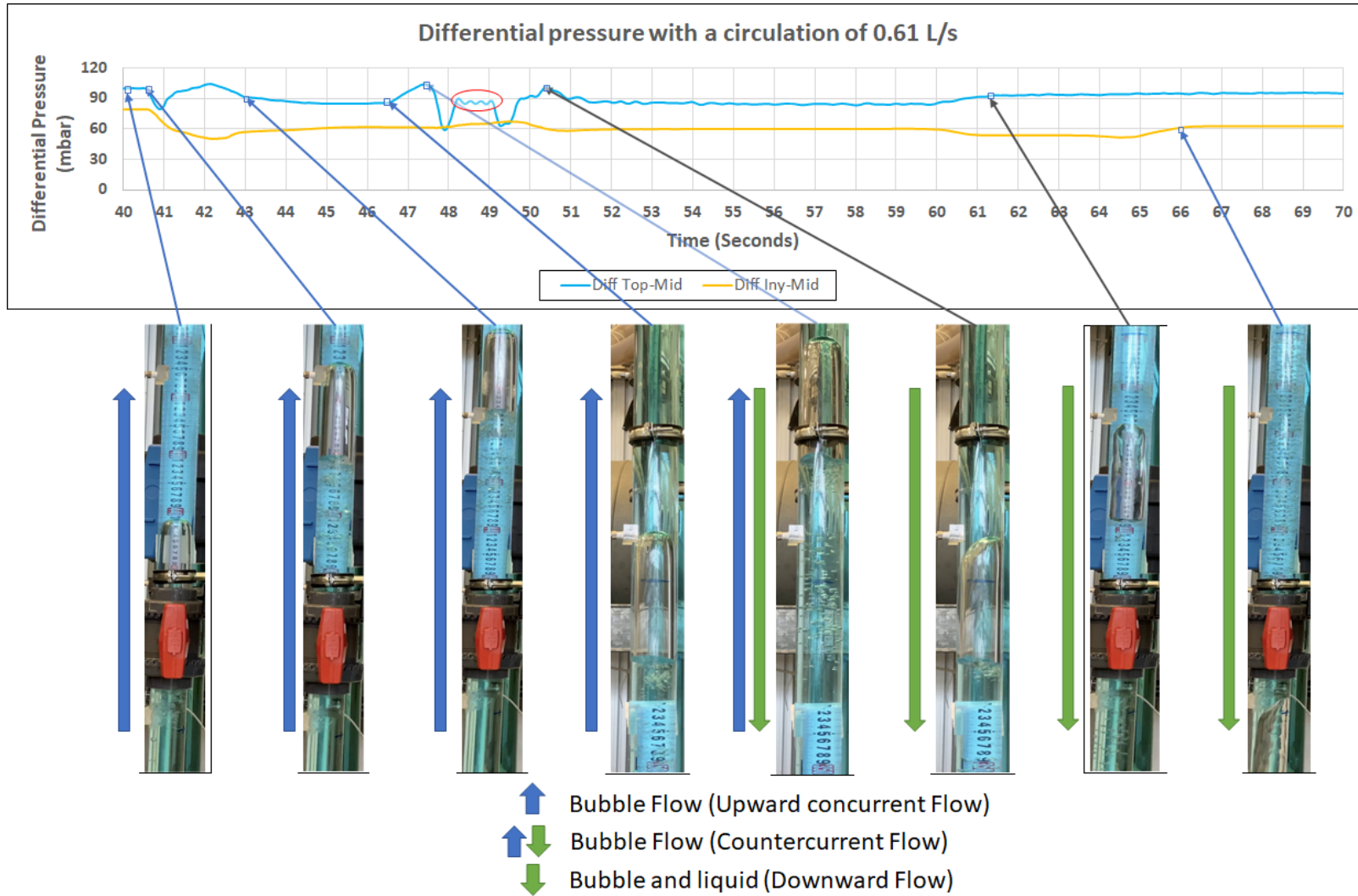


Figure 5.3: *Differential Pressure with flow rate of 0.61 l/s*

Figure 5.4 and Figure 5.5 are the pressure data representation for the second test with increasing the circulation rate up to 0.74 l/s, by an increase in the liquid rate the kick must be Bullheaded faster compared with the first circulation.

Here, the mid sensor measured an absolute pressure of 1332.05 mbar when the valve was open and measured 1316.5 mbar after the fluid column stabilized equivalent to a pressure drop of 15.55 mbar and a liquid level drop of 15.85 cm. The gas bubble spent 49.35 seconds to pass the top sensor and reach the mid sensor at 55.4 seconds, clearly the time interval was reduced up to 6.05 seconds.

On this second test, the pump started circulation at 47.35 seconds and finished the Bullheading at around 58 seconds. Approximately 10.35 seconds it took to push the bubble to the injection sensor where it was released. For this test, the duration of the migration and the bullheading test took 18 seconds, 8 seconds less than the first test.

Figure 5.6 and Figure 5.7 are the pressure data representation for the third experimental test increasing the circulation rate up to 0.90 l/s.

Here the mid sensor, measured an absolute pressure of 1332.02 mbar when the valve was open and measured 1316.02 after the fluid column stabilized equivalent to a pressure drop of 15.55 mbar and a liquid level drop of 16.31 cm. The gas bubble spent 48.75 seconds to pass the top sensor and reach the mid sensor at 52.15 seconds, visibly the movement was reduced up to 3.4 seconds.

For the third experiment, the pump started circulation at 47 seconds and finished the Bullheading at around 54.1 seconds. Approximately 7.1 seconds it took the push of the bubble to reach the injection sensor where it was released.

The pressure oscillations were reduced compared to the previous tests, while increasing the circulation rate, it was easier to stabilize the energy supplied to the pump.

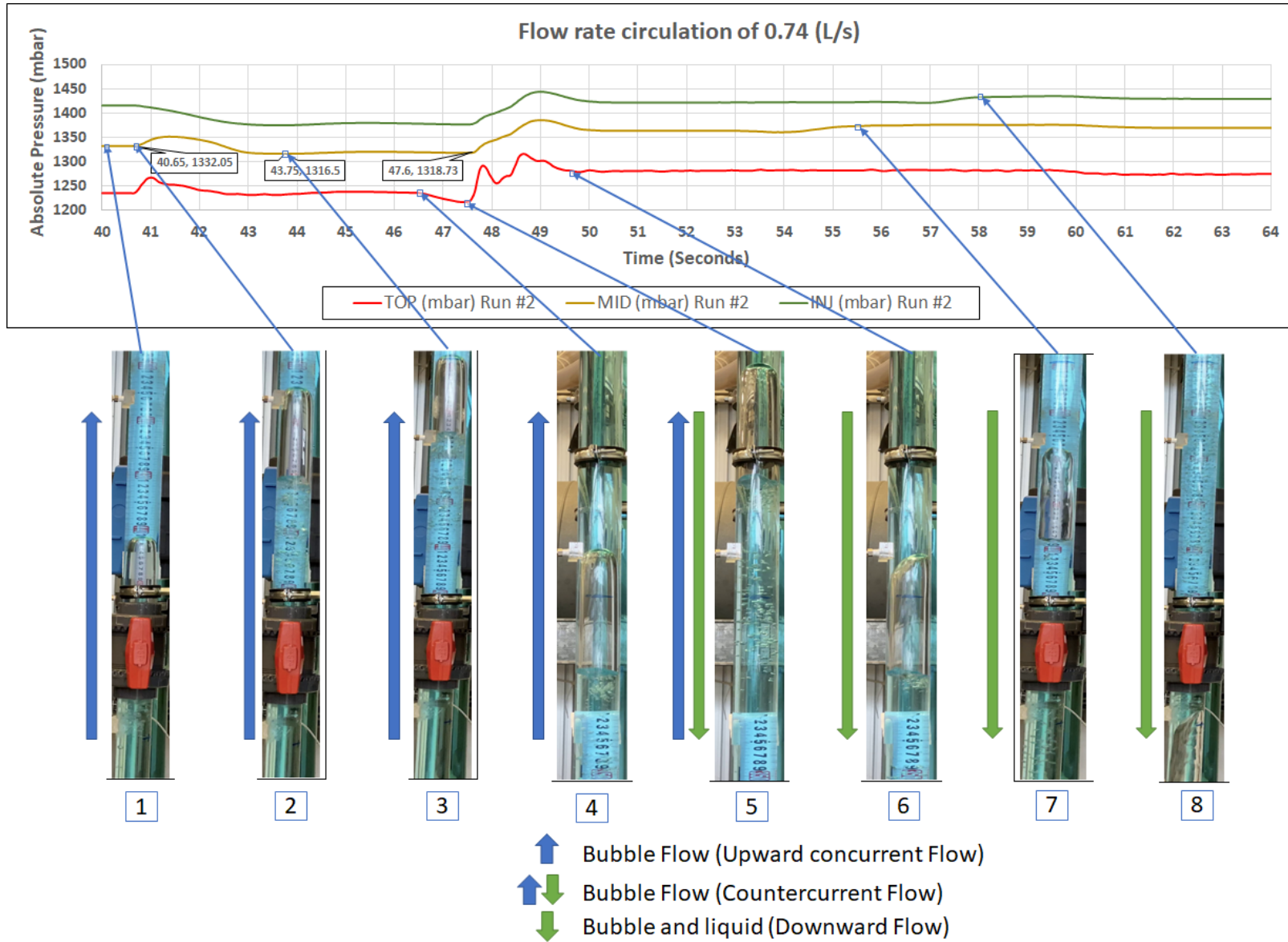


Figure 5.4: Absolute Pressure with flow rate of 0.74 l/s

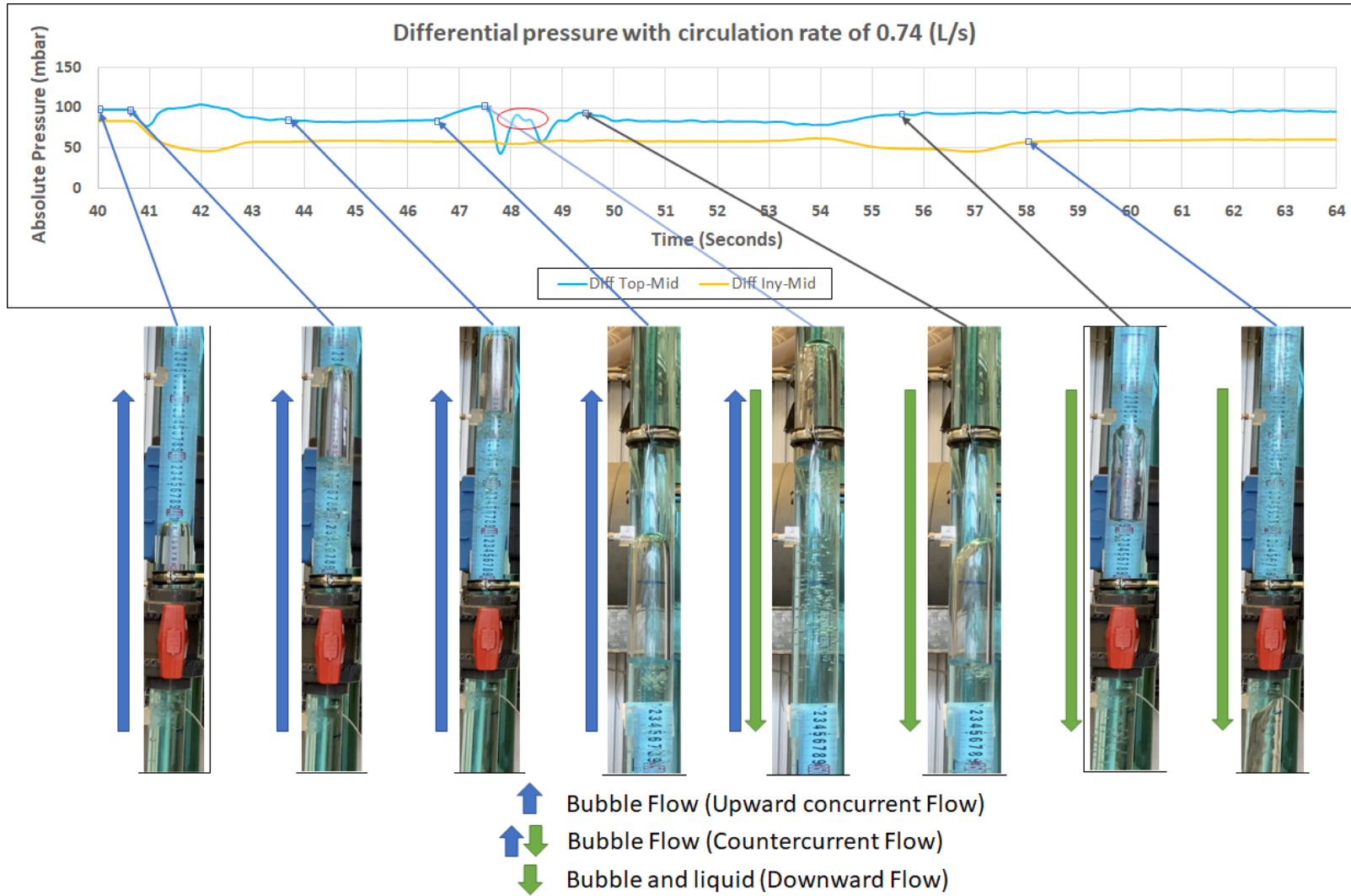


Figure 5.5: *Differential Pressure with flow rate of 0.74 l/s*

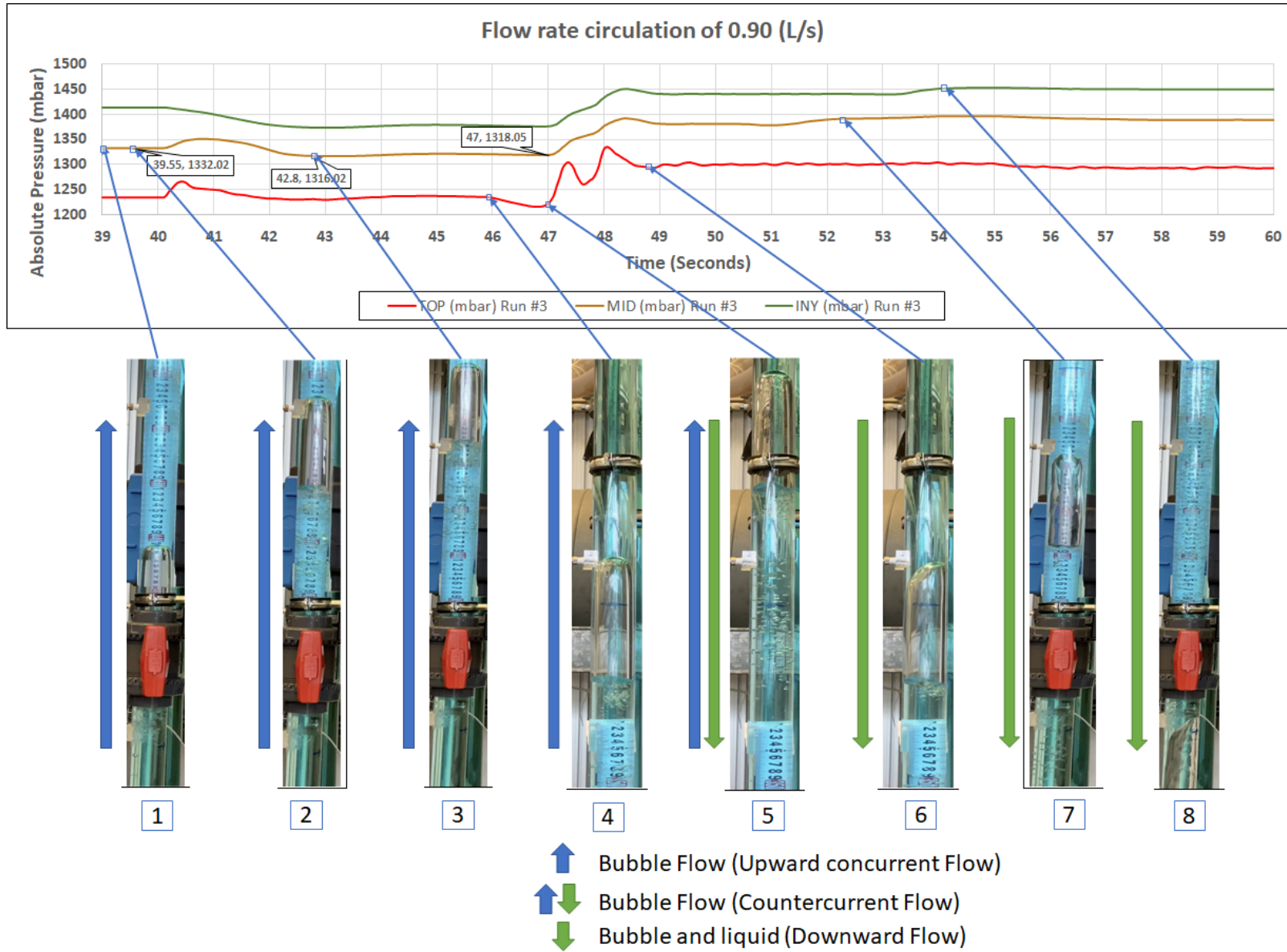


Figure 5.6: Absolute Pressure with flow rate of 0.90 l/s

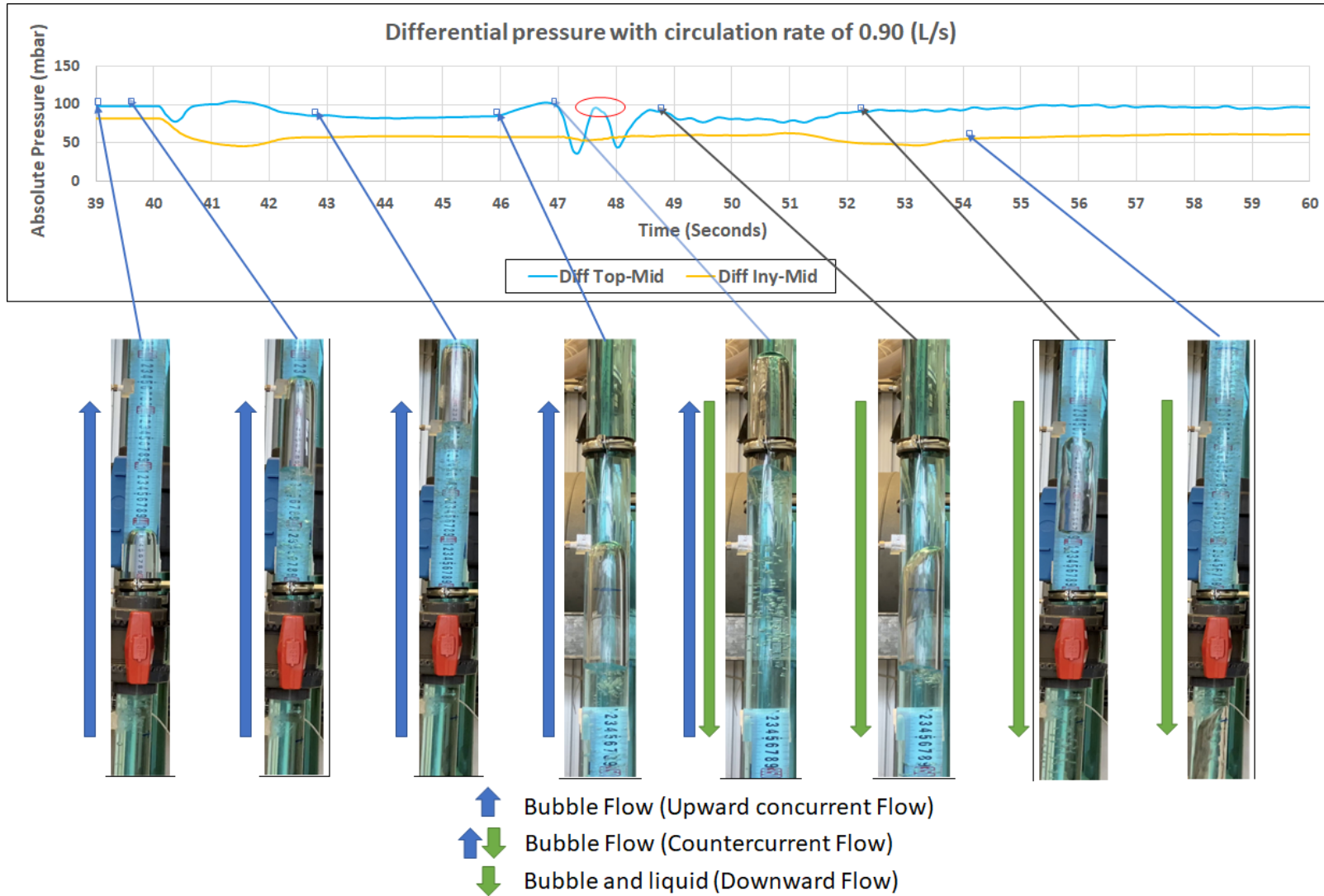


Figure 5.7: *Differential Pressure with flow rate of 0.90 l/s*

Figure 5.8 and Figure 5.9 illustrated the pressure data for the last experimental test with increasing the circulation rate up to 1.08 l/s.

The pressure detected by the Mid sensor measured was 1331.96 mbar, and 1317.5 mbar after the fluid column stabilized equivalent to a pressure drop of 14.46 mbar, and a liquid level drop of 14.74 cm. The gas bubble spent 49.2 seconds to pass the top sensor and reach the mid sensor at 51.05 seconds, a time difference equivalent to 1.82 seconds.

For the last experiment, the pump started circulation at 47.85 seconds similar with all the experimental tests and finished the Bullheading at around 53.1 seconds. Approximately 5.25 seconds the bubble took to reach the injection sensor.

With this test, it was verified that when circulating at the maximum rate of 1.08 l/s, the shortest time to bullhead the bubble was obtained, hence the highest velocity of the gas bubble was seen.

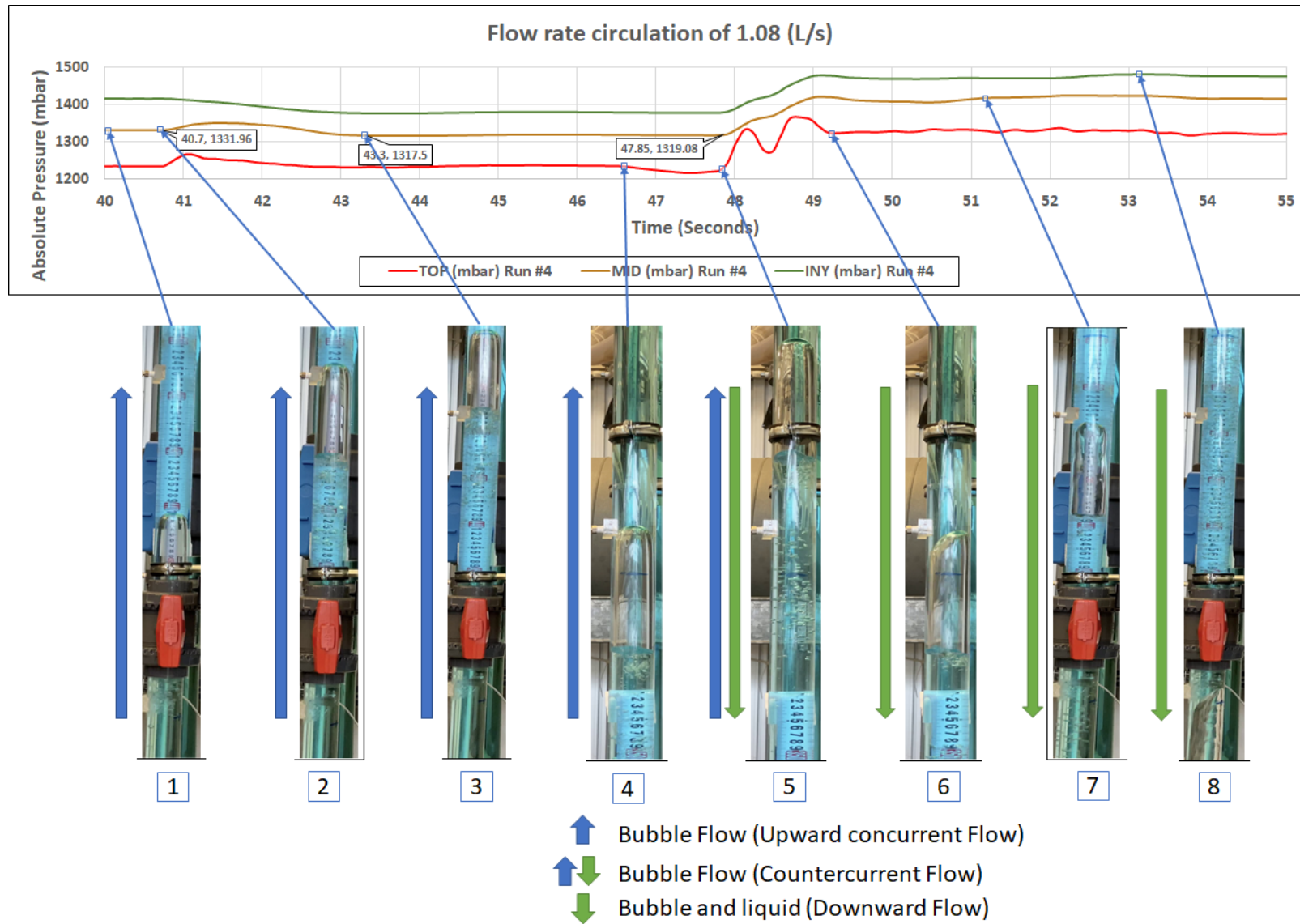


Figure 5.8: Absolute Pressure with flow rate of 1.08 l/s

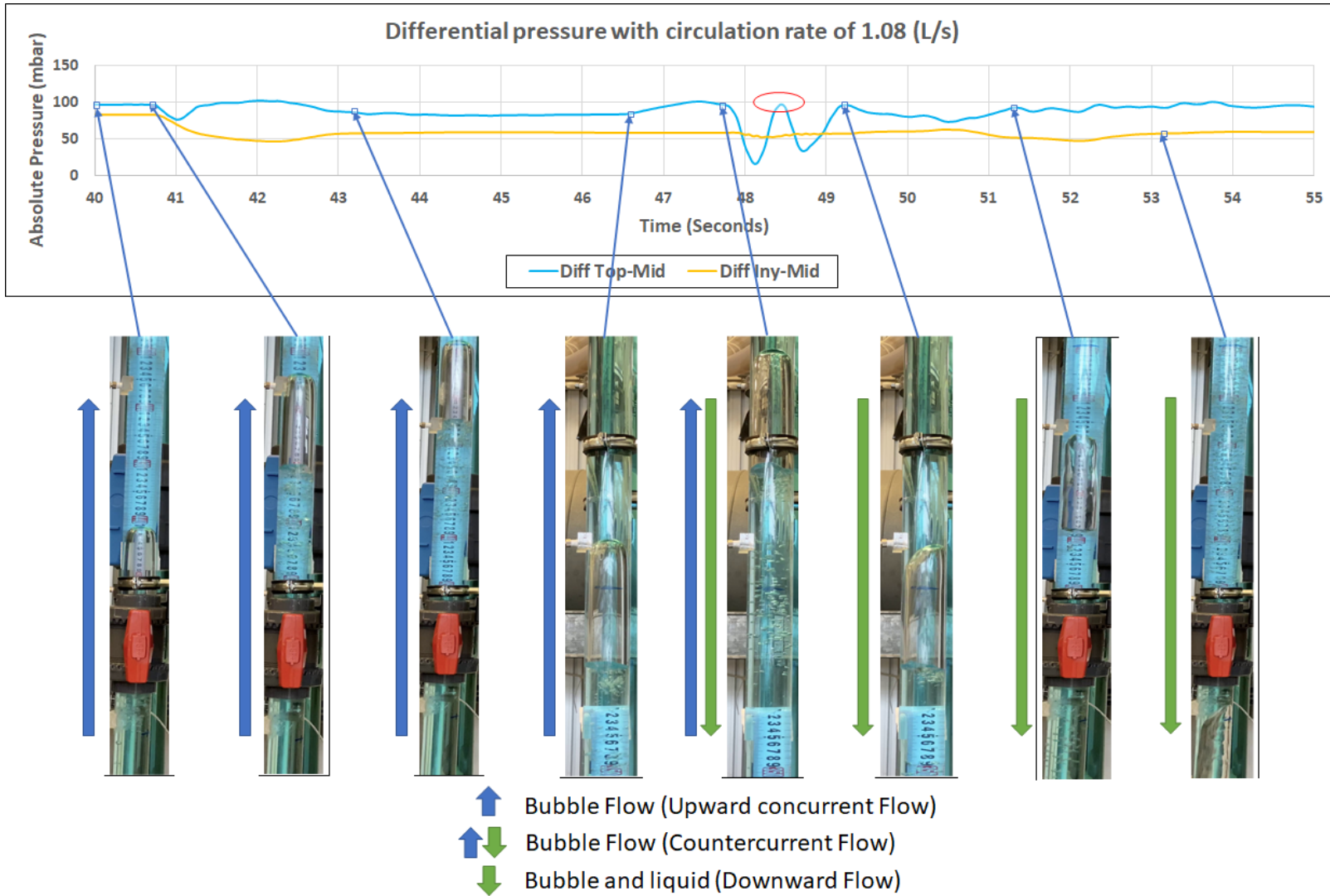


Figure 5.9: Differential Pressure with flow rate of 1.08 l/s

5.2.2 Average Gas Velocity

In the experiment, an average velocity of the gas (ν_g) was calculated using two pressure sensors as discussed previously, i.e Top sensor and Mid sensor. The average gas velocity was then calculated using the distance between the sensors and the time.

The gas velocity is the only parameter that can be compared directly; thus, it is not possible to compare the times need for bullheading in the simulation and experiment directly. this was because, the travelled distances in the experiment and the simulation were different. Hence, only gas velocity can be compared directly.

In the simulation the average gas velocity (ν_g) could be plotted, in the experiment an average ν_g was calculated and is shown in the last column of Table 5.2.

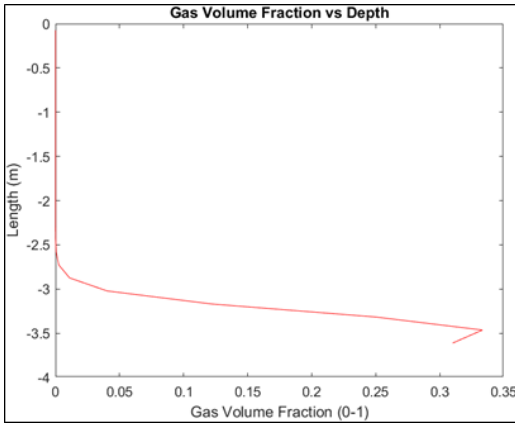
Table 5.2: Average experimental results

Exp. Test	Liquid rate (l/s)	Pressure change (mbar)	Taylor Bubble height (cm)	Volume of air (m ³)	Mass of air (Kg)	Distance (m)	Top sensor (sec)	Mid sensor (sec)	$\Delta t(sec)$	$\nu_g(m/s)$
1 st	0.606	15.46	15.76	0.000190	0.000295	1	50.60	61.25	10.65	-0.094
2 nd	0.735	15.55	15.85	0.000191	0.000296	1	49.35	55.4	6.05	-0.165
3 rd	0.896	16.00	16.31	0.000197	0.000305	1	48.75	52.15	3.40	-0.294
4 th	1.079	14.46	14.74	0.000178	0.000276	1	49.20	51.05	1.85	-0.541

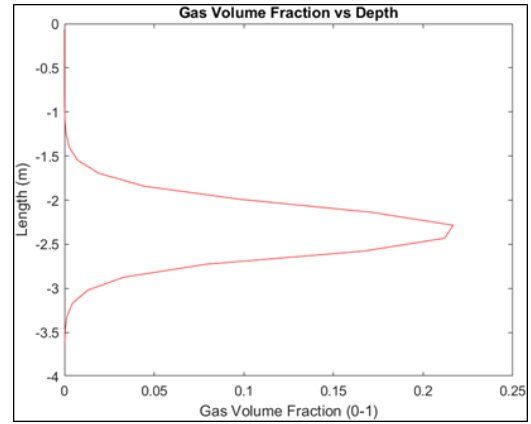
Here the results from the experiment were placed. The inputs to the numerical simulation were the liquid rate and the mass of air calculated previously. For the mass of air theoretically speaking should be the same for each simulation, however the amount of air was not perfectly equal for every injection, hence it was not possible to inject the same amount of gas in every attempt. The distance between the top and mid sensor was always one meter, and the gas velocity was calculated using the distance of one meter divided by the time difference between the Top and Mid sensor time. It must be negative when bullheading the Taylor bubble because downward flow direction causes a negative value.

From Figure 5.10a to Figure 5.10c the depth of the setup versus the gas volume fraction was represented for the flow circulation of 0.61 l/s, the difference lies in the gas distribution in the three different situations mentioned in the section 4.3.4 of Boundary conditions. The simulation time for the gas distribution in the injection was established up to 1.25 seconds and is represented in Figure 5.10a, then the gas volume fraction just before bullheading at 6.25 seconds is represented in Figure 5.10b where the setup conditions change from opening to temporary closing of circulation in the numerical model, subsequent to this moment the bubble begins to be Bull-headed. In addition, it was possible to observe the position of the bubble and predict the average size generated on “y-axis” from the numerical model between -3.5 m to -1.25 m, approximately 2.25 m height.

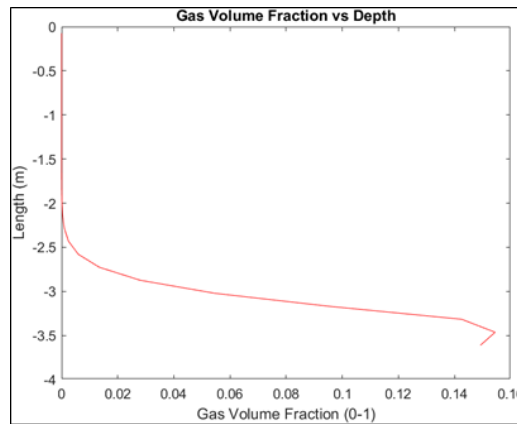
For Figure 5.10c, a 10 second Bullheading time was determined to show that the



(a) Injection interval from 0.0 to 1.25 sec



(b) Migration interval from 1.25 to 6.25 sec



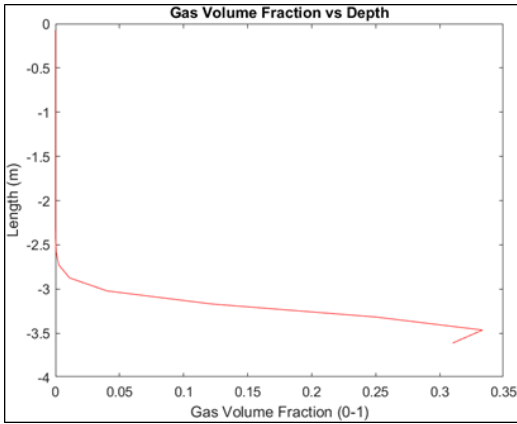
(c) Bullheading interval from 6.25 to 10.0 sec

Figure 5.10: Gas volume fraction - Test 0.61 l/s

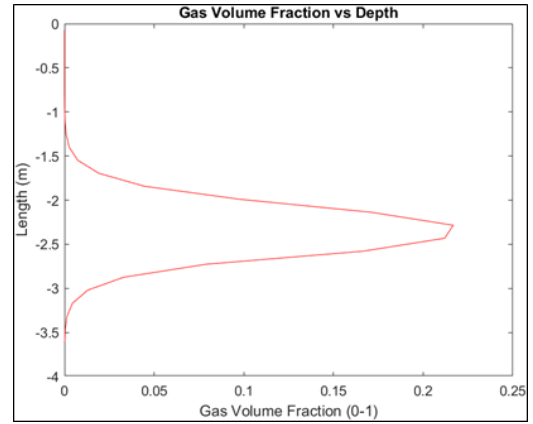
bubble is moving downward. These gas volume fractions were plotted for the four liquid scenarios. For the first two injection and migration situations, the curve behavior was similar. The most noticeable change occurred in the interval where the bubble is partially bullheaded as seen on Figure 5.10c, while between the injection and migration steps the gas fraction was similar since no force has been applied to disturb the shape of the bubble.

From Figure 5.11a to Figure 5.11c, the gas volume fraction is shown for the 10 seconds of simulation, 3.25 seconds after the start of the bullheading (started at 6.25 seconds). For the scenarios of (0.74 l/s) and (0.90 l/s), it could be said that the gas bubble has already been Bullheaded, but not entirely since there is a small partial gas volume, between 2% to 10% and 0.5% to 1.5% respectively. This was analyzed on “x-axis”.

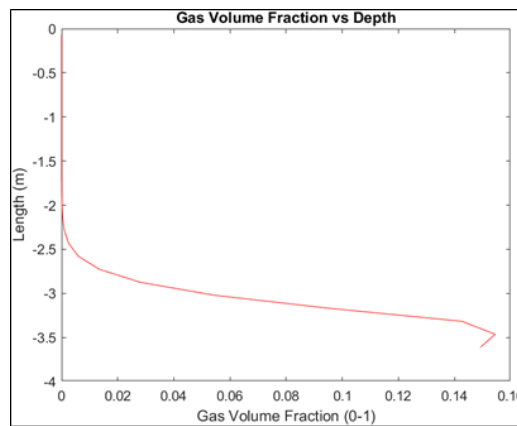
On the other hand, for the last circulation scenario (1.08 l/s), the gas fraction was so small that it could be considered a value to almost zero and indicating that



(a) Bullheading interval with 0.74 l/s



(b) Bullheading interval with 0.90 l/s



(c) Bullheading interval with 1.08 l/s

Figure 5.11: Gas volume fraction at different flow rates

the bubble has already been Bullheaded. Hence, a shorter simulation time would be enough to push the Taylor bubble entirely.

Figure 5.12 represented the gas volume in (m^3) in “y-axis” for the four bullheading rates and on the “x-axis” the simulation time of the entire process. The three situations can be seen with 1.25 seconds for the injection with an increase in the curve, a volume of gas as a flat line from 1.25 seconds to 6.25 seconds where the model changes the closing conditions to opening and ends in the established time of 10 seconds to observe the bullheading of the numerical model.

How fast the curve drops just demonstrate that increasing rate makes the bullheading process faster. But the time interval it uses for displacing the kick in the simulator can not be compared directly with the experiment data since the distances travelled are different in the experiment and the simulation.

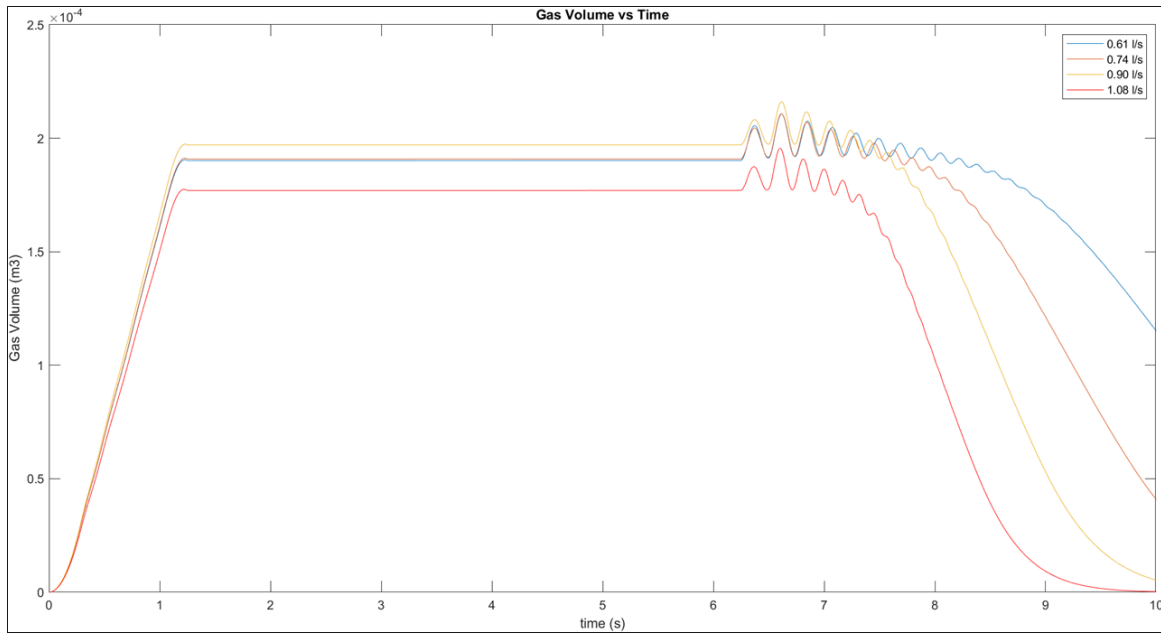


Figure 5.12: *Taylor bubble gas volume for the four Bullheading rates*

Figure 5.13 is the velocity response for a bullheading rate of 0.61 l/s, in the y-axis the depth of the setup is shown from the injection sensor at 3.685 m to the surface and in the x-axis the velocity of the gas phase within an average value of -0.346 m/s. The gas velocity was modeled for 10 seconds of simulation, just after the bullheading process started. The gas velocity between the numerical and the experimental model differs in a high range value, because the average gas value calculated from the experiment was -0.094 m/s.

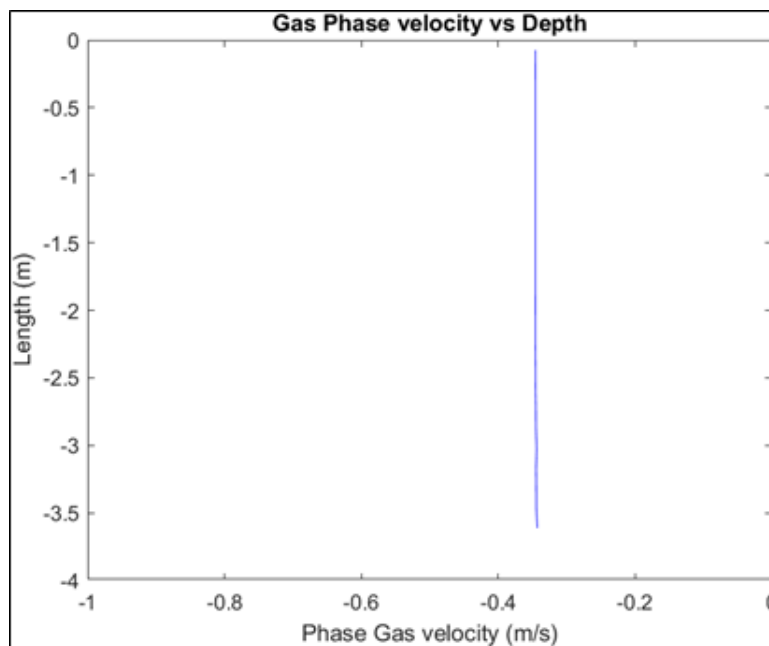


Figure 5.13: *Gas Phase velocity response for a bullheading rate of 0.61 l/s*

Figure 5.14 was the test result for a bullheading circulation rate of 0.74 l/s, the same effect between the gas velocity experimental and numerical difference occurs with the second test. A numerical value of -0.466 m/s was obtained meanwhile the experimental calculated was -0.165 m/s, *an approximate difference of -0.305 m/s between the models.*

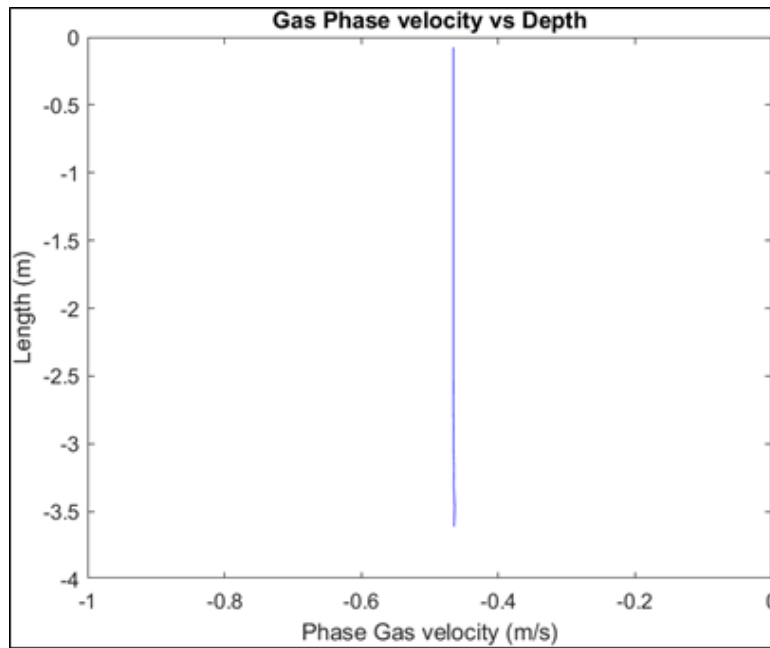


Figure 5.14: *Gas Phase velocity response for a bullheading rate of 0.74 l/s*

An increase in the gas velocity was observed in the Figure 5.15 with similar velocity difference than the previous circulation scenarios, an average value of -0.615 m/s was observed. The maximum gas velocity from the pump circulation can be seen on Figure 5.16, an average value of -0.785 m/s was visualized.

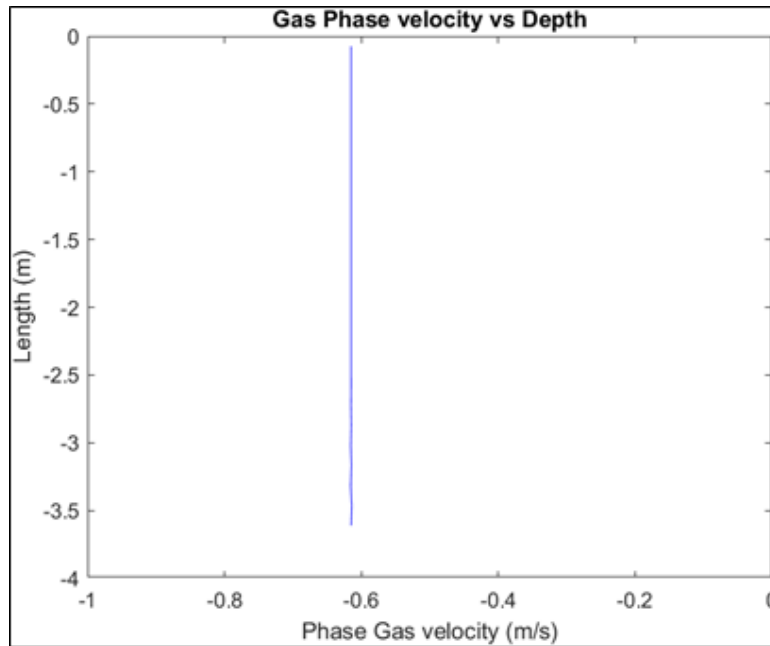


Figure 5.15: *Gas Phase velocity response for a bullheading rate of 0.90 1/s*

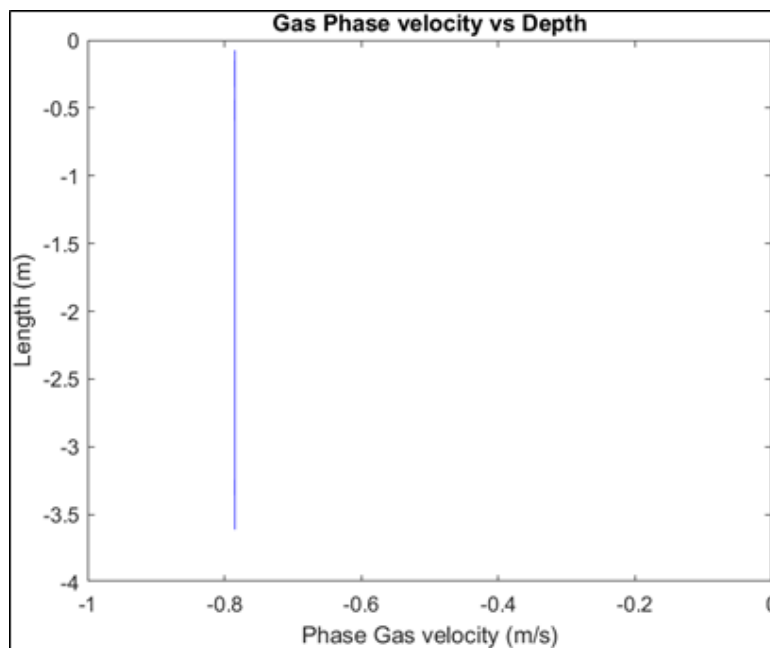


Figure 5.16: *Gas Phase velocity response for a bullheading rate of 1.08 1/s*

A compilation of the gas velocity for each of the liquid circulation scenarios were plotted within the Figure 5.17. A straight-line shape is observed when the data is compiled for a constant period from top to bottom for the small-scale length setup.

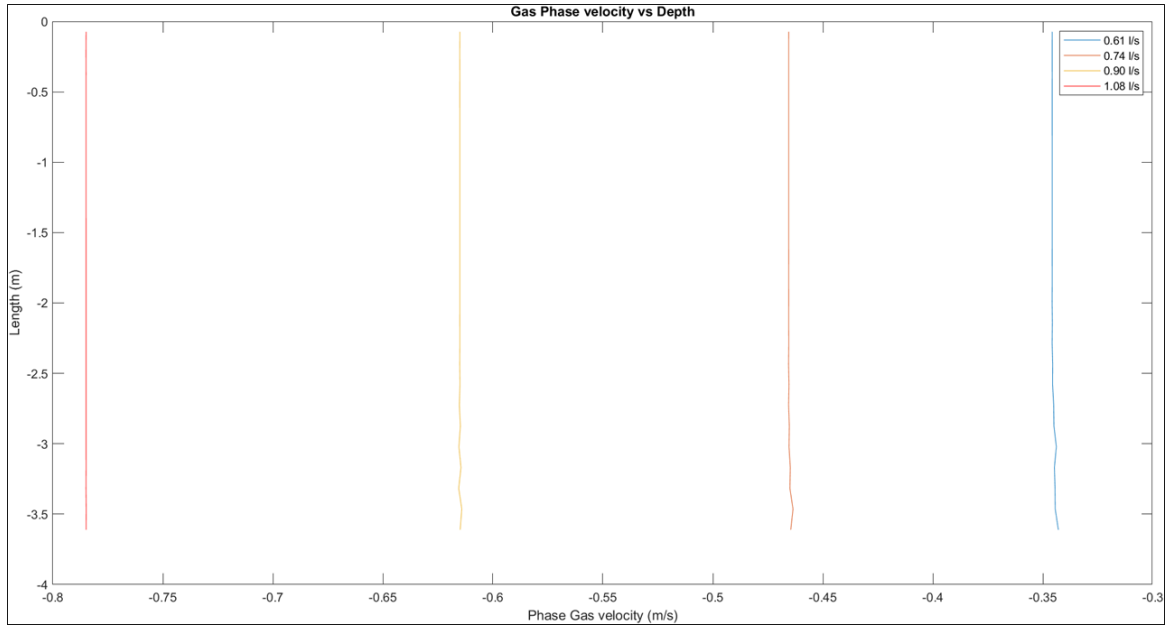


Figure 5.17: *Gas Phase velocity compilation for each circulation rate*

The Table 5.3 showed the liquid circulation scenarios or the bullheading rates being the input of the numerical model, with the results from the experiment and the numerical simulation.

Table 5.3: Gas velocities from the models

Bullheading rate (l/s)	Experimental gas velocity (m/s)	Simulated gas velocity (m/s)
0.606	-0.094	-0.346
0.735	-0.165	-0.466
0.896	-0.294	-0.615
1.079	-0.541	-0.785

For a fixed rate, it was seen that the gas bubble moved faster down in the simulations compared to what was seen in the experiment. The negative gas velocity was larger in the simulation than what was estimated from the experiment when the liquid rate was fixed.

One reason for this can be that the gas was much more concentrated in the experiment. The Taylor bubble was around 15 cm and the gas fraction seemed large. In the simulation however, the gas was much more spread out and with a much lower maximum gas volume fraction. In simple terms, is the same effect as trying to push a fully inflated ball (*Experimental bubble*) in a pool and a little inflated ball (*Simulated bubble*). It will be much easier to push down the little inflated ball.

What we can see from Equation 5.1 is that when α_l is reduced (gas volume fraction

increases) then Q_{liq} increases. What it means is, the more gas volume fraction is present in the system the more pump rate is needed to bullhead.

6 Conclusions and Recommendations

- An experimental facility was built successfully using two transparent tubes with 4.20 m and 4.41 m height, the pipe with 4.20 m height can hold 5.1 liters of fluid while the largest pipe can hold 22.3 liters. the Bullheading experiment was carried out successfully, circulating water through a loop from the water tank to the smaller ID pipe (Downward) passing through the bigger ID pipe (Upward) and returning to the water tank.
- It was interesting to observe the behavior of the Taylor bubble in the three scenarios (injection, migration and bullheading when pumping enough water). During injection the injected bubbles were dispersed and because they did not have where to go because the valve was closed they merged together to create a Taylor bubble. During bubble migration, there was no flow and countercurrent was observed while the water was displaced down as the bubble rise. Finally during bullheading the behavior change once again and cocurrent flow was observed.
- Initially, the experimental design was configured to circulate liquid through the largest pipe. It was not possible because the pump capacity was not enough. However, if a bigger pump is used the configuration allow to make the experiment just switching the hoses from intake and output. This will allow to perform Bullheading tests with higher pressures and bubble velocities when injecting from this side. Also, with some adjustment like an L valve with rotation in one end, a steering wheel device to lock inclination and a extension for the hoses the set-up can be conditioned to simulate bullheading in inclined scenarios.
- It is close to impossible to repeat the same conditions for every test due to the difficulty and the uncertainty of injecting the same gas volume and controlling the same power supply in one attempt.
- If it is desired to continue with the same experimental procedure, it is recommended the use of a flowmeter to mitigate uncertainty of pump performance or change the pump due to the continuous use of tests to which it was subjected, thus decreasing the efficiency for future tests. It is strongly recommended because this will help also to measure the flow rate in real time and thus the velocity calculations will be more accurate. The availability of spare pumps in the laboratory facilitates the development of multiple runs to obtain an average flow rate for higher flow circulations.
- Experiment were carried out to check how the experimental results compare with

theory. A simulator was used which was based on the Drift Flux Model supplemented with a gas slip relation.

- The objective was to see how the theoretical model for gas slippage compares with experimental data for a situation where we are bullheading a Taylor bubble (Slug) flow downward.
- It was also seen difficult to recreate the experiment identically in the simulation. In the simulation, the gas became much more spread out due to a longer injection period and numerical diffusion. It was also difficult to compare the Bullheading time intervals directly since the travelled distances were different in the experiment and simulations. However, it was possible to compare the gas velocities. The more negative gas velocity, the more successful the Bullheading operation is. Table 5.3 showed the different negative gas velocities for each of the Bullheading rates.
- When comparing simulations and experiment, it was found that the experimental gas velocities during Bullheading were less negative than the corresponding gas velocities found from simulation. This means that it was easier to push the gas down in the simulations. This is most likely caused by the fact that the gas was much more spread out in the simulation with a much lower maximum gas volume fraction. refer to Figure 4.4a.
- To improve the output numerical solution, it is recommended to make the kick more concentrated (reducing the elongation of the bubble) by making the injection time shorter and try to reduce the numerical diffusion while increasing the number of well boxes, thus this produce an increase in the computational simulation time while obtaining a more accurate result in the simulation.
- The transient Drift Flux Model was designed to solve a 1D Newtonian fluid model, therefore if one wants to update for a Non-Newtonian model, the numerical scheme must consider the viscosity model that characterizes fluids with a nonlinear viscosity model e.g. drilling fluids (plastic pseudo plastic and dilatant) different than the one for a constant Newtonian fluid model.

References

- [Al-Otaibi et al., 2020] Al-Otaibi, R. F., Al-Haqwi, M., Iturrios, C. O., et al. (2020). First worldwide implementation of pressurized mud cap drilling for a 17×19 in. hole section translates into safer and more cost-effective operations. In *International Petroleum Technology Conference*. International Petroleum Technology Conference.
- [API,] API. Rp 59 (1987) recommended practices for well control operations.
- [Benzoni-Gavage, 1991] Benzoni-Gavage, S. (1991). *Analyse numérique des modèles hydrodynamiques d'écoulements diphasiques instationnaires dans les réseaux de production pétrolière*. PhD thesis, Lyon 1.
- [Brasil, 2020] Brasil, W. (2020). Wellcontrol methods. <https://www.wellcontrol.com.br/?pag=wcworksheets>. Accessed June 2.
- [College, 2020] College, O. n. (2020). Thermal expansion of solids and liquids. <https://courses.lumenlearning.com/physics/chapter/13-2-thermal-expansion-of-solids-and-liquids/>. Accessed June 26.
- [Crumpton, 2018] Crumpton, H. (2018). *Well Control for Completions and Interventions*. Gulf Professional Publishing.
- [EngineeringToolBox, 2004] EngineeringToolBox (2004). Bulk modulus and fluid elasticity. https://www.engineeringtoolbox.com/bulk-modulus-elasticity-d_585.html. Accessed June 26.
- [Fjelde et al., 2016] Fjelde, K., Frøyen, J., Ghauri, A., et al. (2016). A numerical study of gas kick migration velocities and uncertainty. In *SPE Bergen One Day Seminar*. Society of Petroleum Engineers.
- [Gedge et al., 2013] Gedge, B., Dalgit Singh, H. K., Bandico Refugio, E., Ta Quoc, B., Bot, N. V., et al. (2013). Managed pressure drilling-a solution for drilling the challenging and un-drillable wells in vietnam and south east asia. In *SPE Asia Pacific Oil and Gas Conference and Exhibition*. Society of Petroleum Engineers.
- [Ghauri et al., 2016] Ghauri, A. A., Fjelde, K. K., and Frøyen, J. (2016). A transient model for hydraulic simulation of bullheading and pressurized mud cap drilling. In *International Conference on Offshore Mechanics and Arctic Engineering*, volume 49996, page V008T11A029. American Society of Mechanical Engineers.
- [Hasan et al., 2007] Hasan, A., Kabir, C. S., Sayarpour, M., et al. (2007). A basic approach to wellbore two-phase flow modeling. In *SPE annual technical conference and exhibition*. Society of Petroleum Engineers.
- [Koederitz, 1995] Koederitz, W. L. (1995). Gas kick behavior during bullheading operations in vertical wells. *Louisiana State University and Agricultural & Mechanical College*.

- [Lyons et al., 2015] Lyons, W. C., Carter, T., and Lapeyrouse, N. J. (2015). *Formulas and Calculations for Drilling, Production, and Workover: All the Formulas You Need to Solve Drilling and Production Problems*. Gulf Professional Publishing.
- [Malloy, 2007] Malloy, K. P. (2007). Managed pressure drilling-: What is it anyway?: Managed pressure drilling. *World oil*, 228(3).
- [Ortiz, 2019] Ortiz, M. (2019). Basic concepts of pressure gradient. <http://perfob.blogspot.com/2019/04/conceptos-basicos-de-gradientes-de.html>. Accessed May 28.
- [PASCO, 2020] PASCO (2020). Pasco capstone 2.0. <https://www.pasco.com/products/sensors/pasport/ps-2146#compatibility-panel>. Accessed May 15.
- [Pieter et al., 1994] Pieter, O., Avest, D., Grodal, E., Asheim, H., and Meissner, R. (1994). Bull heading to kill live gas wells. In *European Petroleum Conference*.
- [Rabenjafimanantsoa et al., 2011] Rabenjafimanantsoa, A., Time, R. W., and Paz, T. (2011). Dynamics of expanding slug flow bubbles in non-newtonian drilling fluids. *Ann Trans Nord Rheol Soc*, 19:1–8.
- [Schlichting and Gersten, 2016] Schlichting, H. and Gersten, K. (2016). *Boundary-layer theory*. Springer.
- [Sun et al., 2014] Sun, X., Wang, K., Yan, T., Wu, Y., Luan, S., and Shao, S. (2014). Study on applicable conditions and mathematic models of bullheading. *The Open Petroleum Engineering Journal*, 7(1).
- [Taitel et al., 1980] Taitel, Y., Bornea, D., and Dukler, A. (1980). Modelling flow pattern transitions for steady upward gas-liquid flow in vertical tubes. *AIChE Journal*, 26(3):345–354.
- [Taitel et al., 1978] Taitel, Y., Lee, N., and Dukler, A. (1978). Transient gas-liquid flow in horizontal pipes: Modeling the flow pattern transitions. *AIChE Journal*, 24(5):920–934.
- [Time, 2017] Time, R. W. (2017). Course compendium with matlab examples and problems. *University of Stavanger*, page 29.
- [Udegbunam et al., 2015] Udegbunam, J. E., Fjelde, K. K., Evje, S., Nygaard, G., et al. (2015). On the advection-upstream-splitting-method hybrid scheme: a simple transient-flow model for managed-pressure-drilling and underbalanced-drilling applications. *SPE Drilling & Completion*, 30(02):98–109.

A Flow calibration

The pump flow rate tests equivalent to the power supply in voltages are collected in the following tables:

Voltage (V)	Time (s)	Flow rate (l/s)
4.1	47.98	0.417
5.1	34.32	0.583
6.1	29.61	0.675
7.0	25.92	0.772
8.1	22.22	0.989
10.0	18.32	1.092
11.0	16.41	1.219
12.0	14.93	1.332

Voltage (V)	$W_o(Kg)$	$W_f(Kg)$	$W_{dif}(Kg)$	Time (s)	Q (l/s)
4.0	29.87	16	13.87	30.42	0.456
4.4	29.88	16	13.88	28.87	0.481
5.0	29.84	16	13.84	26.79	0.517
5.4	29.86	16	13.86	25.71	0.539
6.0	29.86	16	13.86	23.40	0.592
6.5	29.86	16	13.86	21.71	0.638
7.0	29.84	16	13.84	21.27	0.651
7.5	29.84	16	13.84	19.59	0.706
8.0	29.84	16	13.84	18.57	0.745
8.6	29.84	16	13.84	17.14	0.807
9.0	29.84	16	13.84	16.19	0.855
9.5	29.84	16	13.84	15.60	0.887
10.0	29.84	16	13.84	14.96	0.925
10.5	29.835	16	13.835	14.74	0.939
11.1	29.83	16	13.83	14.34	0.964
11.5	29.83	16	13.83	13.48	1.026
12.0	29.82	16	13.82	13.38	1.033

The following table shows the power supply equivalent to the experimental circulation rates for the final pressure and velocity test of the project.

Voltage (V)	Q (l/s)
4.3	0.469
6.1	0.606
7.8	0.735
9.9	0.896
12.3	1.079

B Numerical model

Here the numerical model is added with the required entries to obtain the approximation of the experimental data, the entries to update the system are highlighted in **RED BOLD COLOR**

```
% Transient two-phase code based on AUSMV scheme: Gas and Water
% The code assumes uniform geometry
% time - Seconds
% p - pressure at new time level (Pa)
% dl - density of liquid at new time level (kg/m3)
% dg - density of gas at new time level (kg/m3)
% eg - phase volume fraction of liquid at new time level (0-1)
% ev - phase volume fraction of gas at new time level (0-1)
% vg - phase velocity of gas at new time level (m/s)
% vl - phase velocity of liquid at new time level (m/s)
% qv - conservative variables at new time level ( 3 in each cell)
% temp - temperature in well (K)
% po - pressure at old time level (Pa)
% dlo - density of liquid at old time level (kg/m3)
% dgo - density of gas at new old level (kg/m3)
% ego - phase volume fraction of liquid at old time level (0-1)
% evo - phase volume fraction of gas at old time level (0-1)
% vgo - phase velocity of gas at old time level (m/s)
% vlo - phase velocity of liquid at old time level (m/s)
% qvo - conservative variables at old time level ( 3 in each cell)
% temp - temperature in well (K)

clear; t = cputime tic,
% Geometry data/ Must be specified
wellddepth = 3.685; %Simulating the Reservoir location (m)
nobox = 25; % Number of boxes in the well
% Note that one can use more refined grid, 50, 100 boxes.
% When doing this, remember to reduce time step to keep the CFL number
% fixed below 0.25.. dt ; cfl x dx/ speed of sound in water. If boxes are
% doubled, then half the time step.
```

```

nofluxes = nobox+1; % Number of cell boundaries
dx = welldepth/nobox; % Boxlength
%dt = 0.005;
% Welldepth. Cell 1 start at bottom
x(1) = -1.0*welldepth+0.5*dx;
for i = 1:nobox-1
x(i+1) = x(i)+ dx;
end

% Sensor locations
xsensor1 = 3.105; % From "Figure 3.3" 4.19 m is the height of the setup, for the experiment
application 3.685m (Injection pressure sensor) - 0.58m (Distance between Inj. and Mid sensors)
= 3.105m (location of Mid sensor).
xsensor2 = 2.105; % Height difference between mid-top is 1m therefore = 2.105 m.

x0(1) = 0.5*dx;
for i = 1:nobox-1
x0(i+1) = x0(i)+dx;
if ((xsensor1 >= x0(i)) && (xsensor1 <= x0(i+1)))

% xint1 will be an interpolation parameter between 0 and 1
% it will be 0 if xsensor is at x0(i)
% it will be 1 if xsensor is at x0(i+1)
xint1 = (xsensor1-x0(i))/(x0(i+1)-x0(i));
box1 = i;
end

if ((xsensor2 >= x0(i)) && (xsensor2 <= x0(i+1)));
% xint1 will be an interpolation parameter between 0 and 1

xint2 = (xsensor2-x0(i))/(x0(i+1)-x0(i));
box2 = i;
end

```

```

% more code here to pick out the correct box
% NB check if we are in middle of cell or at boundary.

% very important: below the timestep is set. make sure that the “cfl” condition is fulfilled. if
number of boxes is changed. “dx” will change and dt must be adjusted to keep the “cfl” number
fixed.

dt = 0.00001; % Timestep (seconds)
dtdx = dt/dx;
time = 0.0; % initial time.
endtime = 15; % Time for ending simulation (seconds)
nosteps = endtime/dt; %Number of total timesteps. Used in for loop.
timebetweensavingtimedata = 0.001; % How often in s we save data vs time for plotting.
nostepsbeforesavingtimedata = timebetweensavingtimedata/dt;

% Slip parameters used in the gas slip relation.  $v_g = K v_{mix} + S$ 
k = 1.2;
s = 0.2169;

% Boundary condition at outlet
% pbondout = 100000; % Pascal (1 bar)
pbondout = 101100; % Pascal (1 bar)

% Initial temperature distribution. (Kelvin)
% Note that this is only used if we use density models that depend on
% temperature
%tempbot = 110+273;
%temptop = 50+273;

tempbot = 20+273;
temptop = 20+273;

```

```

tempgrad = (tempbot-temptop)/welldepth;
tempo(1) = tempbot-dx/2*tempgrad;
for i = 1:nobox-2
tempo(i+1) = tempo(i)-dx*tempgrad;
end
tempo(nobox) = tempo(nobox-1)-dx*tempgrad;
temp = tempo;

% Different fluid density parameters
% Note how we switch between different models later.
% These parameters are used when finding the primitive variables pressure, densities in an
analytical manner.
% Changing parameters here, you must also change parameters inside the density routines roliq
and rogas.
% Simple Water density model & Ideal Gas. See worknote Extension of AUSMV
scheme.

rho0 = 1000; % Water density at STC (Standard Condition) kg/m3
Bbeta = 2.2*10^9; % Parameter that depend on the compressibility of water
Alpha = 0.000207; % Parameter related to thermal expansion/compression
R = 286.9; % Ideal gas parameter
P0 = 100000; % Pressure at STC (Pa)
T0 = 20+273.15; % Temperature at STC (K)

% Very simple models (PET510 compendium)

al = 1500; % Speed of sound in water.
rt = 100000; % Ideal gas parameter in model rhog = p/rt (rt = ag^2)
rho0 = 1000; % Water density at STC (Standard Condition) kg/m3
P0 = 100000; % Pressure at STC (Pa)
T0 = 20+273.15; % Temperature at STC (K)

% Viscosities (Pa*s)/Used in the frictional pressure loss model (dpfric).
viscl = 0.001; % Liquid phase

```

```
viscg = 0.0000182; % Gas phase
```

```
% Gravity constant
```

```
g = 9.81; % Gravitational constant m/s2
```

```
% Well opening. opening = 1, fully open well, opening = 0 (<0.01), the well  
% is fully closed. This variable will control what boundary conditions that  
% will apply at the outlet (both physical and numerical): We must change  
% this further below in the code if we want to change status on this.
```

```
wellopening = 1.0; % This variable determines if  
% the well is closed or not, wellopening = 1.0 -> open. wellloopening = 0  
%-> Well is closed. This variable affects the boundary treatment.
```

```
bullheading = 0.0; % This variable can be set to 1.0 if we want to simulate  
% a bullheading operation. But the normal is to set this to zero.
```

```
% Specify if the primitive variables shall be found either by  
% a numerical or analytical approach. If analytical = 1, analytical  
% solution is used. If analytical = 0. The numerical approach is used.  
% using the itsolver subroutine where the bisection numerical method  
% is used. We use analytical.
```

```
analytical = 1;
```

```
% Initialization of rest of geometry.  
% Here we specify the outer and inner diameter and the flow area  
% We assume 12.25 x 5 inch annulus. But this can be modified.
```

```
for i = 1:nobox
```

```
%do(i) = 0.331;
```

```
do(i) = 0.0392;
```

```
di(i) = 0.0;
```

```
area(i) = 3.14/4*(do(i)*do(i)- di(i)*di(i));
```

```
end
```

```
% Initialization of slope limiters. These are used for
```

```
% reducing numerical diffusion and will be calculated for each timestep.
```

```
% They make the numerical scheme second order.
```

```
for i = 1:nobox
```

```
sl1(i) = 0;
```

```
sl2(i) = 0;
```

```
sl3(i) = 0;
```

```
sl4(i) = 0;
```

```
sl5(i) = 0;
```

```
sl6(i) = 0;
```

```
end
```

```
% Now comes the initialization of the physical variables in the well.
```

```
% First primitive variables, then the conservative ones.
```

```
% Below we initialize pressure and fluid densities. We start from top of
```

```
% the well and calculated downwards. The calculation is done twice with
```

```
% updated values to get better approximation. Only hydrostatic
```

```
% considerations since we start with a static well.
```

```
for i = 1:nobox
```

```
eg(i) = 0.0; % Gas volume fraction
```

```
ev(i) = 1-eg(i); % Liquid volume fraction
```

```
end
```

```
p(nobox) = pboundout+0.5*9.81*dx*...
```

```
(ev(nobox)*rho_liq(P0,T0)+eg(nobox)*rho_gas(P0,T0)); % Pressure (Pa)
```

```
dl(nobox) = rho_liq(p(nobox),tempo(nobox)); % Liquid density kg/m3
```

```
dg(nobox) = rho_gas(p(nobox),tempo(nobox)); % Gas density kg/m3
```

```

for i = nobox-1:-1:1
p(i) = p(i+1)+dx*9.81*(ev(i+1)*dl(i+1)+eg(i+1)*dg(i+1));
dl(i) = rholiq(p(i),tempo(i));
dg(i) = rogas(p(i),tempo(i));
end

```

```

for i = nobox-1:-1:1
rhoavg1 = (ev(i+1)*dl(i+1)+eg(i+1)*dg(i+1));
rhoavg2 = (ev(i)*dl(i)+eg(i)*dg(i));
p(i) = p(i+1)+dx*9.81*(rhoavg1+rhoavg2)*0.5;
dl(i) = rholiq(p(i),tempo(i));
dg(i) = rogas(p(i),tempo(i));
end

```

```

% Intitialize phase velocities, volume fractions, conservative variables
% and friction and hydrostatic gradients.
% The basic assumption is static fluid, one phase liquid.

```

```

for i = 1:nobox
vl(i) = 0; % Liquid velocity new time level.
vg(i) = 0; % Gas velocity at new time level
eg(i) = 0.0; % Gas volume fraction
ev(i) = 1-eg(i); % Liquid volume fraction
qv(i,1) = dl(i)*ev(i)*area(i); % Conservative variable for liquid mass (kg/m)
qv(i,2) = dg(i)*eg(i)*area(i); % Conservative variable for gas mass (kg/m)
qv(i,3) = (dl(i)*ev(i)*vl(i)+dg(i)*eg(i)*vg(i))*area(i); %Conservative var. for mixture
moementum
fricgrad(i) = 0; % Pa/m
hydgrad(i) = g*(dl(i)*ev(i)+eg(i)*dg(i)); % Pa/m
end

```

```

% Section where we also initialize values at old time level

```

```

for i = 1:nobox
dlo(i) = dl(i);
dgo(i) = dg(i);

```



```

po(i) = p(i);
ego(i) = eg(i);
evo(i) = ev(i);
vlo(i) = vl(i);
vgo(i) = vg(i);
qvo(i,1) = qv(i,1);
qvo(i,2) = qv(i,2);
qvo(i,3) = qv(i,3);
end

% Intialize fluxes between the cells/boxes

for i = 1:nofluxes
for j =1:3
flc(i,j) = 0.0; % Flux of liquid over box boundary
fgc(i,j) = 0.0; % Flux of gas over box boundary
fp(i,j) = 0.0; % Pressure flux over box boundary
end

% Main program. Here we will progress in time. First some intializations and definitions to take
out results. The for loop below runs until the simulation is finished.

countsteps = 0;
counter = 0;
printcounter = 1;
%box10(printcounter) = p(10)-p(5)
%box10(printcounter) = eg(10)

pin(printcounter) = (p(1)+dx*0.5*hydgrad(1))/100000; % Pressure in bar at bottom for time
storage
pout(printcounter) = pbondout/100000; % Pressure at outlet of uppermost cell
pnobox(printcounter) = p(nobox)/100000; % Pressure in middle of uppermost cell
liquidmassrateout(printcounter) = 0; % liquid mass rate at outlet kg/s
gasmassrateout(printcounter) = 0; % gass mass rate at outlet kg/s

```

```

bullvol(printcounter) = 0; % Vector that stores accumulated bullheading volume

timeplot(printcounter) = time; % Array for time and plotting of variables vs time
pitvolume = 0;
pitrates = 0;
pitgain(printcounter) = 0;

kickvolume = 0;
bullvolume = 0;

% Code for sensors.

% sensor1:
psensor1(printcounter) = (1-xint1)*p(box1)+xint1*p(box1+1)
psensor1(printcounter) = psensor1(printcounter)/100000;

psensor2(printcounter) = (1-xint2)*p(box2)+xint2*p(box2+1)
psensor2(printcounter) = psensor2(printcounter)/100000;

pdifftrykk(printcounter) = psensor1(printcounter)-psensor2(printcounter)
% The temperature is not updated but kept fixed according to the initialization.
% Now comes the for loop that runs forward in time. This is repeated for every timestep.

for i = 1:nosteps
countsteps = countsteps+1;
counter = counter+1;
time = time+dt; % Step one timestep and update time.

% Then a section where specify the boundary conditions.
% Here we specify the inlet rates of the different phases at the bottom of the pipe in kg/s. We
interpolate to make things smooth.
% It is also possible to change the outlet boundary status of the well here. First, we specify rates
at the bottom and the pressure at the outlet

```

% in case we have an open well. This is a place where we can change the code to control simulations. If the well shall be close, wellopening must be set to 0. It is also possible to reverse the flow (bullheading).

% In the example below, we take a gas kick and then circulate this out of the well without closing the well. (how you not should perform well control)

% Note there are two variables wellopening and bullheading that can be changed in the control structure below to close the well or start reversing the flow i.e. pumping downwards.

% Note that if we will change to bullheading throughout the control structure, the variable inletligmassrate has to be defined as negative since pumping downwards at outlet will be in negative direction (positive direction of flow has been chosen to be
% upwards)

% NB, NOTE THAT THIS IS ONE OF THE MAIN PLACES WHERE YOU HAVE TO
ADJUST THE
% CODE TO CONTROL THE SIMULATION SCENARIO.

%XX = 4; % Gasrate in kg/s

XX = 0.000280;

%YY = 40; % Liquidrate in kg/s

%YY = 0.0;

%bullheadingrate = 3; %(3 kg/s = 3 l/s)

bullheadingrate = 0.59056;

if (time>=0) && (time<0.25)

inletligmassrate = 0.0;

inletgasmassrate = XX*time/0.25;

elseif (time>0.25) && (time<1.0)

inletligmassrate = 0.0;

inletgasmassrate = XX;

```

elseif (time>1.0) && (time<1.25)
    inletligmassrate = 0.0;
    inletgasmassrate = XX-XX*(time-1.0)/0.25;
elseif (time>1.25) && (time<6.25)
    welopening = 0.0;
    inletligmassrate = 0.0;
    inletgasmassrate = 0.0;
elseif ((time>6.25) && (time<6.5))
welopening = 1.0;
    bullheading = 1.0;
    inletligmassrate = -1.0*bullheadingrate*(time-6.25)/0.25;
    inletgasmassrate = 0;

intparam = (time-6.25)/(6.5-6.25);
% 0 when time = 2.0
% 1 when time = 2.25
k = 1.2*(1-intparam)+1.12*intparam; % k = 1.2 when time = 2.0 % k = 1.12 when time =
2.25
% This is the way Abrar Ghauri did it in his thesis. page V in appendix
% Check page 87 also in the thesis.
% Code for accumulating bullheading volume
% unit is m3
bullvolume = bullvolume+inletligmassrate*dt/rholiq(P0,T0)*(-1.0);

elseif (time>6.5)
    k = 1.12; % just to make sure k = 1.12
    welopening =1.0;
    bullheading = 1.0;
    inletligmassrate = -1.0*bullheadingrate;
    inletgasmassrate = 0;
    % Code for accumulating bullheading volume
    % unit is m3
    bullvolume = bullvolume+inletligmassrate*dt/rholiq(P0,T0)*(-1.0);
end

```

```

% elseif (time>=1.0 & time <= 2.0)
%   bullheading = 1.0;
%   inletgasmassrate = 0.0;
%   inletligmassrate = -1.0*YY*(time-1.0)/(2.0-1.0);
% else
%   bullheading = 1.0;
%   inletgasmassrate = 0.0;
%   inletligmassrate = -1.0*YY;
% end
% % if (time < 10)
% %
% %   inletligmassrate = 0.0;
% %   inletgasmassrate = 0.0;
% %
% % elseif ((time>=10) & (time < 20))
% %   inletligmassrate = YY*(time-10)/10; % Interpolate the rate from 0 to value wanted.
% %   inletgasmassrate = XX*(time-10)/10;
% %
% % elseif ((time >=20) && (time<200))
% %   inletligmassrate = YY;
% %   inletgasmassrate = XX;
% % % elseif ((time >=200) & (time<210))
% % % % inletligmassrate = YY-YY*(time-200)/10;
% % %   inletligmassrate = YY-YY*(time-200)/10;
% % %   inletgasmassrate = XX-XX*(time-200)/10;
% % elseif (time > 210)
% % %   inletligmassrate = 0;
% % %   inletgasmassrate = 0;
% % %   wellopening = 0;
% %   inletligmassrate = YY;
% %   inletgasmassrate = XX;
% % end

```

```

% The commented code below are from some previous runs. It shows. e.g. how
% we can close the well.
%elseif((time>=500)&(time<510))
% inletligmassrate = YY-YY*(time-500)/10;
% inletgasmassrate = XX-XX*(time-500)/10;
% elseif(time>=510)
% inletligmassrate = 0;
% inletgasmassrate = 0;
% wellopening = 0.0;
% end

%XX = 4;
% XX (kg/s) is a variable for introducing a kick in the well.
%YY = 15; % Liquid flowrate (kg/s) (1 kg/s = 1 l/s approx)
% if (time < 10)
%
% inletligmassrate = 0.0;
% inletgasmassrate = 0.0;
%
% elseif ((time>=10) & (time < 20))
% inletligmassrate = 0*(time-10)/10;
% inletgasmassrate = XX*(time-10)/10;
%
% elseif ((time >=20) & (time<110))
% inletligmassrate = 0;
% inletgasmassrate = XX;
%
% elseif ((time>=110)& (time<120))
% inletligmassrate = 0;
% inletgasmassrate = XX-XX*(time-110)/10;
% elseif ((time >= 120 & time < 130))
% inletligmassrate = 0;
% inletgasmassrate = 0;
% elseif ((time >= 130) & (time < 300))

```

```

% inletligmassrate = 0;
% inletgasmassrate = 0;
% elseif ((time >= 300) & (time < 310))
% inletligmassrate = YY*(time-300)/10;
% inletgasmassrate = 0;
% elseif((time >= 310))
% inletligmassrate = YY;
% inletgasmassrate = 0;
% end

kickvolume = kickvolume+inletgasmassrate/dgo(1)*dt; % Here we find the kickvolume

% initially induced in the well.
% Here we specify the physical outlet pressure. Here we have given the pressure as
% constant. It would be possible to adjust it during openwell conditions
% either by giving the wanted pressure directly (in the command lines
% above) or by finding it indirectly through a chokemodel where the chokeopening
% would have had to be an input parameter. The chokeopening variable would equally had
% to be adjusted inside the controle structure given above.

pressureoutlet = pbondout;

% Based on these given physical boundary values combined with use
% of extrapolations techniques
% for the remaining unknowns at the boundaries, we will define the mass and
% momentum fluxes at the boundaries (inlet and outlet of pipe).

% inlet/bottom fluxes first.
if (bullheading <= 0)
% Here we pump from bottom
flc(1,1) = inletligmassrate/area(1);
flc(1,2) = 0.0;
flc(1,3) = flc(1,1)*vlo(1);
fgc(1,1) = 0.0;

```

```

fgc(1,2) = inletgasmassrate/area(1);
fgc(1,3) = fgc(1,2)*vgo(1);
fp(1,1) = 0.0;
fp(1,2) = 0.0;

% Old way of treating the boundary
% fp(1,3) = po(1)+0.5*(po(1)-po(2)); %Interpolation used to find the
% pressure at the inlet/bottom of the well.
% New way of treating the boundary
fp(1,3) = po(1)...
    +0.5*dx*(dlo(1)*evo(1)+dgo(1)*ego(1))*g...
    +0.5*dx*fricgrad(1);
else
% Here we pump from the top. All masses are assumed to flow out of the
% well into the formation. We use first order extrapolation.
flc(1,1) = dlo(1)*evo(1)*vlo(1);
flc(1,2) = 0.0;
flc(1,3) = flc(1,1)*vlo(1);

fgc(1,1) = 0.0;
fgc(1,2) = dgo(1)*ego(1)*vgo(1);
fgc(1,3) = fgc(1,2)*vgo(1);

fp(1,1) = 0.0;
fp(1,2) = 0.0;
%fp(1,3) = 20000000; (Pa) %
%This was a fixed pressure set at bottom when bullheading
fp(1,3) = 135000; % (Pa)
end
% Outlet fluxes (open & closed conditions)
if (wellopening>0.01)

% Here open end condntions are given. We distinguish between bullheading
% & normal circulation.

```



```

if (bullheading <= 0) % Here we dont bullhead, i.e we circulate from bottom
% Here the is normal ciruclation and open well)
flc(nofluxes,1) = dlo(nobox)*evo(nobox)*vlo(nobox);
flc(nofluxes,2) = 0.0;
flc(nofluxes,3) = flc(nofluxes,1)*vlo(nobox);
fgc(nofluxes,1) = 0.0;
fgc(nofluxes,2) = dgo(nobox)*ego(nobox)*vgo(nobox);
% fgc(nofluxes,2)=0; Activate if gas is sucked in!?
fgc(nofluxes,3) = fgc(nofluxes,2)*vgo(nobox);
fp(nofluxes,1) = 0.0;
fp(nofluxes,2) = 0.0;
fp(nofluxes,3) = pressureoutlet;
else
% Here we are bullheading.
flc(nofluxes,1) = inletligmassrate/area(nobox);
flc(nofluxes,2) = 0.0;
flc(nofluxes,3) = flc(nofluxes,1)*vlo(nobox);
fgc(nofluxes,1) = 0.0;
fgc(nofluxes,2) = 0.0;
fgc(nofluxes,3) = 0.0;
fp(nofluxes,1) = 0.0;
fp(nofluxes,2) = 0.0;
fp(nofluxes,3) = po(nobox)...
    -0.5*dx*(dlo(nobox)*evo(nobox)+dgo(nobox)*ego(nobox))*g...
    +0.5*dx*fricgrad(nobox); %check sign here on friction
% Physically, the friction should be added when going from mid point in upper cell to outlet.
But if fricgrad(nobox) is negative there should be a minus in front of the term to have + in the
end.
end
else
% Here closed end conditions are given

flc(nofluxes,1) = 0.0;
flc(nofluxes,2) = 0.0;

```

```

flc(nofluxes,3) = 0.0;
fgc(nofluxes,1) = 0.0;
fgc(nofluxes,2) = 0.0;
fgc(nofluxes,3) = 0.0;
fp(nofluxes,1) = 0.0;
fp(nofluxes,2) = 0.0;
% Old way of treating the boundary
% fp(nofluxes,3) = po(nobox)-0.5*(po(nobox-1)-po(nobox));
% New way of treating the boundary
fp(nofluxes,3) = po(nobox)...-0.5*dx*(dlo(nobox)*evo(nobox)+dgo(nobox)*ego(nobox))*g;
% -0.5*dx*fricgrad(nobox); % Neglect friction since well is closed.
end

```

```

% Implementation of slopelimiters. They are applied on the physical
% variables like phase densities, phase velocities and pressure.

```

```

% It was found that if the slopelimiters were set to zero in
% the boundary cells, the pressure in these became wrong. E.g. the upper
% cell get an interior pressure that is higher than it should be e.g. when
% being static (hydrostatic pressure was too high). The problem was reduced
% by copying the slopelimiters from the interior cells. However, both
% approaches seems to give the same BHP pressure vs time but the latter
% approach give a more correct pressure vs depth profile. It is also better
% to use when simulating pressure build up where the upper cell pressure
% must be monitored. It should be checked more in detail before concluding.
% BUT; there has been mass conservation problems with the scheme for the
% case where the slopelimiters were copied (see master thesis of Keino)
% A possible fix has been included below where the slopelimiter related to
% the gas volume fraction is set to zero in the first cell.

```

```

for i = 2:nobox-1
sl1(i) = minmod(dlo(i-1),dlo(i),dlo(i+1),dx);
sl2(i) = minmod(po(i-1),po(i),po(i+1),dx);
sl3(i) = minmod(vlo(i-1),vlo(i),vlo(i+1),dx);

```

```

sl4(i) = minmod(vgo(i-1),vgo(i),vgo(i+1),dx);
sl5(i) = minmod(ego(i-1),ego(i),ego(i+1),dx);
sl6(i) = minmod(dgo(i-1),dgo(i),dgo(i+1),dx);
end

% Slopelimiters in outlet boundary cell are set to zero!
%   sl1(nobox) = 0;
%   sl2(nobox) = 0;
%   sl3(nobox) = 0;
%   sl4(nobox) = 0;
%   sl5(nobox) = 0;
%   sl6(nobox) = 0;

% Slopelimiters in outlet boundary cell are copied from neighbour cell!
sl1(nobox) = sl1(nobox-1);
sl2(nobox) = sl2(nobox-1);
sl3(nobox) = sl3(nobox-1);
sl4(nobox) = sl4(nobox-1);
sl5(nobox) = sl5(nobox-1);
sl6(nobox) = sl6(nobox-1);

% Slopelimiters in inlet boundary cell are set to zero!
% sl1(1) = 0;
% sl2(1) = 0;
% sl3(1) = 0;
% sl4(1) = 0;
% sl5(1) = 0;
% sl6(1) = 0;

% Slopelimiters in inlet boundary cell are copied from neighbour cell!
sl1(1) = sl1(2);
sl2(1) = sl2(2);
sl3(1) = sl3(2);
sl4(1) = sl4(2);
sl5(1) = sl5(2);

```

```
sl6(1) = sl6(2);
```

```
% FIX FOR OMITTING THE GAS MASS CONSERVATION PROBLEM
```

```
sl5(1) = 0;
```

```
% Now we will find the fluxes between the different cells.
```

```
% NB - IMPORTANT - Note that if we change the compressibilities/sound velocities of
```

```
% the fluids involved, we may need to do changes inside the csound function.
```

```
% But the effect of this is unclear.
```

```
for j = 2:nofluxes-1
```

```
% First order method is from here: If you want to test this, activate this
```

```
% and comment the second order code below.
```

```
% cl = csound(ego(j-1),po(j-1),dlo(j-1),k);
```

```
% cr = csound(ego(j),po(j),dlo(j),k);
```

```
% c = max(cl,cr);
```

```
% pll = psip(vlo(j-1),c,evo(j));
```

```
% plr = psim(vlo(j),c,evo(j-1));
```

```
% pgl = psip(vgo(j-1),c,ego(j));
```

```
% pgr = psim(vgo(j),c,ego(j-1));
```

```
% vmixr = vlo(j)*evo(j)+vgo(j)*ego(j);
```

```
% vmixl = vlo(j-1)*evo(j-1)+vgo(j-1)*ego(j-1);
```

```
% pl = pp(vmixl,c);
```

```
% pr = pm(vmixr,c);
```

```
% mll = evo(j-1)*dlo(j-1);
```

```
% mlr = evo(j)*dlo(j);
```

```
% mgl = ego(j-1)*dgo(j-1);
```

```
% mgr = ego(j)*dgo(j);
```

```
% flc(j,1) = mll*pll+mlr*plr;
```

```
% flc(j,2) = 0.0;
```

```
% flc(j,3) = mll*pll*vlo(j-1)+mlr*plr*vlo(j);
```

```

%   fgc(j,1) = 0.0;
%   fgc(j,2) = mgl*pgl+mgr*pgr;
%   fgc(j,3) = mgl*pgl*vgo(j-1)+mgr*pgr*vgo(j);

%   fp(j,1)= 0.0;
%   fp(j,2)= 0.0;
%   fp(j,3)= pl*po(j-1)+pr*po(j);

% First order methods ends here

% Second order method starts here:
% Here slopelimiter is used on all variables except phase velocities

psll = po(j-1)+dx/2*s12(j-1);
pslr = po(j)-dx/2*s12(j);
dsll = dlo(j-1)+dx/2*s11(j-1);
dslr = dlo(j)-dx/2*s11(j);
dgl1 = dgo(j-1)+dx/2*s16(j-1);
dglr = dgo(j)-dx/2*s16(j);

vlv = vlo(j-1)+dx/2*s13(j-1);
vlh = vlo(j)-dx/2*s13(j);
vgv = vgo(j-1)+dx/2*s14(j-1);
vgh = vgo(j)-dx/2*s14(j);

gvv = ego(j-1)+dx/2*s15(j-1);
gvh = ego(j)-dx/2*s15(j);
lvv = 1-gvv;
lvh = 1-gvh;

cl = csound(gvv,psll,dsll,k);
cr = csound(gvh,pslr,dslr,k);
c = max(cl,cr);
pll = psip(vlo(j-1),c,lvh);

```

```

plr = psim(vlo(j),c,lvv);
pgl = psip(vgo(j-1),c,gvh);
pgr = psim(vgo(j),c,gvv);
vmixr = vlo(j)*lvh+vgo(j)*gvh;
vmixl = vlo(j-1)*lvv+vgo(j-1)*gvv;

pl = pp(vmixl,c);
pr = pm(vmixr,c);

mll = lvv*dsl;
mlr = lvh*dslr;
mgl = gv v*dgll;
mgr = gv h*dglr;

flc(j,1) = mll*pll+mlr*plr;
flc(j,2) = 0.0;
flc(j,3) = mll*pll*vlo(j-1)+mlr*plr*vlo(j);
fgc(j,1) = 0.0;
fgc(j,2) = mgl*pgl+mgr*pgr;
fgc(j,3) = mgl*pgl*vgo(j-1)+mgr*pgr*vgo(j);

fp(j,1) = 0.0;
fp(j,2) = 0.0;
fp(j,3) = pl*psll+pr*pslr;

%%% Second order method ends here

% Here sloplimiters is used on all variables. This has not worked so well yet. Therefore it is
commented away.

%   psll = po(j-1)+dx/2*s12(j-1);
%   pslr = po(j)-dx/2*s12(j);
%   dsll = dlo(j-1)+dx/2*s11(j-1);
%   dslr = dlo(j)-dx/2*s11(j);

```

```

%   dgl1 = dgo(j-1)+dx/2*s16(j-1);
%   dglr = dgo(j)-dx/2*s16(j);

%   vlv = vlo(j-1)+dx/2*s13(j-1);
%   vlh = vlo(j)-dx/2*s13(j);
%   vgv = vgo(j-1)+dx/2*s14(j-1);
%   vgh = vgo(j)-dx/2*s14(j);

%   gvv = ego(j-1)+dx/2*s15(j-1);
%   gvh = ego(j)-dx/2*s15(j);
%   lvv = 1-gvv;
%   lvh = 1-gvh;

%   cl = csound(gvv,psll,dsl1,k);
%   cr = csound(gvh,pslr,dslr,k);
%   c = max(cl,cr);

%   pll = psip(vlv,c,lvh);
%   plr = psim(vlh,c,lvv);
%   pgl = psip(vgv,c,gvh);
%   pgr = psim(vgh,c,gvv);
%   vmixr = vlh*lvh+vgh*gvh;
%   vmixl = vlv*lvv+vgv*gvv;

%   pl = pp(vmixl,c);
%   pr = pm(vmixr,c);
%   mll = lvv*dsl1;
%   mlr = lvh*dslr;
%   mgl = gvv*dgl1;
%   mgr = gvh*dglr;

%   flc(j,1) = mll*pll+mlr*plr;
%   flc(j,2) = 0.0;
%   flc(j,3) = mll*pll*vlv+mlr*plr*vlh;

```

```

%   fgc(j,1) = 0.0;
%   fgc(j,2) = mgl*pgl+mgr*pgr;
%   fgc(j,3) = mgl*pgl*vgv+mgr*pgr*vgh;
%   fp(j,1) = 0.0;
%   fp(j,2) = 0.0;
%   fp(j,3) = pl*psll+pr*pslr;

```

```
end
```

% Fluxes have now been calculated. We will now update the conservative variables in each of the numerical cells.

% The source terms can be calculated by using a for loop.

% Note that the model is sensitive to how we treat the model for low Reynolds numbers (possible discontinuity in the model)

```
for j = 1:nobox
```

```
fricgrad(j) = dpfric(vlo(j),vgo(j),evo(j),ego(j),dlo(j),dgo(j), ...
```

```
po(j),do(j),di(j),viscl,viscg); % Pa/m
```

```
hydgrad(j) = g*(dlo(j)*evo(j)+dgo(j)*ego(j)); % Pa/m
```

```
end
```

```
sumfric = 0;
```

```
sumhyd = 0;
```

```
for j = 1:nobox
```

% Here we solve the three conservation laws for each cell and update

% the conservative variables qv

```
ar = area(j);
```

% Liquid mass conservation

```
qv(j,1) = qvo(j,1)-dtdx*((ar*flc(j+1,1)-ar*flc(j,1))...
    +(ar*fgc(j+1,1)-ar*fgc(j,1))...
    +(ar*fp(j+1,1)-ar*fp(j,1)));
```

% Gas mass conservation:


```

qv(j,2) = qvo(j,2)-dtdx*((ar*flc(j+1,2)-ar*flc(j,2))...
            +(ar*fgc(j+1,2)-ar*fgc(j,2))...
            +(ar*fp(j+1,2)-ar*fp(j,2)));

```

```

% Mixture momentum conservation:

```

```

qv(j,3) = qvo(j,3)-dtdx*((ar*flc(j+1,3)-ar*flc(j,3))...
            +(ar*fgc(j+1,3)-ar*fgc(j,3))...
            +(ar*fp(j+1,3)-ar*fp(j,3)))...
            -dt*ar*(fricgrad(j)+hydgrad(j));

```

```

% Add up the hydrostatic pressure and friction in the whole well.

```

```

sumfric = sumfric+fricgrad(j)*dx;
sumhyd = sumhyd+hydgrad(j)*dx;
end

```

```

% Section where we find the physical variables (pressures, densities etc)

```

```

% from the conservative variables. Some tricks to ensure stability. These are induced to avoid
negative masses.

```

```

gasmass = 0;
liqmass = 0;
for j = 1:nobox

```

```

% Remove the area from the conservative variables to find the
% the primitive variables from the conservative ones.

```

```

qv(j,1) = qv(j,1)/area(j);
qv(j,2) = qv(j,2)/area(j);

```

```

if (qv(j,1) < 0.00000001) % Trick to avoid negative masses.
qv(j,1) = 0.00000001;
end

```

```

if (qv(j,2) < 0.00000001) % Trick to avoid negative masses.
qv(j,2) = 0.00000001;

```

end

```
% Here we summarize the mass of gas and liquid in the well respectively.  
% These variables are important to show that the scheme is conserving  
% mass. (if e.g. gas leaks in our out of the well unintentionally in the simulation  
% without being specified in the code,something fundamental is wrong.
```

```
gasmass = gasmass+qv(j,2)*area(j)*dx;
```

```
liqmass = liqmass+qv(j,1)*area(j)*dx;
```

```
% Below, we find the primitive variables pressure and densities based on  
% the conservative variables q1,q2. One can choose between getting them by  
% analytical or numerical solution approach specified in the beginning of  
% the program. Ps. For more advanced density models, this must be changed.
```

```
if (analytical == 1)
```

```
% Analytical solution:
```

```
% here the simple density models used in PET 510 Wellflow modelling  
% compendium is used.
```

```
% % %    t1=rho0-P0/al^2;
```

```
% % %    Coefficients:
```

```
% % %    a = 1/(al*al);
```

```
% % %    b = t1-qv(j,1)-rt*qv(j,2)/(al*al);
```

```
% % %    c = -1.0*t1*rt*qv(j,2);
```

```
% % %    Note here we use the very simple models from the PET510 course
```

```
% % %    p(j)=(-b+sqrt(b*b-4*a*c))/(2*a); % Pressure
```

```
% % %    dl(j)=rholiq(p(j),temp(j)); % Density of liquid
```

```
% % %    dg(j)=rogas(p(j),temp(j)); % Density of gas
```

```
%    The code below can be activated if we want to switch to the other set of density models.  
Also then remember to do the changes inside functions rogas og rholiq if we change density  
models.
```

```

x1 = rho0-P0*rho0/Bheta-rho0*Alpha*(temp(j)-T0);
x2 = rho0/Bheta;
x3 = -qv(j,2)*R*temp(j);
a = x2;
b = x1+x2*x3-qv(j,1);
c = x1*x3;
p(j) = (-b+sqrt(b*b-4*a*c))/(2*a); % Pressure
dl(j) = rholiq(p(j),temp(j));
dg(j) = rogas(p(j),temp(j));
else

%Numerical Solution: This might be used if we use more complex
%density models. Has not been used for years.
[p(j),error] = itsolver(po(j),qv(j,1),qv(j,2)); % Pressure
dl(j) = rholiq(p(j),temp(j)); % Density of liquid
dg(j) = rogas(p(j)); % Density of gas
% In case a numerical solution is not found, the program will write out "error":
if error > 0
error
end

% Find phase volume fractions
eg(j) = qv(j,2)/dg(j);
ev(j) = 1-eg(j);

% Reset average conservative variables in cells with area included in the variables.
qv(j,1) = qv(j,1)*area(j);
qv(j,2) = qv(j,2)*area(j);
end % end of loop

% Below we find the phase velocities by combining the conservative variable defined by the
mixture momentum equation with the gas slip relation.
% At the same time we try to summarize the gas volume in the well. This

```

```

% also measure the size of the kick.
gasvol = 0;
for j = 1:nobox

% The interpolations introduced below are included to omit a singularity in the slip relation
when the gas volume fraction becomes equal to 1/K. In addition, S is interpolated to zero
when approaching one phase gas flow. In the transition to one phase gas flow, we have no slip
conditions (K=1, S=0)

% We will let the k0,s0,k1,s1 be arrays to make it easier to incorporate
% different flow regimes later. In that case, the slip parameters will
% vary from cell to cell and we must have slip parameter values for each
% cell.

ktemp = k;
stemp = s;

k0(j) = ktemp;
s0(j) = stemp;

% Interpolation to handle that (1-Kxgasvolumefraction) does not become zero
if ((eg(j) >= 0.7) & (eg(j) <= 0.8))
xint = (eg(j)-0.7)/0.1;
k0(j) = 1.0*xint+k*(1-xint);
elseif (eg(j) > 0.8)
k0(j) = 1.0;
end

% Interpolate S to zero in transition to pure gas phase
if ((eg(j) >= 0.9) & (eg(j) <= 1.0))
xint = (eg(j)-0.9)/0.1;
s0(j) = 0.0*xint+s*(1-xint);
end

% Note that the interpolations above and below can be changed
% if numerical stability problems

```

```

% are encountered.
if (eg(j) >= 0.999999)
% Pure gas
k1(j) = 1.0;
s1(j) = 0.0;
else
% Two phase flow
k1(j) = (1-k0(j)*eg(j))/(1-eg(j));
s1(j) = -1.0*s0(j)*eg(j)/(1-eg(j));
end

help1 = dl(j)*ev(j)*k1+dg(j)*eg(j)*k0;
help2 = dl(j)*ev(j)*s1+dg(j)*eg(j)*s0;

vmixhelp1 = (qv(j,3)/area(j)-help2)/help1;
vg(j)=k0(j)*vmixhelp1+s0(j);
vl(j)=k1(j)*vmixhelp1+s1(j);

% Variable for summarizing the gas volume content in the well.
gasvol=gasvol+eg(j)*area(j)*dx;
end

% Old values are now set equal to new values in order to prepare computation of next time
level.

po=p;
dlo=dl;
dgo=dg;
vlo=vl;
vgo=vg;
ego=eg;
evo=ev;
qvo=qv;

% Section where we save some timedependent variables in arrays.

```

```

% e.g. the bottomhole pressure. They will be saved for certain
% timeintervalls defined in the start of the program in order to ensure
% that the arrays do not get to long!

if (counter>=nostepsbeforesavingtimedata)
printcounter=printcounter+1;
time % Write time to screen.

% Outlet massrates (kg/s) vs time
liquidmassrateout(printcounter)=dl(nobox)*ev(nobox)*vl(nobox)*area(nobox);
gasmassrateout(printcounter)=dg(nobox)*eg(nobox)*vg(nobox)*area(nobox);

% Outlet flowrates (lpm) vs time
liquidflowrateout(printcounter)=liquidmassrateout(printcounter)/...
rho(liq,P0,T0)*1000*60;
gasflowrateout(printcounter)=gasmassrateout(printcounter)/...
rho(gas,P0,T0)*1000*60;

% Hydrostatic and friction pressure (bar) in well vs time
hyd(printcounter)=sumhyd/100000;
fric(printcounter)=sumfric/100000;

% Volume of gas in well vs time (m3). Also used for indicating kick
% size in well.

volgas(printcounter)=gasvol;

% Total phase masses (kg) in the well vs time
% Used for checking mass conservation.

massgas(printcounter)=gasmass;
massliq(printcounter)=liqmass;

```

```

% pout calculates the pressure at the outletboundary. I.e. upper edge
% of uppermost cell. Corresponds where the well ends at surface. The
% reason we do this is the fact than in AUSMV is all variables defined
% in the mid point of the numerical cells.
pout(printcounter)=(p(nobox)-0.5*dx*...
(dlo(nobox)*evo(nobox)+dgo(nobox)*ego(nobox))*g-dx*0.5*fricgrad(nobox))/100000;
% pin (bar) defines the pressure at the inlet boundary, I.e lower edge
% of the lowermost cell. Corresponds to TD of well.
pin(printcounter)=
(p(1)+0.5*dx*(dlo(1)*evo(1)+dgo(1)*ego(1))*g+0.5*dx*fricgrad(1))/100000;

% Pressure in the middle of top box (bar).
pnobox(printcounter)=p(nobox)/100000; %

%box10(printcounter)=p(10)-p(5)
%box10(printcounter)=eg(10)

psensor1(printcounter) = (1-xint1)*p(box1)+xint1*p(box1+1);
psensor1(printcounter) = psensor1(printcounter)/100000;

psensor2(printcounter) = (1-xint2)*p(box2)+xint2*p(box2+1);
psensor2(printcounter) = psensor2(printcounter)/100000;

pdifftrykk(printcounter)= psensor1(printcounter)-psensor2(printcounter);

% Here we store the accumulated bullheading volume in the vector
% that is going to be used for plotting.
bulvol(printcounter)= bullvolume; % Unit is m3

% Time variable
timeplot(printcounter)=time;

counter = 0;
end

```

```

% end of stepping forward in time.
% Printing of result ssection
countsteps % Marks number of simulation steps.

% Plot commands for variables vs time. The commands can also
% be copied to command screen where program is run for plotting other variables.

toc,
e = cputime-t

% Plot bottomhole pressure
plot(timeplot,pin)

% Show cfl number used.
disp('cfl')
cfl = al*dt/dx

%plot(timeplot,pin,'r'); title ('Pbottomhole vs Time'); xlabel('time (s)'); ylabel('bottomhole
(bar)');
%plot(timeplot,hyd,'m'); title ('Hydrostatic vs Time'); xlabel('time (s)');
ylabel('Hydrostatic(bar)');
%plot(timeplot,fric,'c'); title ('Friction vs Time'); xlabel('time (s)'); ylabel('Friction Factor
(dimensionless)');
%plot(timeplot,liquidmassrateout,'g'); title ('Liquidmassrateout vs Time'); xlabel('time (s)');
ylabel('Liquid mass rate (Kg/s)');
%plot(timeplot,gasmassrateout,'b'); title ('Gasmassrate vs Time'); xlabel('time (s)'); ylabel('Gas
mass rate (Kg/s)');
%plot(timeplot,volgas,'r'); title ('Gas Volume vs Time'); xlabel('time (s)'); ylabel('Gas Volume
(m3)');
%plot(timeplot,liquidflowrateout,'b'); title ('Liquid flow rate vs Time'); xlabel('time (s)');
ylabel('Liquid rate (lpm)');
%plot(timeplot,gasflowrateout,'r'); title ('Gas flow rate vs Time'); xlabel('time (s)'); ylabel('Gas
rate (lpm)');

```



```

%plot(timeplot,massgas,'r'); title ('gas mass vs Time'); xlabel('time (s)'); ylabel('Gas mass (kg)');
%plot(timeplot,massliq,'b'); title ('liquid mass vs Time'); xlabel('time (s)'); ylabel('Liquid mass
(kg)');
%plot(timeplot,pout,'b'); title ('Pressure at the outlet vs Time'); xlabel('time (s)'); ylabel('Outlet
Pressure (bar)');
%plot(timeplot,pnobox,'b'); title ('Pressure middle top box vs Time'); xlabel('time (s)');
ylabel('Middle Pressure (bar)');
%Plot commands for variables vs depth/Only the last simulated
% values at endtime is visualised

%plot(vl,x,'g'); ; title ('Liquid Phase velocity vs Depth'); xlabel('Phase liquid velocity (m/s)');
ylabel('Length (m)');
plot(vg,x,'b'); title ('Gas Phase velocity vs Depth'); xlabel('Phase Gas velocity (m/s)');
ylabel('Length (m)');
%plot(eg,x,'r'); title ('Gas Volume Fraction vs Depth'); xlabel('Gas Volume Fraction (0-1)');
ylabel('Length (m)');
%plot(p,x,'b'); title ('Pressure at new time level vs Depth'); xlabel('Pressure (Pa)');
ylabel('Length (m)');
%plot(dl,x,'c'); title ('Density of Liquid at new time level vs Depth'); xlabel('Liquid density
(Kg/m3)'); ylabel('Length (m)');
%plot(dg,x,'m'); title ('Density of Gas at new time level vs Depth'); xlabel('Gas density
(Kg/m3)'); ylabel('Length (m)');

```

C 3D set-up pieces

